1993

# Uranium-lead zircon geochronology study of the Bird River greenstone belt, southeastern Manitoba.

Xiaodong. Wang
*University of Windsor*

# U-PB ZIRCON GEOCHRONOLOGY STUDY OF THE BIRD RIVER GREENSTONE BELT, SOUTHEASTERN MANITOBA

by

Xiaodong Wang

A Thesis
Submitted to the
Faculty of Graduate Studies and Re[illegible]h
through the Department of Geolog[illegible]
in Partial Fulfillment of the Requirements
for the Degree of Master of Science
at the University of Windsor

Windsor, Ontario, Canada

1993

ISBN 0-315-87370-1

Canada

Name WANG - XIAODONG

*Dissertation Abstracts International* is arranged by broad, general subject categories. Please select the one subject which most nearly describes the content of your dissertation. Enter the corresponding four-digit code in the spaces provided.

U-Pb Geochronology Study of Southeastern Manitoba. 0372 U·M·I

SUBJECT TERM SUBJECT CODE

## Subject Categories

# THE HUMANITIES AND SOCIAL SCIENCES

### COMMUNICATIONS AND THE ARTS
- Architecture 0729
- Art History 0377
- Cinema 0900
- Dance 0378
- Fine Arts 0357
- Information Science 0723
- Journalism 0391
- Library Science 0399
- Mass Communications 0708
- Music 0413
- Speech Communication 0459
- Theater 0465

### EDUCATION
- General 0515
- Administration 0514
- Adult and Continuing 0516
- Agricultural 0517
- Art 0273
- Bilingual and Multicultural 0282
- Business 0688
- Community College 0275
- Curriculum and Instruction 0727
- Early Childhood 0518
- Elementary 0524
- Finance 0277
- Guidance and Counseling 0519
- Health 0680
- Higher 0745
- History of 0520
- Home Economics 0278
- Industrial 0521
- Language and Literature 0279
- Mathematics 0280
- Music 0522
- Philosophy of 0998
- Physical 0523
- Psychology 0525
- Reading 0535
- Religious 0527
- Sciences 0714
- Secondary 0533
- Social Sciences 0534
- Sociology of 0340
- Special 0529
- Teacher Training 0530
- Technology 0710
- Tests and Measurements 0288
- Vocational 0747

### LANGUAGE, LITERATURE AND LINGUISTICS
- Language
  - General 0679
  - Ancient 0289
  - Linguistics 0290
  - Modern 0291
- Literature
  - General 0401
  - Classical 0294
  - Comparative 0295
  - Medieval 0297
  - Modern 0298
  - African 0316
  - American 0591
  - Asian 0305
  - Canadian (English) 0352
  - Canadian (French) 0355
  - English 0593
  - Germanic 0311
  - Latin American 0312
  - Middle Eastern 0315
  - Romance 0313
  - Slavic and East European 0314

### PHILOSOPHY, RELIGION AND THEOLOGY
- Philosophy 0422
- Religion
  - General 0318
  - Biblical Studies 0321
  - Clergy 0319
  - History of 0320
  - Philosophy of 0322
- Theology 0469

### SOCIAL SCIENCES
- American Studies 0323
- Anthropology
  - Archaeology 0324
  - Cultural 0326
  - Physical 0327
- Business Administration
  - General 0310
  - Accounting 0272
  - Banking 0770
  - Management 0454
  - Marketing 0338
- Canadian Studies 0385
- Economics
  - General 0501
  - Agricultural 0503
  - Commerce-Business 0505
  - Finance 0508
  - History 0509
  - Labor 0510
  - Theory 0511
- Folklore 0358
- Geography 0366
- Gerontology 0351
- History
  - General 0578
  - Ancient 0579
  - Medieval 0581
  - Modern 0582
  - Black 0328
  - African 0331
  - Asia, Australia and Oceania 0332
  - Canadian 0334
  - European 0335
  - Latin American 0336
  - Middle Eastern 0333
  - United States 0337
- History of Science 0585
- Law 0398
- Political Science
  - General 0615
  - International Law and Relations 0616
  - Public Administration 0617
- Recreation 0814
- Social Work 0452
- Sociology
  - General 0626
  - Criminology and Penology 0627
  - Demography 0938
  - Ethnic and Racial Studies 0631
  - Individual and Family Studies 0628
  - Industrial and Labor Relations 0629
  - Public and Social Welfare 0630
  - Social Structure and Development 0700
  - Theory and Methods 0344
- Transportation 0709
- Urban and Regional Planning 0999
- Women's Studies 0453

# THE SCIENCES AND ENGINEERING

### BIOLOGICAL SCIENCES
- Agriculture
  - General 0473
  - Agronomy 0285
  - Animal Culture and Nutrition 0475
  - Animal Pathology 0476
  - Food Science and Technology 0359
  - Forestry and Wildlife 0478
  - Plant Culture 0479
  - Plant Pathology 0480
  - Plant Physiology 0817
  - Range Management 0777
  - Wood Technology 0746
- Biology
  - General 0306
  - Anatomy 0287
  - Biostatistics 0308
  - Botany 0309
  - Cell 0379
  - Ecology 0329
  - Entomology 0353
  - Genetics 0369
  - Limnology 0793
  - Microbiology 0410
  - Molecular 0307
  - Neuroscience 0317
  - Oceanography 0416
  - Physiology 0433
  - Radiation 0821
  - Veterinary Science 0778
  - Zoology 0472
- Biophysics
  - General 0786
  - Medical 0760

### EARTH SCIENCES
- Biogeochemistry 0425
- Geochemistry 0996
- Geodesy 0370
- Geology 0372
- Geophysics 0373
- Hydrology 0388
- Mineralogy 0411
- Paleobotany 0345
- Paleoecology 0426
- Paleontology 0418
- Paleozoology 0985
- Palynology 0427
- Physical Geography 0368
- Physical Oceanography 0415

### HEALTH AND ENVIRONMENTAL SCIENCES
- Environmental Sciences 0768
- Health Sciences
  - General 0566
  - Audiology 0300
  - Chemotherapy 0992
  - Dentistry 0567
  - Education 0350
  - Hospital Management 0769
  - Human Development 0758
  - Immunology 0982
  - Medicine and Surgery 0564
  - Mental Health 0347
  - Nursing 0569
  - Nutrition 0570
  - Obstetrics and Gynecology 0380
  - Occupational Health and Therapy 0354
  - Ophthalmology 0381
  - Pathology 0571
  - Pharmacology 0419
  - Pharmacy 0572
  - Physical Therapy 0382
  - Public Health 0573
  - Radiology 0574
  - Recreation 0575
  - Speech Pathology 0460
  - Toxicology 0383
- Home Economics 0386

### PHYSICAL SCIENCES
#### Pure Sciences
- Chemistry
  - General 0485
  - Agricultural 0749
  - Analytical 0486
  - Biochemistry 0487
  - Inorganic 0488
  - Nuclear 0738
  - Organic 0490
  - Pharmaceutical 0491
  - Physical 0494
  - Polymer 0495
  - Radiation 0754
- Mathematics 0405
- Physics
  - General 0605
  - Acoustics 0986
  - Astronomy and Astrophysics 0606
  - Atmospheric Science 0608
  - Atomic 0748
  - Electronics and Electricity 0607
  - Elementary Particles and High Energy 0798
  - Fluid and Plasma 0759
  - Molecular 0609
  - Nuclear 0610
  - Optics 0752
  - Radiation 0756
  - Solid State 0611
- Statistics 0463

#### Applied Sciences
- Applied Mechanics 0346
- Computer Science 0984
- Engineering
  - General 0537
  - Aerospace 0538
  - Agricultural 0539
  - Automotive 0540
  - Biomedical 0541
  - Chemical 0542
  - Civil 0543
  - Electronics and Electrical 0544
  - Heat and Thermodynamics 0348
  - Hydraulic 0545
  - Industrial 0546
  - Marine 0547
  - Materials Science 0794
  - Mechanical 0548
  - Metallurgy 0743
  - Mining 0551
  - Nuclear 0552
  - Packaging 0549
  - Petroleum 0765
  - Sanitary and Municipal 0554
  - System Science 0790
- Geotechnology 0428
- Operations Research 0796
- Plastics Technology 0795
- Textile Technology 0994

### PSYCHOLOGY
- General 0621
- Behavioral 0384
- Clinical 0622
- Developmental 0620
- Experimental 0623
- Industrial 0624
- Personality 0625
- Physiological 0989
- Psychobiology 0349
- Psychometrics 0632
- Social 0451

## ABSTRACT

The Archean Bird River greenstone belt of southeastern Manitoba is in the Superior Province of the Canadian Shield. It is made up of mafic to felsic volcanic rocks and associated metasedimentary rocks. Felsic plutonic rocks intrude and surround these supracrustal rocks. To the north of the belt is the Maskwa Lake granitoid batholith which belongs to the English River domain, and to the south, the belt borders with the Lac du Bonnet and Pointe du Bois granitoid batholiths of the Winnipeg River domain. The evolution of the belt and the granitoid terrains occurred over a time span of over 300 Ma, from ca. 3000 Ma to 2660 Ma. U-Pb zircon ages indicate a major volcanic and plutonic event in the area in the period of 2740-2730 Ma. Age for the Lac du Bonnet batholith is 2660 $\pm$ 3 Ma. The Pointe du Bois batholith which was thought to be older than the Bird River greenstone belt, yields an age of 2729 $\pm$ 9 Ma. Two ages for the Maskwa Lake batholith indicate that this batholith must be a granitoid complex incorporating rafters of older materials; the ages are: 2725 $\pm$ 6 Ma and 2782 $\pm$ 11 Ma. The age of the supracrustal rocks is inferred to be between ca. 2730 to 3000 Ma. The Peterson felsic volcanic is dated at 2740 $\pm$ 4 Ma; stratigraphically below this, the Bird River chromite sill has an age of 2745 $\pm$ 5 Ma , which is coeval and cogenetic with some of the mafic volcanism here. Sphene from a subvolcanic diorite stock of similar age yield a metamorphic age of 2715 Ma. An age of 2844 inferred for a granodiorite body adjacent to the Maskwa Lake batholith may be related to a still older volcanism here. By comparison with greenstone belts to the north and northeast, it is possible that the volcanism may be as old as 3000 Ma. However, the nature of the basement, sialic or simatic, remains unknown.

## ACKNOWLEDGEMENTS

I sincerely thank my advisor, Dr. A. Turek, for his patience and guidance throughout this study. I also wish to thank Dr. Cheong Bin Kim from Chonnam National University of Korea, for his help with sample collecting in field and mineral preparation and chemical separation in the laboratory, as well as for drafting one map. This project was made possible through funding to Dr. A. Turek by the Natural Sciences and Engineering Research Council of Canada and the Province of Ontario Visa Differential Scholarship which I received here at University of Windsor.

TABLE OF CONTENTS

## LIST OF TABLES

## LIST OF FIGURES

# CHAPTER I

## INTRODUCTION

The Bird River greenstone belt of southeastern Manitoba is one of many important Archean greenstone belts in the Superior Province of the Canadian Precambrian Shield. This east-west trending belt is in the English River domain. To the north is the Rice Lake greenstone belt and to the northeast is the Red Lake greenstone belt, both in the Uchi domain of the Superior Province. South of the Bird River belt is the Winnipeg River domain (Fig.2.1).

The Bird River greenstone belt contains many economic mineral deposits, eg., lithium- tantalum- cesium- bearing pegmatites and sub-economic nickel and chromium deposits. Both the geology and geochronology of the area have not been well investigated. The regional geological survey of the area was done in 1948 and 1952. A 1987 compilation map of the area is based on the above maps together with information contained in unpublished and published university theses. A Rb-Sr geochronology study was done in the 1970's, and the ages are secondary and reflect regional metamorphism. A M.Sc. thesis done at University of Windsor by Timmins (1985) was a U-Pb zircon dating and palaeomagnetic project. The preliminary U-Pb ages reported in that thesis were older than the Rb-Sr metamorphic ages, while the palaeomagnetic ages were reflecting the regional metamorphic events. These results, however, were reported but never published.

Absolute age determinations in greenstone belts are essential chrono-stratigraphic tools. This U-Pb geochronology study was undertaken to establish such a chrono-stratigraphy and to complete the dating started by Timmins in 1985. The rock samples used

in this study can be divided into two sets. The first set are samples: MA-4, MA-6, MA-10 and MA-17, these were collected in the summer of 1983 by E.A. Timmins and T. Vandall. The chemistry and mass spectrometry runs were done by A. Turek and Pat E. Smith in 1984 at University of Kansas on 3 of the above samples. The second set of 8 samples, including sample MA-21, MA-23 and MA-26, was collected in the summer of 1992 by the writer, A. Turek and C.B. Kim. The zircons from the first set of samples were reanalyzed, here at Windsor in this study, in 1992, together with the newly collected set.

The purpose of this thesis is to :

1. To determine new U-Pb ages and to improve on the previous geochronology study of the Bird River greenstone belt.

2. To verify and modify, if necessary, the existing stratigraphic sequence in the study area.

3. To compare the obtained U-Pb zircon ages for the Bird River greenstone belt to those in the adjacent Rice Lake and Red Lake greenstone belts, which have been recently studied by several workers, and which appear geologically to be very similar belts. All of this is related to the evolution of the Bird River greenstone belt.

This thesis is divided into seven chapters:

Chapter I is the introduction. Chapter II summarizes and discusses several aspects of the regional geology in the study area. Chapter III gives an outline of the theoretical aspect of the U-Pb geochronology. Chapter IV describes analytical procedures, from sample preparation to mass spectrometry analysis, including a mass spectrometry data smoothing technique developed in the laboratory. Chapter V presents the analytical results for the 8

samples analyzed in this study. For convenience, the related figures and tables have been put together at the end of that chapter. Chapter VI is a discussion of the analytical results. It postulates a revised stratigraphy for the Bird River area, and includes regional correlation of igneous activities in the study area and the adjacent areas. Chapter VII gives the conclusions of this thesis.

# CHAPTER II

## REGIONAL GEOLOGY

The Bird River Archean greenstone belt is in southeastern Manitoba, between latitudes 50°20' to 50°30'N and longitudes 95°09' to 95°50'W, approximately 130 km northeast of Winnipeg, and is close to the town of Lac du Bonnet (Fig. 2.1 and Fig. 2.2). The area is centred on the western boundary of the Nopiming Provincial Park along Provincial highway 314.

The first reconnaissance geological mapping in this area was conducted along the main water courses in 1912 by the Geological Survey of Canada. During the 1920's and 1930's the Survey mapped parts of the area at one mile to the inch. In 1948 and 1951, more detailed mapping, at 1/2 mile to the inch, was done by the Manitoba Mine Branch (Springer, 1948; Davies, 1951). The most interesting parts of the area, geologically and economocally, were mapped, at 1,000 feet to the inch, by the Manitoba Mines Branch in 1954, 1955, and 1956. However, much of the geological information in this thesis is based on the most recent study of this area which was done by Trueman (1980), and Cerny et al. (1981).

The Bird River greenstone belt, trends east-west, is approximately 50 km long and 10 km wide. It is in the Superior Province of the Canadian Shield and is a broad easterly plunging anticlinorium-synclinorium bounded by 4 batholiths: Maskwa Lake Batholith on the north; Lac du Bonnet Batholith, Point Du Bois Batholith and White Shell Batholith on the south (Fig. 2.2.).

The next greenstone belt to the north is the Rice Lake belt and is made up of lithologically similar rocks. Consequently the term Rice Lake Group was applied to the

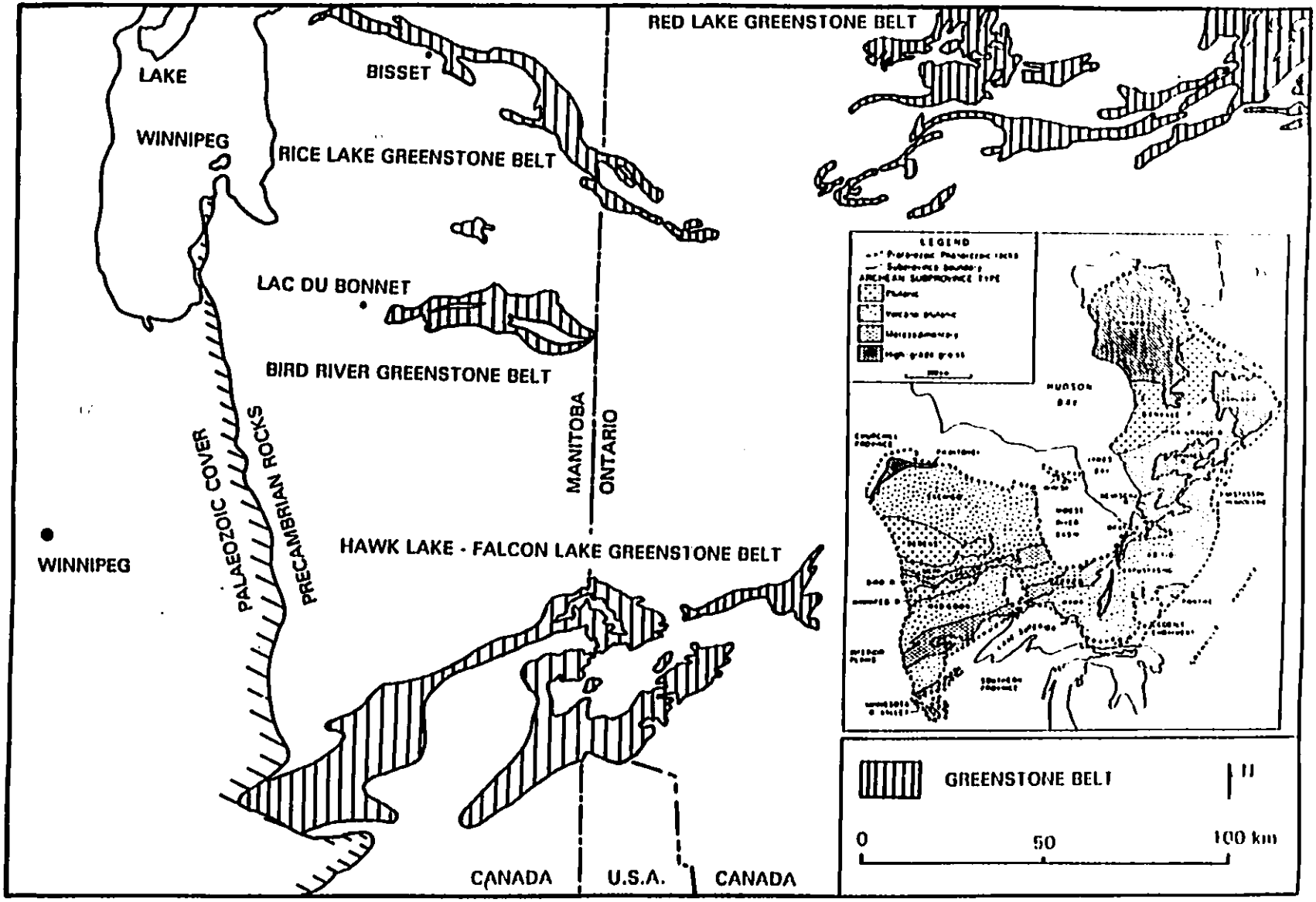


**Fig. 2.1.** Greenstone belts of southeastern Manitoba and northwestern Ontario. Insert map shows subdivisions of Canadian Shield (Card and Ciesielski, 1986).

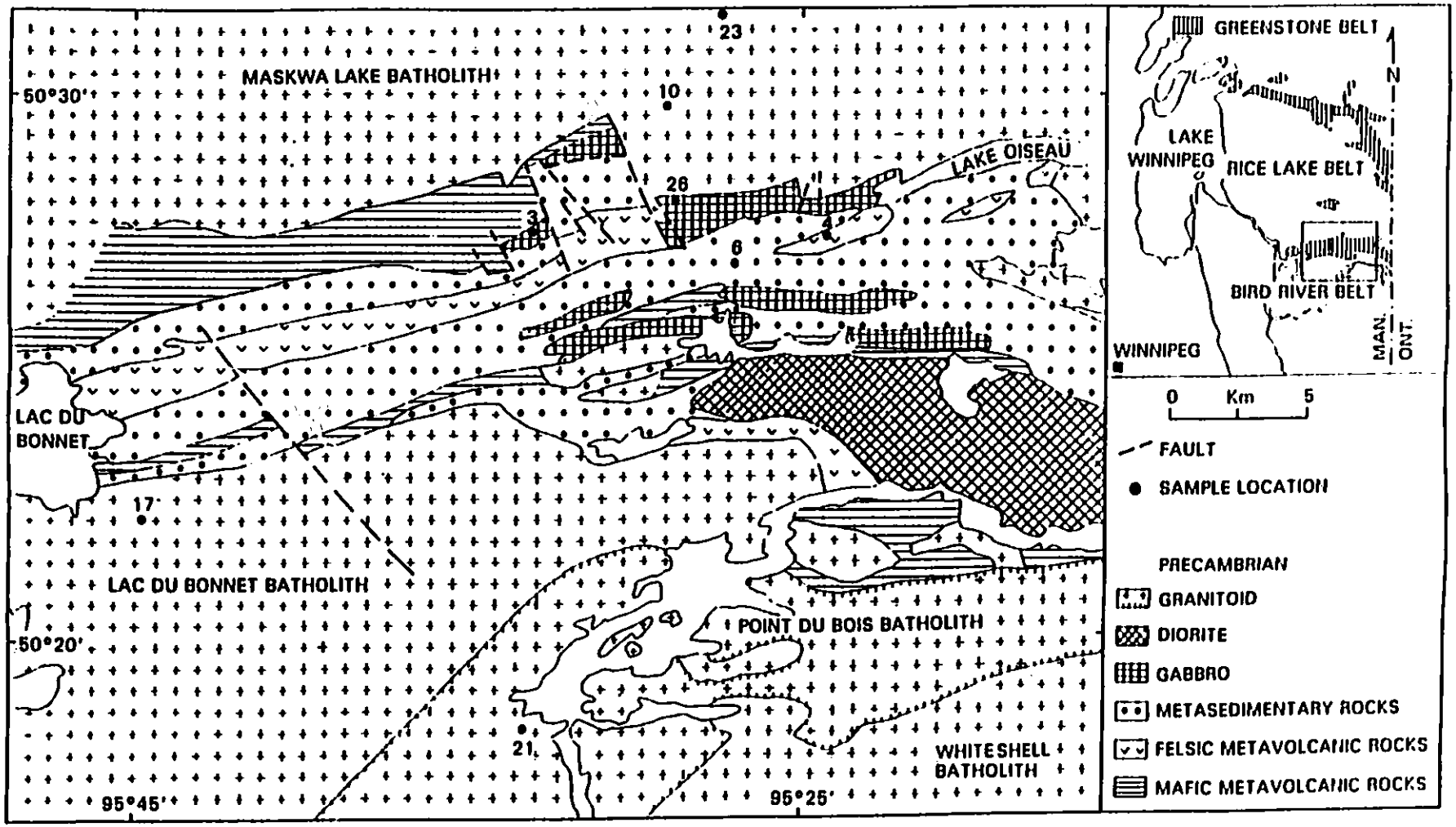


**Fig. 2.2.** Geological map of the Bird River greenstone belt (based on Kowerchuk and Weber, 1987).

Bird River area. However, following the work of Trueman (1980) and Cerny et al. (1981) in the Bird River area and the work of McRitchie and Weber (1971) in the Rice Lake area, the rocks in these two belts have been subdivided into individual formations. The Bird River belt has been subdivided into 6 formations separated by three unconformities. These are (from oldest to youngest): the Eaglenest Formation, a meta-sedimentary unit followed by the Lamprey Falls Formation, Peterson Creek Formation, Bernic Lake Formation, meta-volcanic and meta-sedimentary rocks, and the Flanders Lake Formation and the Booster Lake Formation which are meta-sedimentary rocks. These supracrustal rocks are intruded by igneous rocks ranging in composition from ultramafic and gabbroic rocks to granites and pegmatites (Table 2.1). Detailed descriptions of these formations are in Cerny et al. (1981), Davies (1952, 1955, 1956, 1957), McRitchie and Weber (1971), and Trueman (1980).

## General geology

### Supracrustal rocks

The Archean supracrustal rocks contained in the 6 formations of the greenstone belt are mainly meta-volcanic rocks and meta-sedimentary rocks.

The Eaglenest Formation, considered to be the oldest unit in the greenstone belt on the basis of stratigraphy, is composed of metamorphosed volcanic rocks, pebbly wackes and volcanic sandstones. Less abundant are biotite schists and amphibolites of uncertain origin that outcrop between bands of tonalitic and dioritic intrusive materials near the southern contact. The dominant subunit is a volcanic wacke which outcrops on the northern shore of

**Table 2.1.** Table of formations for the Archean rocks of the Bird River Area, Manitoba (based on Tureman, 1980).

| Formation | Supracrustal Rocks | Intrusive Rocks |
|---|---|---|
| | | Pegmatite, granite |
| | | Lac du Bonnet quartz monzonite |
| | | Maskwa Lake batholith |
| Booster Lake | Metamorphosed grey-wacke mudstone. | |
| | unconformity | |
| Flanders Lake | Lithic meta-arenite meta-conglomerate. | |
| | uncomformity | |
| Bernic Lake | Clastic derivatives meta-rhyolite meta-diorite meta-andesite | Metamorphosed: gabbro, diorite, quartz-feldspar porphyries, granodiorite. |
| | uncomformity | |
| Peterson Creek | Meta-rhyolite clastic equivalents | |
| Lamprey Falls | Meta-basalt | Bird River Sill meta-gabbro |
| Eaglenest Lake | Metamorphosed volcanic wacke | |

Eaglenest Lake. It is dark grey to buff weathering, fine to coarse grained, and moderately to strongly schistose. The wacke is poorly bedded and lacks sorting with its clasts showing strong deformation and flattening parallel to the schistosity. These rocks are obviously derived from a volcanic source, but their relative age is uncertain. This formation may represent its true position in the stratigraphic succession as the oldest unit in the area, but it may also represent a faulted segment of the Bernic Lake Formation (Trueman, 1980; Cerny et al., 1981).

The Lamprey Falls Formation contains predominantly mafic meta-volcanics and related hypabyssal intrusive rocks. Metamorphosed pillow basalts are the dominant rock types of this formation and range from a dark grey-black to green in colour. The pillows are characterized by a fine to medium grain size, massive to weakly schistose texture, and display well selvaged pillow structures. Other rock types in the formation include tuffs, hyaloclastite, aquagene breccias, megacrystic basalts, porphyritic and amygdaloidal meta-basalts and iron formation. These rocks outcrop extensively along the Winnipeg River and north of Bird River with both locations being marked by faults and intrusive contacts. The maximum thickness of this formation is about 3 km (Cerny et al., 1981).

The Peterson Creek Formation consists essentially of rhyolite flows. Specific rock types of this formation include metamorphosed flow-banded rhyolites (quartz porphyry), rhyolite breccia, rhyolite tuffs and epiclastic sandstone derivatives. Some of the rocks in this formation were subaerially erupted, transported, reworked, and redeposited subaqueously as felsic sandstones. The meta-rhyolite flows are buff to greenish weathering, porphyritic with quartz being the dominant phenocryst, aphanitic to fine grained, flow-banded, and weakly

schistose. The thickness of the flows range from 6 to 20 m. The clastic felsic meta-volcanic rocks are subdivided into tuffs, lapillistone and pyroclastic breccia. Pyroclastic breccia and lapillistone predominate in the western and central Bird River area, and they grade eastwards into lapillistone, tuffaceous units and ultimately into their derived epiclastic counterparts. All the rocks in this formation are in fault contact with and along both flanks of the synclinorium formed by the Lamprey Falls Formation, and in turn are overlain and interfolded with mixed rocks of the Bernic Lake Formation (Trueman, 1980; Cerny et al., 1981).

The Bernic Lake Formation is lithologically similar to the clastic rocks of the Eaglenest Formation. It consists of metamorphosed basalt, andesite, dacite, rhyolite, iron formation, polymictic conglomerate and sandstone. The dominant rocks in this formation are polymictic and oligomictic meta-conglomerates, they are clastically interlayered with each other and with other rock types. The polymictic meta-conglomaterates are typically dark grey to black in colour and are fine to coarse grained with clasts ranging from pebble to boulder size. The oligomictic meta-conglomerate is typically greyish weathering, fine to coarse grained with a grey to black strongly schistose matrix. Clasts are pebble to boulder size and are intermediate to felsic in composition. The oligomictic meta-conglomerate is dominant in the southern exposure of the Bernic Lake Formation. The flow rocks in this formation are mainly metabasalts and are typically pillowed flows. They are greyish to black in colour and are marked by a moderately to strongly developed schistosity. The meta-basalts form two prominent units, one in the Bernic Lake area and the other just south of the Bird River (Trueman, 1980; Cerny et al., 1981).

The Flanders Lake Formation includes polymictic meta-conglomerates and related meta-arenites. The dominant rock type in this formation is the meta-arenite. It is typically greyish weathering, moderately well bedded and sorted, and displays a schistose foliation that develops into a gneissosity close to intrusive contacts. The meta-conglomerates in this formation are distinctive. They are characterized by abundant stretched pebble and cobble-sized clasts differing in composition. Primary bedding structures are locally preserved in the meta-conglomerates which suggest that deposition was by turbidity and debris flow mechanisms with subsequent reworking in a fluviatile regime (Posehn, 1976; Trueman, 1980; Cerny et al., 1981).

The Booster Lake Formation consists of two dominant rock types, greywacke and mudstone turbidites with minor iron formation and conglomerate units. The turbidites are typically buff weathered, well bedded, fine to coarse grained and moderately schistose. There are abundant primary structures in the turbidites. These structures include the graded bedding phase of the classical Bouma sequence. The conglomerate units contained in the turbidites are well exposed and consist of clasts up to 2 m in diameter (Trueman, 1980; Cerny et al., 1981).

Intrusive rocks

Intrusive rocks within the belt have been subdivided by Trueman (1980) into syn-volcanic, syntectonic and late-tectonic rocks on the basis of field relationships, composition and internal structure.

Synvolcanic intrusive rocks: Synvolcanic intrusive rocks in this area include the Bird River sill and the intrusive stocks of the Bernic Lake Formation and Lamprey Falls Formation.

The Bird River sill is intruded along the contact between the Lamprey Falls Formation and the Bernic Lake Formation. It is a layered unltramafic to gabbroic body formed by gravitational settling and accumulation of layers of olivine, chromite and plagioclase. There are 5 principal units in the sill: a feeder dike, a layered ultramafic cummulate, a picrite layer, a grabbroic cummulate, and a granophyre.

The layered ultramafic cummulate is about 200 m in thickness and contains serpentinized peridotite as the predominant rock type. The two main rock types in this unit are dunite and peridotite, both of them contain varying amount of chromite. Abundant primary structures can be found in this unit, including features such as bifurcation and disruption of chromite layers, graded bedding and flame structures.

The picrite layer is about 10 m in thickness and forms the uppermost layer of the ultramafic portion of the sill. It is identified by the disappearance of original olivine and the first appearance of cumulus plagioclase.

The layered gabbroic unit includes several rock types: anorthositic gabbro, laminated and glomero-porphyritic gabbro, and anorthosite. It is the thickest portion of the sill, about 380 m in thickness.

The granophyre unit is about 6 to 9 m in thickness and is supposed to be the last crystallization product of the sill. It is sandwiched between the downward accumulation of the

overlying anorthosite and the upward accumulation of the gabbros. (Gait, 1964; Trueman, 1971,1980; Bannatyne and Trueman,1982).

The intrusive stocks in the area show both mutually intrusive relationships and differentiation from gabbro to diorite. The meta-gabbro is typically grey to black weathering, medium to coarse-grained, and is believed to be the earliest intrusive phase of these composite rocks. The meta-diorite occurs as intrusive stocks near Bernic Lake and as thin sills north and east of Osis Lake. It is grey weathering, medium to coarse grained, equigranular and moderately schistose. (Jackson, 1967; Trueman,1980; Cerny et al., 1981).

Syntectonic intrusive rocks: The Maskwa Lake Batholith is assigned to a syntectonic association because its emplacement correlates with the second regional metamorphic event in the area. The related schistosities are parallel to the intrusive boundaries of the batholith. There are two intrusive phases exhibited in the Maskwa Lake Batholith: a coarse grained, equigranular to porphyritic, massive to locally gneissic, dark grey to buff colored diorite; and an equigranular, medium to coarse grained, massive, pink to buff colored granite. In addition, the Marijane Lake batholith which extents to the east of the study area is also considered a type of syntectonic intrusive body. It is a weakly foliated, equigranular, medium to coarse grained, buff colored granite. (Carlson, 1958; Ermanovics et al., 1979; Trueman, 1980; Cerny et al., 1981).

Late-tectonic intrusive rocks: The late-tectonic intrusive rocks in this area include the Lac du Bonnet quartz monzonite batholith, related sills, stocks and dikes of pegmatitic granite and pegmatites.

The Lac du Bonnet quartz monzonite is a composite intrusion of batholithic size. It contains areas of quartz diorite enclosed by two phases of granite: one phase is biotite rich, the other is devoid of biotite. The quartz monzonite is massive to weakly foliated, coarse grained, biotite-bearing and buff to reddish in colour. Its northern intrusive boundary isolates the southern contact of the Bird River greenstone belt, and its southern contact marks the northern extent of the Winnipeg River batholithic belt. The size of the Lac du Bonnet batholith is bigger than 2,500 $km^2$ and outcrops in the southern part of the Bird River greenstone belt (Fig.2.2).

The related pegmatites are generally coarse grained assemblages of quartz, feldspars, and micas; they appear to occupy previously formed bedding, schistosity and faulting structures that were formed in the second and third deformation event in the area. Thus the relative age of the pegmatites in the area must be very young (Hall and Hajnal, 1973; Hall, 1974; Beakhouse, 1977; Ermanovics et al., 1979; Trueman, 1980; Cerny et al., 1981).

## Structural geology

The Bird River Archean greenstone Belt forms the central part of the western extremity of a broad linear crustal feature termed the English River gneissic belt. It is a broad easterly plunging anticlinorium-synclinorium. The Maskwa Lake Batholith is on its northern contact and the Lac du Bonnet Batholith is on its southern contact (Fig. 2.2). Trueman (1980) subdivided this belt into 6 formations (as discussed above) and several synvolcanic, syntectonic, and late-tectonic intrusive events.

It is believed that the Archean meta-sedimentary and meta-volcanic units in the area display 4 deformational and metamorphic events. Across the entire study area, two major folding events and two major faulting events are suggested based on structural and petrographic analysis. The higher metamorphic grade rocks are concentrated in the eastern and southern map area, and the lower metamorphic grade rocks are concentrated in the western and northern map areas. Moreover, there are original sedimentary structures preserved in the west and north parts of the area. All these suggest that the belt has undergone differential uplift. Correlating depth with metamorphism, the southern and eastern parts of the greenstone belt must be metamorphosed at a grater depth with a higher metamorphic grade than the northern and western areas. (Dwidebi, 1966; Wilson, 1971; Trueman, 1980).

There is a major fault in the west part of the Bird River greenstone belt, about 5 km east of Lac du Bonnet. This fault trends northwest and is more than 10 km in length. It crosses into the Lac du Bonnet Batholith, so it must be younger than the batholith. A group of small faults appear in the north part of the greenstone belt, most of them trend northwest and extend from 1 km to 5 km in lengths. They cross into the Maskwa Lake Batholith, thus they too must be younger than the batholith (Trueman, 1980; Cerny et al., 1981).

## Mineral deposits

There are 4 types of mineral deposits in the Bird River area; these are: chromium, lithium and beryllium, base metals, and miscellaneous minerals.

Chromite ($FeCr_2O_4$) in the area occurs as stratiform deposit within the lower, peridotite, part of the Bird River sill. The chromite horizon lies parallel to, and 175 feet or so

below, the gabbro-peridotite contact. Bands of dense and disseminated chromite are separated by layers of peridotite containing variable but small amounts of chromite. The chromite deposits have two principal types, differing only in the thickness and distribution of chromiferous bands. Dense chromite ore contains 40% to 75% chromite in small irregular to rounded and octahedral grains about 0.5 mm across. Typical disseminated ore contains about 25% chromite. Many of the chromite crystals contain small silicate nuclei. The chromic oxide content of different bands varies from a few precent for chromiferous peridotite to 30 precent for dense ore (Davies et al., 1962).

Lithium and beryllium minerals are contained in pegmatite dikes which occur in volcanic and granitic rocks close to the margins of large granitic intrusions. Most of the lithium dikes are in volcanic rocks; the beryllium dikes, if in volcanic rocks, occur closer to the granitic intrusion than the lithium dikes. Many beryllium pegmatites occur within the granite. The most important dikes are those containing lithum minerals and these may be either vertical or nearly horizontal bodies. Most of the flat, zoned dikes are coarse grained, containing crystals several inches to several feet across. Much of the spodumene, however, is intergrown with quartz and very large crystals of pure spodumene are rare. Most of the valuable silicate minerals (spodumene, amblygonite, beryl, petalite, pollucite) are white or near white in colour and may be easily confused with one another or even with quartz and feldspar (Davies et al., 1962).

Base metal deposits in the area containing copper and nickel occur in or along the edges of gabbro and peridotite. The deposits west of the Bird River occur at the contacts between granite, and peridotite and gabbro. A series of sulphide lenses composed of massive

and disseminated pyrrhotite, pentlandite, chalcopyrite, cubanite, pyrite, and magnetite were found in the deposits. One of the sulphide zones was drilled by Maskwa Nickel Chrome Mines Limited in 1953. Reserves to a depth of 500 feet are reported to be 1,213,000 tons averaging 1.23% nickel and 0.37% copper (Davies et al., 1962).

Miscellaneous minerals in the area include fuchsite, rose quartz, feldspar, and gold. Fuchsite, chromium-bearing mica, occurs south of the Winnipeg River in "pearl rock" (silicified basalt), at the contact between granite and basalt. Rose quartz forms the core zone of a pegmatite dike north of Birse Lake. Feldspar is abundant in most pegmatite dikes in the area. Gold associated with sphalerite and galena was discovered between Maskwa Lake and Little Bear Lake in 1924. Irregular quartz veins, cutting sheared lamprophyre dikes that intrude granite, are mineralized with pyrite containing gold. Gold also occurs in the native state and as tellurides in the quartz. However, surface indications are that the veins are very small and the gold content is generally low (Davies et al., 1962).

## Previous geochronology

Some of the very first chemical absolute ages were determined in the 1940's on pegmatite minerals from Bird River area (Ahrens, 1955). However, the first attempt at working out the geochronology of the area was done by Penner and Clark (1971) and Farquharson (1975). These were Rb-Sr whole rock ages, which due to regional metamorphism, are for most part updated. Timmins et al. (1985) then attempted U-Pb zircon ages as part of a paleomagnetic study of the area.

The published and reported ages for the surrounding Bird River area are given in Table 2.2. All the ages in Table 2.2 are for Archean rocks, hence it is obvious that a significant number of ages has been affected by metamorphic and diagenetic processes, all above rocks should be older than 2600 Ma, age of the Kenoran orogeny.

**Table 2.2.** Table of radiometric ages of the Archean rocks in the Bird River Area and surrounding area, Manitoba.

| Rock unit | Age (ma)* | Method | Remark |
|---|---|---|---|
| Pegmatite-Tanco Mine | 2320 | Rb-Sr | Penner & Clark, 1971. |
| Lac du Bonnet quartz monzonite | 2442±127<br>2623±89 | Rb-Sr<br>Rb-Sr | Penner & Clark, 1971.<br>Farquharson, 1975. |
| Maskwa Lake Batholith | 2584±132 | Rb-Sr | Penner & Clark, 1971. |
| Bird River volcanics | 2593±34 | Rb-Sr | Penner & Clark, 1971. |
| Huron Claim uraninite | 2475 | U-Pb (207/206) | Nier et al., 1941. |
| Huron Claim uraninite | 2580±100 | U-Pb (207/206) | Cummings et al., 1955. |
| Huron Claim uraninite Salt | 2535±160 | U-Pb (207/206) | Cummings et al., 1955. |
| Huron Claim muscovite | 2150±180 | K-Ar | Steven & Sbillibeer, 1956. |
| Huron Claim albite | 2030±170 | K-Ar | Steven & Sbillibeer, 1956. |
| Silverleaf Claim lepidolite | 2623±69<br>2623±88<br>2613±64 | Rb-Sr<br>Rb-Sr<br>Rb-Sr | Aldrich et al., 1956.<br>Eckelmann & Gast, 1957. |
| Silverleaf Claim microcline | 2290±137 | Rb-Sr | Eckelmann & Gast, 1957. |
| Silverleaf Claim lepidolite | 2613±64 | Rb-Sr | Gast et al., 1958. |
| Silverleaf Claim microcline | 2290±137 | Rb-Sr | Gast et al., 1958. |
| Rennie batholith | 2548±313 | Rb-Sr | Farquharson & Clark, 1971. |

Table 2.2 continued:

| | | | |
|---|---|---|---|
| Whiteshell porphyritic rock | 2554±111 | Rb-Sr | Farquharson & Clark, 1971. |
| Caddy Lake quartz monzonite | 2504±12 | Rb-Sr | Farquharson & Clark, 1971. |
| Maskwa Lake quartz diorite | 2779±32 | U-Pb | Timmins et al., 1985. |
| | 2779±64 | U-Pb | Timmins, 1985. |
| Bird River Sill | 2745±5 | U-Pb | Timmins et al., 1985. |
| | 2745±6 | U-Pb | Timmins, 1985. |
| Peterson Lake lapilli tuff | 2741 | U-Pb | Timmins,et al., 1985. |

* Ages have been recalculated using $\lambda\ (Rb^{87}) = 1.42 \times 10^{-11}\ yr^{-1}$ to conform to modern decay constants (Steiger and Jäger, 1977).

# CHAPTER III

# THEORY OF THE U-PB GEOCHRONOLOGY

## Basic theory

Absolute age determinations in geochronology are based on the decay of a radioactive parent isotope to a stable radiogenic daughter isotope, since decay is a function of time. There is extensive literature coverage of geochronology and isotope geochemistry. The most recent comprehensive text is by Faure (1986).

According to the theories of Rutherford and Soddy which were developed in the early 1900's, the decay rate of a radioactive parent nuclide is proportional to the number of atoms N remaining at any time t. This can be expressed mathematically as :

$$-\frac{dN}{dt} \propto N \qquad (1)$$

or :

$$-\frac{dN}{dt} = \lambda N \qquad (2)$$

Where $\lambda$ is the constant of proportionality and is called decay constant, it is related to the half life of the particular radionuclide.

From the above, the following time equation can be developed:

$$t = \frac{1}{\lambda} \ln\left(\frac{D^*}{P} + 1\right) \qquad (3)$$

Where T is time, $\lambda$ is decay constant, P is number of parent atoms present now, $D^*$ is number of daughter atoms produced in time t. If the system contained daughter atoms at start of time t, t=0, then $D^* = D - D_o$ ; where $D_o$ is number of daughter atoms present initially, and D is total number of atoms, radiogenic and initial.

The above equation is the law of radioactivity, and is used to calculate the age of the rock or mineral for all parent-daughter radioactive clocks.

To measure the isotope ratios in a sample, a mass spectrometer has to be used. The basic principle of a mass spectrometer is as follows: when a moving ion of mass **m** and charge e is acted upon by a potential difference of V volts, and enters a magnetic field, it will be deflected into a circular path. Equation (4) is the governing equation for the motion of this ion in the magnetic field .

$$\frac{m}{e} = 4.825 \bullet 10^5 \bullet \frac{B^2 r^2}{V} \qquad (4)$$

Where **m** is in atomic mass units, V in volts, e in units of electric charge, **B** is the strength of the magnetic field measured in gauss, **r** is the radius of path measured in centimetres. According to this principle, a mass spectrometer is designed to separate charged atoms and molecules in magnetic fields governed by equation (4). There are usually three parts in a mass spectrometer : a source of a positively charged monoenergetic beam of ions, a magnetic analyzer, and an ion collector ( Fig. 3.1 ). All three parts of a mass spectrometer are evacuated to pressure of the order $10^{-6}$ to $10^{-9}$ torr before any measurement work.

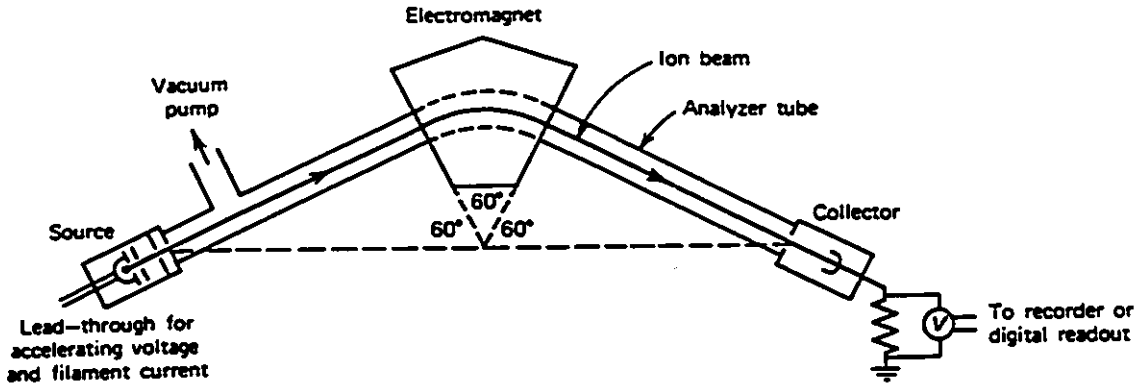


**Fig. 3.1.** Schematic diagram of a 60° sector mass spectrometer showing arrangement of ion source, electromagnet, and collector (after Faure, 1986).

In this study, the U and Pb isotope ratios were measured on a 30 cm (12 inch), 90° mass spectrometer at the University of Windsor, Mass Spectrometer Lab. A single filament was used for ionization, an accelerating voltage of 3950 volts was used for lead, and a 3050 volts accelerating voltage was used for uranium.

## The U-Pb-Th method of dating

The decay of $^{238}U$, $^{235}U$ and $^{232}Th$ is a series decay involving several intermediate daughter products before reaching the stable daughter product: $^{206}Pb$, $^{207}Pb$ and $^{208}Pb$ respectively.

The series decay process in summary is :

$$^{238}U \rightarrow {}^{206}Pb + 8He + 6\beta^-$$

$$^{235}U \rightarrow {}^{207}Pb + 7He + 4\beta^-$$

$$^{232}Th \rightarrow {}^{208}Pb + 6He + 4\beta^-$$

Pb in its own right has four naturally occurring stable isotopes: $^{204}Pb$, $^{206}Pb$, $^{207}Pb$, and $^{208}Pb$. Therefore, there is a difference between radiogenic Pb which is composed of masses 206, 207, 208 and common Pb which is 204, 206, 207, 208. Thus common Pb contents is addition to masses 206, 207, 208, and mass 204. Moreover, the abundance of the other three isotopes is variable. $^{204}Pb$ is therefore an indicator of common Pb and makes it possible to correct for presence of common Pb at time of crystallization. In the U-Pb clock, it is necessary to correct for presence of initial daughter products. The age equation (3) above can be transformed to the following equations :

$$t_{206} = \frac{1}{\lambda_1} \ln\left(\frac{(^{206}Pb/^{204}Pb) - (^{206}Pb/^{204}Pb)_i}{(^{238}U/^{204}Pb)} + 1\right) \qquad (5)$$

$$t_{207} = \frac{1}{\lambda_2} \ln\left(\frac{(^{207}Pb/^{204}Pb) - (^{207}Pb/^{204}Pb)_i}{(^{235}U/^{204}Pb)} + 1\right) \qquad (6)$$

Where $\lambda_1$ and $\lambda_2$ are decay constants for $^{238}U$ and $^{235}U$ respectively; i indicates the initial Pb isotope ratio of the rock or mineral system, other ratios represent those measured at the time of analysis. The above equations correct for any inherited Pb. As mass spectrometers measure directly isotope ratios, it is more convenient to work with ratios of isotope rather than concentrations. For this reason, Equation (5) and (6) can be rewritten as

follows :

$$^{206}Pb = (^{206}Pb)_i + {}^{238}U(e^{\lambda_1 t} - 1) \quad (7)$$

$$^{207}Pb = (^{207}Pb)_i + {}^{235}U(e^{\lambda_2 t} - 1) \quad (8)$$

Dividing Equation (8) by (7) a third derived age equation results :

$$\left(\frac{^{207}Pb}{^{206}Pb}\right)^{*} = \frac{{}^{235}U(e^{\lambda_2 t} - 1)}{{}^{238}U(e^{\lambda_1 t} - 1)} \quad (9)$$

Where $\left(\frac{^{207}Pb}{^{206}Pb}\right)^{*}$ is the radiogenic Pb ratio, corrected for initial Pb. Equation (9) is a transcendental equation and can not be solved for t except by iteration. Thus the U-Pb method can give three ages: the $^{206}Pb/^{238}U$, $^{207}Pb/^{235}U$ age and $^{207}Pb/^{206}Pb$ age.

The U-Pb method dating can be used for any geological material that contains U, but for various geological and practical reasons the ideal is the mineral zircon ($ZrSiO_4$). Zircons contain trace quantities of U and Th substitution for Zr, since they have similar ionic radii and charge. Zircon shows excellent retention of U and radiogenic Pb, the amount of the inherited common Pb is very small because Pb has a larger ionic radius and lower charge than Zr. The high U and Th content relative to any inherited Pb in zircons makes this rare mineral a very sensitive geochronometer. However, the determination of the Th-Pb ages is not very successful since Th is not as strongly held as U and in practice they are not measured, or if measured are generally disregarded.

## The U-Pb concordia diagram

The U-Pb clock provides three ages. When all three ages agree, they are said to be concordant. If, however, the system has been disturbed, the three ages are different, but it is still possible to derive the true age. This is done by a mathematical technique, which is shown graphically as plot of $^{206}Pb/^{238}U$ vs $^{207}Pb/^{235}U$ called a concordia diagram.

The concordia diagram (Fig. 3.2) was developed by Wetherill (1956). The equation for the concordia plot follow from equations (7) and (8) and are :

$$\frac{^{206}Pb^*}{^{238}U} = e^{\lambda_1 t} - 1 \qquad (10)$$

$$\frac{^{207}Pb^*}{^{235}U} = e^{\lambda_2 t} - 1 \qquad (11)$$

Where $^{206}Pb^* = {}^{206}Pb - (^{206}Pb)_i$ , $^{207}Pb^* = {}^{207}Pb - (^{207}Pb)_i$ .

Equation (19) and (20) are parametric equations. The curve is the locus of all concordant U-Pb systems, and each point on the concordia represents a finite age for a concordant mineral.

There is another kind of concordia diagram (Fig. 3.3) which was introduced by Tera and Wasserburg (1972), and was used by them to interpret U-Pb data of lunar rocks (1974). The Tera-Wasserburg concordia was subsequently modified by Wendt (1984), however, the most useful and conventional concordia diagram is the one shown in Fig. 3.2.

If the three U-Pb ages are concordant, the U-Pb ratios will plot on the concordia curve. This means there has been no loss or gain of parent or daughter, i.e. closed system

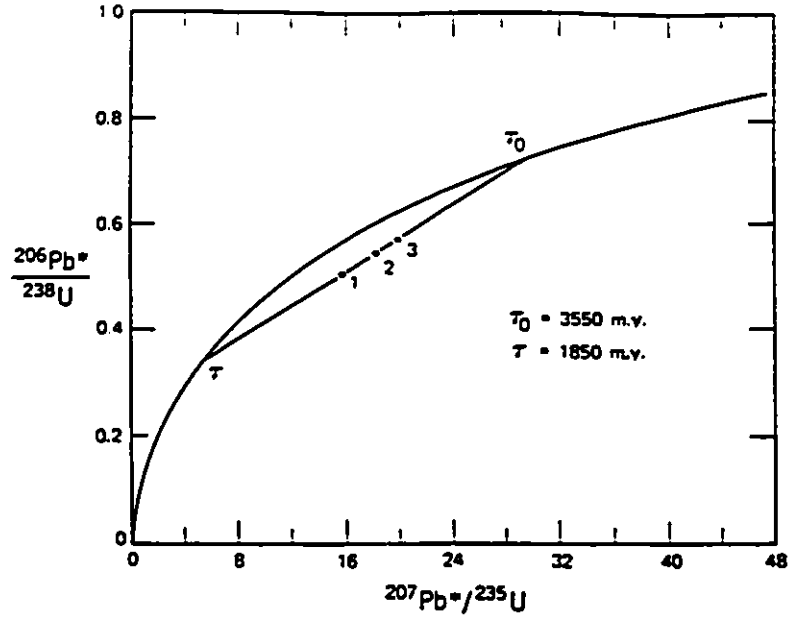


**Fig. 3.2.** An example of the concordia diagram. The curve is called concordia, data point are 1,2,3; the chord is called discordia, and the intercepts are ages (after Faure, 1986).

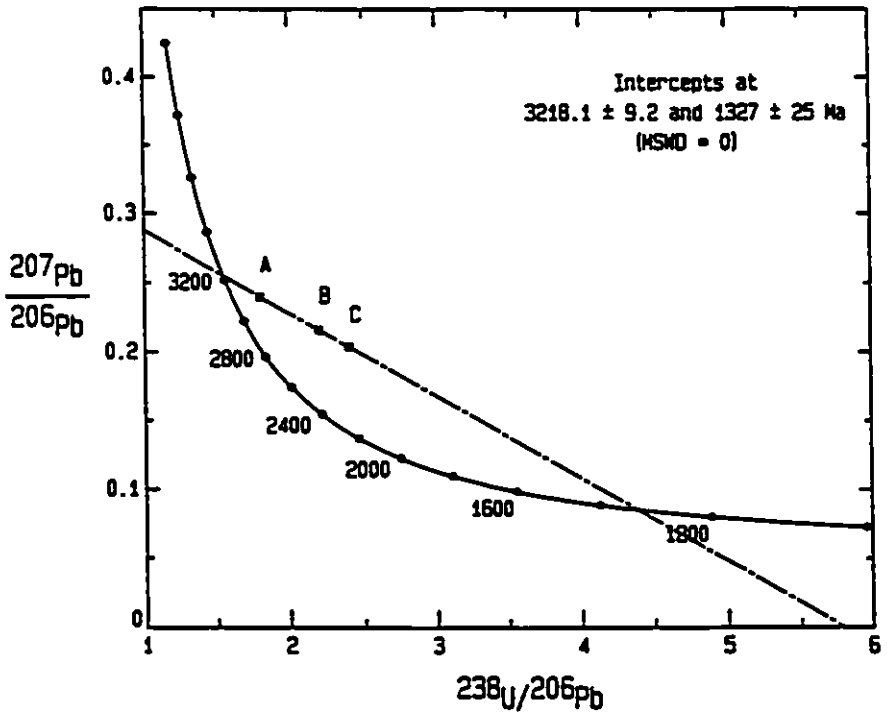


**Fig. 3.3.** The Tera-Wasserburg concordia diagram (from simulated data).

behaviour. However, if the system has been open, the U-Pb ratio for that sample will not fall on the concordia curve, and the ages are discordant.

Generally, most rocks or minerals are not totally closed systems and in the U-Pb system the loss of some lead (or gain of uranium) is likely. Zircon crystals may lose varying fractions of their radiogenic lead even though all of them experienced the same set of conditions. Therefore, it is often possible to recover several zircon fractions from a single rock sample, these date points plot below the concordia and are collinear (Fig. 3.2). The line is called " discordia ". The intercepts of the discordia with the concordia curve yield two ages, shown on Fig. 3.2 as $\tau_o$ and $\tau$. $\tau_o$ represents the time elapsed since original crystallization, point $\tau$ represents the time elapsed since closure of the mineral system following a period of time in which the system experienced an episodic or continuous lead loss. The lead loss in a rock or mineral system may happen at any time between time $\tau_o$ and $\tau$. It seems to be related to the size of the zircon crystals, to their uranium concentrations, and to the radiation damage in the crystals. Smaller crystal grains and those having high uranium concentrations may suffer greater lead losses than larger grains or those containing less uranium.

Several models have been developed to explain the lead loss. These models are discussed below :

## The Pb-loss models

### Episodic Pb-loss model

This model, developed by Wetherill (1956), is the simplest. Lead is lost in a period

of time that is much shorter than the total time since crystallization. The episodic events that cause the Pb-loss in the zircons, or any other U bearing mineral, can be caused by metamorphism or chemical weathering. The lower intercept of discordia with the concordia is the age of the episodic lead loss. Fig. 3.4 shows a concordia diagram with intercepts at 500 Ma and 2700 Ma. This diagram means that the rock crystallized at 2700 Ma. The zircons evolved through time along the concordia curve until the Pb-loss event at 500 Ma ago, which partially reset the age. After this Pb-loss event, however, the system was again closed, and the zircons continued to evolve along the concordia curve until the present time.

For this episodic Pb-loss model, the lower intercept has to have a geological meaning, and sometimes it dose. For example, in Fig. 3.4, if the 500 Ma event is a known tectonic or metamorphic event in the study area then the lower interecept has a geological means. However, if in the given region there is no geological evidence for a metamorphic type of event then this model is invalid, and another explanation is needed, and hence the continuous diffusion model was developed.

The continuous diffusion model

This model was proposed by Tilton (1960). It treats the Pb-loss as a continuous rather than episodic process. Tilton (1960) observed that for a set of 16 minerals from five continents having $^{207}Pb/^{206}Pb$ ages greater than 2300 Ma, a discordia line with intercepts at 2800 Ma and 600 Ma existed. If the discordia line can be explained by the episodic Pb-loss model, the lower intercept would imply that there was a worldwide metamorphic event 600 Ma ago, but there is no evidence for this. Tilton's model proposes continuous diffusion of lead from the crystal at a rate which is governed by the diffusion coefficient "D", the

effective radius of the mineral "a" and the concentration gradient. A differential equation can be used to estimate the amount of diffusion from a given mineral over time was derived by using Fick's law. The 2800 Ma - 600 Ma discordia line can be explained if the Pb-loss was continuous since time of formation. An example of a continuous diffusion discordia line is shown in Fig. 3.4. In the model, the discordia line is linear until it approaches the origin, then becomes non-linear. The upper intercept obtained from the extrapolation of the discordia still represent the original age of crystallization, but the lower intercept will has no geological significance.

The dilatancy model

This model was proposed by Goldich and Mudrey (1972). It is based on the fact that minerals such as zircons suffer radiation damage due to the alpha-decay of U and Th and their daughter atoms, and the extent of the radiation damage of the minerals increases with their age and the amount of U and Th in them. Goldich and Mudrey (1972) suggest that radiation damage would lead to the formation of micro-capillary channels that permit water to enter the crystal, this water would be very tightly held until uplift and erosion reduced the pressure on the minerals resulting in release of the capillary water together with dissolved radiogenic Pb.

According to this model, the loss of radiogenic Pb is related to uplift and erosion of rocks in a given region, and lower concordia intercept is the age of that uplift and erosion. This is still an episodic loss but the episode is not a metamorphic event.

Multiple stage Pb-loss situation

The above three models are so called single Pb-loss models. In some cases, the

U/Pb ratios obtained from samples are so complicated that no single Pb-loss model discussed above can explain the observed ages. Minerals may have suffered more than one single stage of Pb-loss. For example, in the time span from 2700 Ma to 500 Ma, the minerals may have suffered a metamorphic event, a dilatancy Pb-loss event and a continuous diffusion loss of Pb. In addition, there may also be loss of intermediate daughter elements (eg. $^{222}Rn$). All of which can make the interpretation of such a date impossible or at least highly speculative.

### Loss of intermediate daughter products

The decay of U to Pb produces a number of intermediate daughter elements, Radon is one of them. Radon, being a gas, may be more prone to leakage rather than a solid intermediate daughter product. Radon has two isotopes, $^{222}Rn$ and $^{219}Rn$, half lives are 3.8 days and 3.9 seconds, respectively. Loss of radon would be most likely from $^{222}Rn$ which is in the $^{238}U \rightarrow {}^{206}Pb$ decay series. That would decrease the $^{238}U/^{206}Pb$ value on the concordia plot and data points would translate vertically down on the concordia (Fig. 3.4). The effect of radon loss would be such that on a concordia diagram, data points would not be collinear, thought it is possible they may show a linear relation depending on the original disposition of the points and the amount of radon loss.

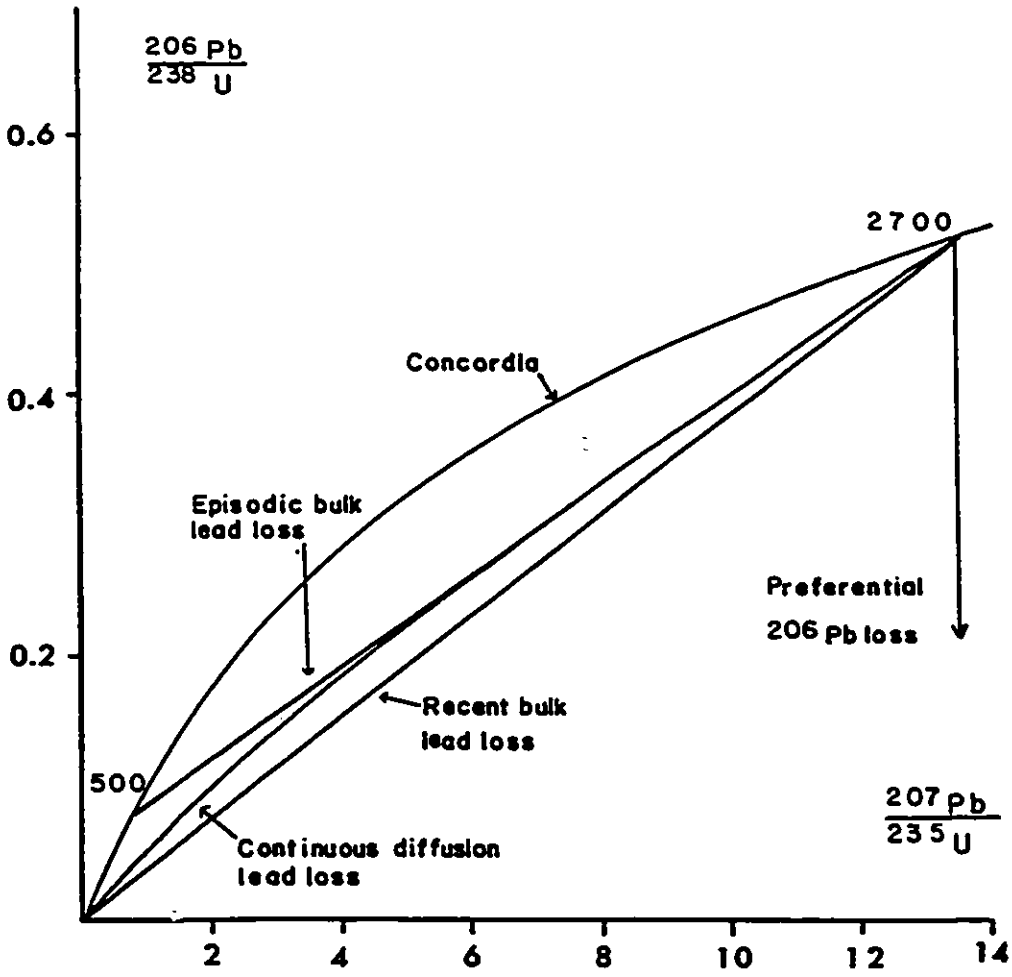


Fig. 3.4. Concordia diagram showing the various models of Pb loss (Doe, 1970).

# CHAPTER IV

# ANALYTICAL PROCEDURE

## Sample preparation

In the field, fresh and unweathered samples of approximately 30-50 kg each were collected. In the laboratory, they were then crushed using a Chipmunk jaw crusher to about 1 cm fragments. This was then reduced to a powder of -70 Tyler mesh size using the Braun pulverizer. This powdered rock was then processed using the Wifley table to concentrate the heavy minerals. The typical heavy mineral concentrate taken off the table would be 500-1000 ml in volume. After drying the sample was sieved through a -60 Tyler mesh screen, coarse material present, if any, was discarded. Strong magnetic minerals were removed by a hand magnet and discarded. The rest of the sample was sorted magnetically using the Carpco induced roll magnetic separator, with the magnetic fraction again being discarded. The non-magnetic portion was then processed by gravity separation using heavy liquids. Ethylene tetrabromide (SG = 2.96) removed the feldspars and quartz while methylene iodide (SG = 3.10) removed most of the mafic minerals. The heavy liquid concentrate contains zircons (SG = 4.7) plus some mafic minerals, apatite, sphene, sulphide, etc. At this stage, the concentrate was usually boiled in 50% $HNO_3$ which dissolves the sulphide and any other soluble minerals. This zircon concentrate is further refined by using the Frantz isodynamic separator.

At this stage, this heavy non-magnetic concentrate should be all zircons except for some extraneous grains and composite grains. However, the quality of the zircons is variable and it is necessary to remove the altered grains and any composite grains. To do this

the sample was sieved via nylon screens into a series of size ranges using 70, 100, 200, 325 Tyler mesh nylon screens. The different fractions (-70+100, -100+200, -200+325, -325) are then sorted according to their magnetic susceptibility using the Frantz isodynamic separator by changing the inclination of the magnet. The best quality zircons are the totally non-magnetic ones and also the smallest grain size fractions.

The above sequence of steps is somewhat generalized. In many instances, the order of the separation steps may be changed as well as additional steps may be required. Frequently at this stage samples may be abraded (Krogh, 1982) or recrushed in an agate mortar to remove any adhering mineral coating and surface alteration.

Hand picking to remove extraneous and altered grains was done under a binocular microscope with the zircons immersed in ultrapure ethanol. Selected samples were then repeatedly washed for about 3 hours in 25% $HNO_3$ and ultrapure water.

From this point onwards the samples were kept in a very clean lab where the air is filtered through HEPA filters. This is done to exclude any Pb contamination even from the air.

### Sample dissolution and ion separation

All reagents used in the dissolution and separation were ultrapure. They have been triple distilled in teflon (Mattison, 1972). The pressure bombs and beakers are also made of teflon (TFE or FEP) which have been extensively cleaned. All the chemistry was done in positive flow clean air hoods to prevent contamination by Pb present in air.

The zircon samples were weighed out into teflon pressure bombs. A desirable amount of sample is 1-2 mg, but may be as small as one grain. To dissolve the zircons 0.5 ml concentrated HF and 1 drop of concentrated $HNO_3$ was added to the bome. The pressure bombs were assembled and heated at 195°C for 7 days. They were disassembled, samples were evaporated to dryness and converted to a chloride by adding 0.5 ml of 6N HCl and heated again in the pressure bombs for 1 day. After this, samples are ready for spiking and ion exchange.

The 0.5 ml sample was usually aliquoted into 0.3 ml for an IC (isotope composition) sample run, and 0.2 ml for the ID (isotope dilution) sample run. The IC sample is for measurement of isotope ratios while the ID sample is for determination of concentration of U and Pb isotopes. To the weighed portion of the ID sample is added a known quantity of the mixed $^{208}Pb$-$^{235}U$ tracer or spike. Both aliquots are dried down, taken up in either 3N (for ID) or 1N (for IC) HCl and loaded onto micro ion exchange columns containing 0.5 ml of Dowex AG1-X8 200-400 mesh anion exchange resin. The detailed procedure for this is given in Appendix B. Once off the columns the samples are taken to dryness.

The Pb and U samples are loaded onto cleaned and outgassed Re ribbon filaments for analysis on the mass spectrometer. The sample is taken up with 1 $\mu$l of 1/4 N $H_3PO_4$ and 1 $\mu$l of silica gel which act as binding agents between the Re and the Pb and U.

## Mass spectrometry

In the determination of U-Pb ages, as currently done in this laboratory, three mass spectrometer runs are required on the two (IC and ID) aliquotes of the sample.

On the IC sample, the following Pb ratio are measured: $^{208}Pb/^{206}Pb$, $^{207}Pb/^{206}Pb$, $^{204}Pb-/^{206}Pb$. These ratios give the isotopic composition of the Pb in the zircon sample. They vary from sample to sample depending on the amount of initial Pb incorporated at the time of crystallization plus the amount of Pb isotopes, $^{206}Pb$, $^{207}Pb$, $^{208}Pb$, that was produced by the decay of U and Th present in the zircon sample. On the other hand, the isotopic composition of U is constant, presently the ratio of $^{235}U/^{238}U$ is 1/137.88. (Steiger and Jäger, 1977).

The ID sample, as processed above, contains both U and Pb plus the added [$^{235}U$] and [$^{208}Pb$] of the tracer. Two mass spectrometer runs are done on this ID sample. The Pb ID run is done first to measure the $^{208}Pb/^{206}Pb$ ratio. The filament current is then turned up to increase the temperature for U to vaporise and the $^{235}U/^{238}U$ ratio is measured. From these two ratios and the IC ratios, the abundance of each isotope may be calculated. However, for practical reasons, the important quantities are the ratios : $^{207}Pb/^{235}U$, $^{206}Pb/^{238}U$, $^{207}Pb/^{206}Pb$, as they yield the three ages of the U-Pb system. The $^{204}Pb/^{206}Pb$ ratio is also important in that it is used to correct for the common Pb present at the time of crystallization, this is a small correction. The isotopic composition of this inherited Pb can be directly measured by measuring the Pb isotopic composition in the feldspar from the same rock, however, for Precambrian rocks the usual practice is to correct for common Pb using an equation developed by Stacey and Kramers (1975).

Isotope ratio measurements on mass spectrometers have to be corrected for mass fractionation and mass discrimination. In U and Pb work, this is done by determining a fractionation factor based on the measured versus the certified value on NBS (National Bureau of Standards) Pb isotope standards. For the mass spectrometer in this laboratory, the

fractionation (and mass discrimination) correction has been determined as 0.01% per a.m.u. (atom mass unit), and has been used throughout this study. Correction for blank, which in this laboratory has been determined as 0.08 ng, $^{206}Pb$ and $^{235}U$, was also made. The composition of that blank was taken as: $^{206}Pb/^{204}Pb = 18.7$, $^{207}Pb/^{204}Pb = 15.7$ and $^{208}Pb/^{204}Pb = 38.4$, which corresponds to modern Pb found in laboratory reagents.

Once the critical U and Pb ratios of the sample have been calculated. The absolute ages can be calculated as well as the concentration of U and Pb based on the equations shown in the previous chapter of this thesis. These calculations have been done using existing computer programs in this laboratory. The preferred treatment of the U-Pb data is to plot the results on concordia diagrams and to determine the upper and lower intercepts on the plot. In this thesis, the concordia plots were evaluated using the statistical procedure and computer program developed by Ludwig (1992). The input $2\sigma$ errors used in the Ludwig regression were 1% in both the $^{207}Pb/^{235}U$ and $^{206}Pb/^{238}U$ with a correlation between them of 0.98. The regression uses a weighting so that the more concordant point has more influence on the regression than a discordant point. It also calculates a probability of fit, which is a measure of the goodness of fit of the data points. A probability of 15% or greater means that the fit of the points is within experimental error. Less than 15% indicates presence of a geological error.

In this study, all errors reported for the ages are 95% confidence limits, unless otherwise stated. The decay constants used in this study are: for $^{235}U$, $\lambda^{235} = 9.8485 \times 10^{-10} yr^{-1}$, for $^{238}U$, $\lambda^{238} = 1.55125 \times 10^{-10}\ yr^{-1}$ (Steiger and Jäger, 1977).

In the course of this study, standard samples were measured. The NBS Pb isotope standard was measured and is shown in Table 4.1. Several samples were also re-run here on this mass spectrometer that were previously run on an extended geometry VG Sector mass spectrometer at the University of Kansas. These results are shown in Table 4.2., and attest to the high quality of results being reported in this thesis.

## Mass spectrometer data smoothing technique

In the course of this study, a technique for smoothing the mass spectrometer voltmeter signal has been developed. Fig. 4.1 and Fig. 4.2 shows the procedure to calculate an isotope ratio. Magnet peak switching is done automatically by a dedicated computer. The readings taken are 10 s on peak and background with a 5 s delay for the magnet to resettle. To measure the $^{208}Pb/^{206}Pb$ ratio (Fig. 4.1.), readings are taken on zero (mass 206.5), mass 206, 208, 206 and zero again. After subtracting the zero (it is always kept as a positive reading), the average of the 206 readings is divided by the 208 peak reading to get the ratio of $^{206}Pb/^{208}Pb$. Ten similar comparisons are made. If a ratio is out of line, usually outside the $2\sigma$ error limit, that whole data set is rejected. Fig. 4.1 shows two signal spikes on mass 206 and 208, which means that these two sets of data would be rejected. However, that spike occurred in a fraction of a second, and because of that, three readings of 10 s each have to be rejected. The peak signal is an average of 10 one second readings. Each one second reading is an integration of 15,000 readings. If only one of these readings is in error, the whole set of three peaks would have to be rejected.

**Table 4.1.** Isotope ratios measured on NBS standard Pb sample

| | $^{208}Pb/^{206}Pb$ | $^{207}Pb/^{206}Pb$ | $^{204}Pb/^{206}Pb$ |
|---|---|---|---|
| certified value | 2.1681±0.0008 | 0.91464±0.0003 | 0.05904±0.00037 |
| Run 605 | 2.1664±0.0006 | 0.9140 ±0.0004 | 0.05922±0.00003 |
| Run 642 | 2.1692±0.0014 | 0.91498±0.00079<br>0.91533±0.00031 | 0.05887±0.00008 |
| Run 981 | 2.1677±0.0011 | 0.91492±0.00067 | 0.05839±0.00002 |
| Run 982 | 2.1677±0.0008 | 0.91478±0.00026 | |

**Table 4.2.** Comparison of isotope ratios measured on two mass spectrometers

| | $^{208}Pb/^{206}Pb$ | $^{238}U/^{235}U$ |
|---|---|---|
| Zircon 02-89-9C | | |
| at Windsor | 2.70114±0.001%(1)<br>2.69827±0.0005%(2) | 0.10343±0.00005%(2)<br>0.10349±0.00010%(2) |
| at Kansas | 2.70378±0.006%(2) | 0.10323±0.00010%(1)<br>0.10396±0.06%(2) |
| Zircon 02-89-9D | | |
| at Windsor | 3.3237±0.004%(1)<br>3.3237±0.001%(2) | 0.08984±0.0002%(2) |
| at Kansas | 3.3248±0.01%(2) | 0.08942±0.03%(2) |

Note: (1) 1 V beam ; (2) 300 MV beam ; errors are %SD.

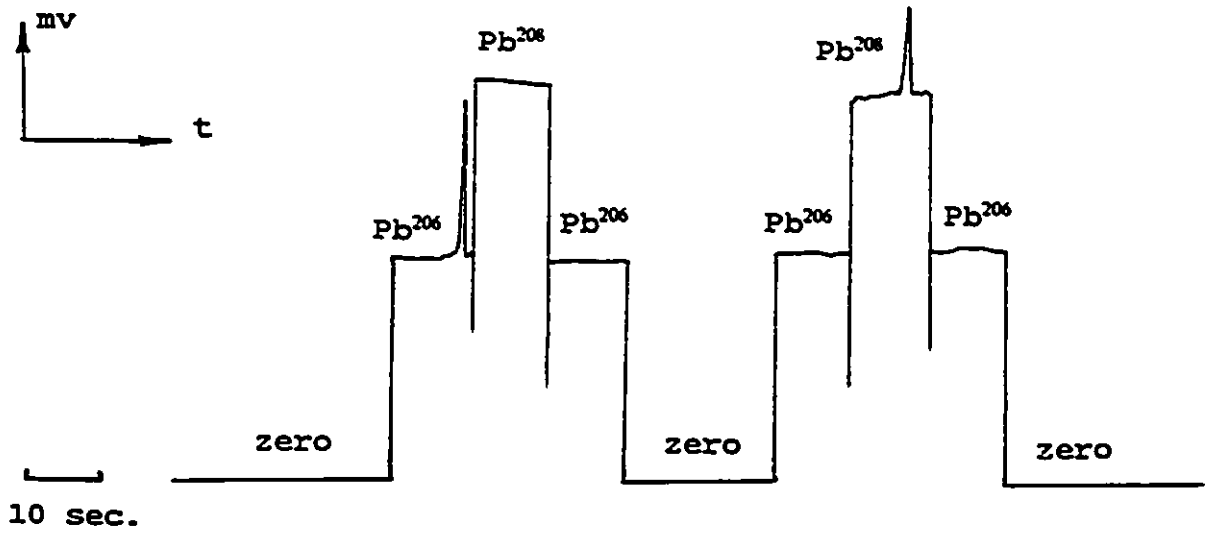


Fig. 4.1. Two sets of the mass spectrometer data obtained for ID Run No. 707, showing a resonably stable signal with spikes.

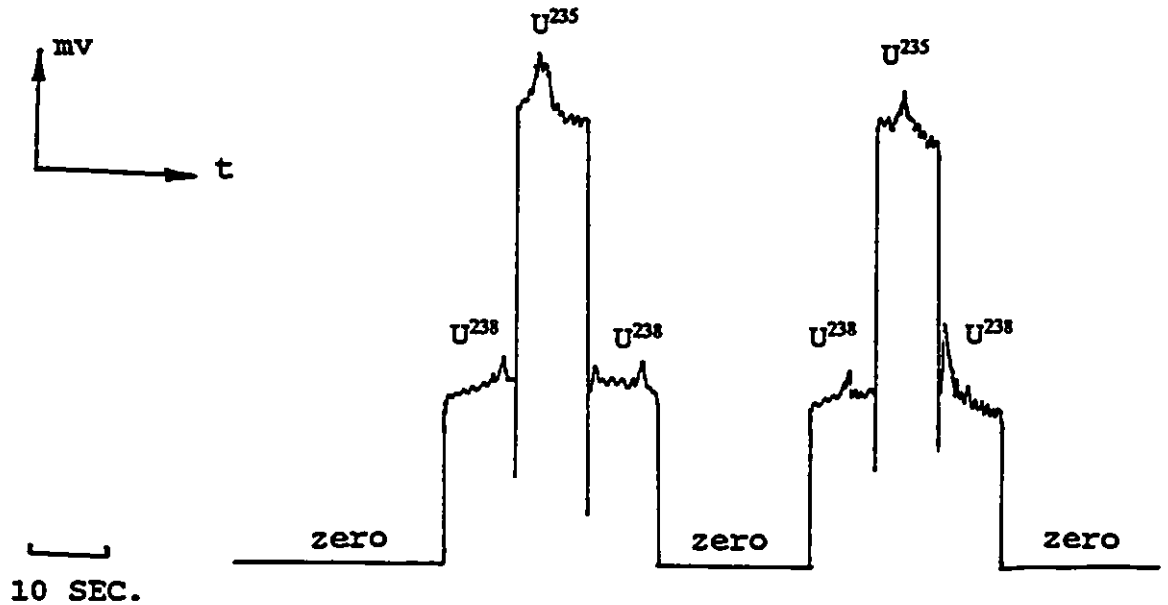


Fig. 4.2. Two sets of the mass spectrometer data obtained for ID Run No. 759, showing a fluctuating beam with high noise.

The program developed here can delete an erroneous reading in such a way that the rest of the data is usable and the data for the three peaks (1 ratio set) are salvageable. To do this, the program examines the 10 one second numbers, if one of these is outside the statistical width ($2\sigma$ error), it is rejected and thus the average data for the other 9 one second reading are used. The beam, in 10 s, can be rising or falling as well as being very noisy (Fig. 4.2); in this case, an average value cannot be used for rejection purposes. Therefore a regression line is calculated for the 10 one second readings and any value outside the limits of the regression is rejected. The midpoint values of the regression lines for the 3 peaks are used to calculate the isotope ratio. The flowchart for this computer program is given in Fig. 4.3.

To use this smoothing technique, the mass spectrometer run is the same as usual, results are printed in real time, but all the raw digital volt meter data are also saved on disk. After completion of the run, that data file is processed offline. The experience with the use of this method is that when the beam is very stable there will be few or even no rejections with this regression smoothing. However, if the beam is noisy, the regression may produce a slightly different mean value compared to the averaging method, but most importantly the standard error for the ratio will be lower. Fig. 4.2 shows a very noisy beam for which data would not be taken until the signal had stabilized. Using the regression smoothing technique, data can be collected and will yield the right ratio with an acceptable error. The value of this regression smoothing is that data can be collected sooner; also in some situations when a run would be aborted because of a noisy sample or low signal, that run can be salvaged.

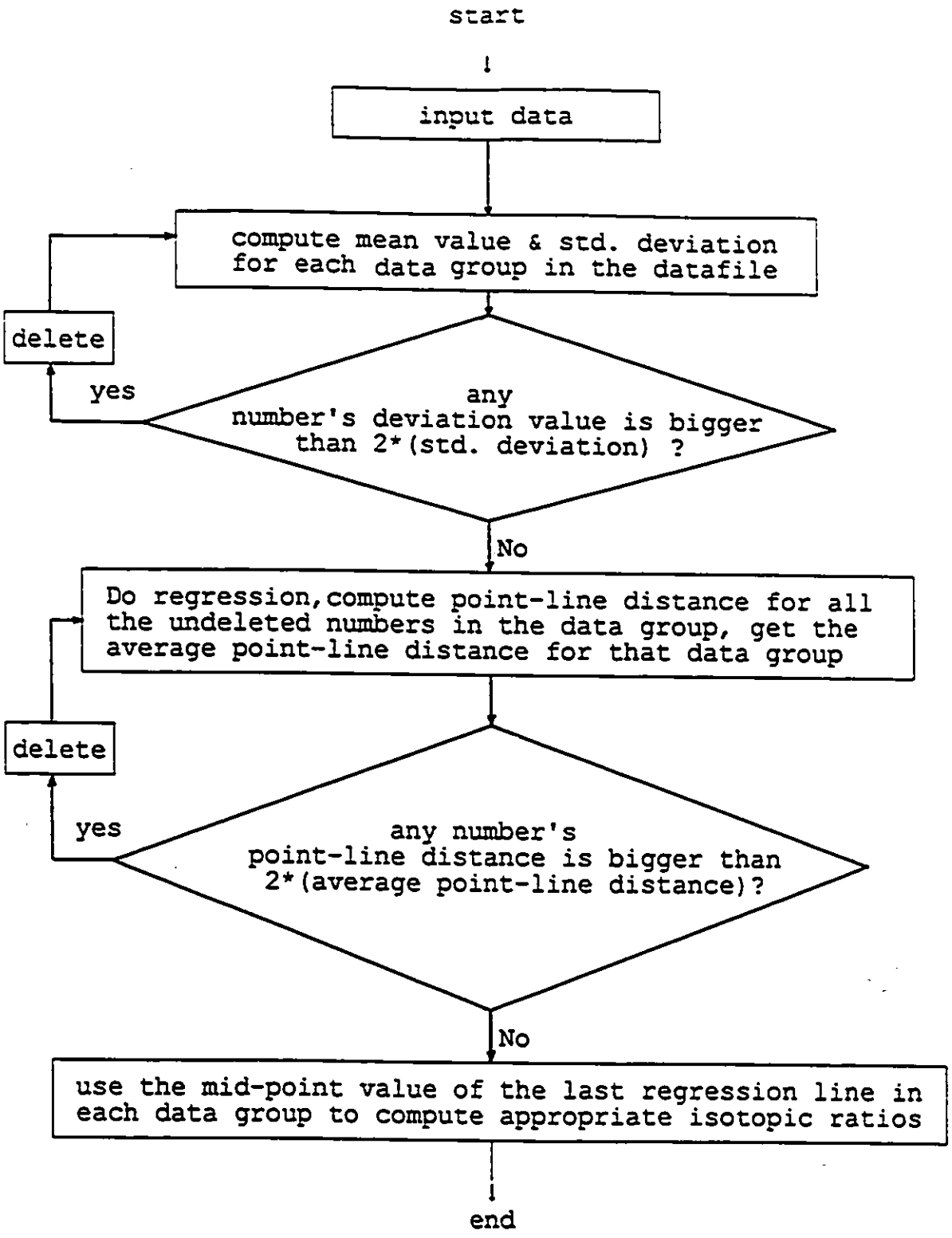


**Fig. 4.3.** The flowchart for the data processing program.

An example of the data processing result using this data smoothing technique is shown in Appendix C.

This technique was developed independently in this laboratory, however, the Australia National University (A. Turek pers. com.) laboratory has also devised a similar data smoothing procedure.

# CHAPTER V

# ANALYTICAL RESULTS

This thesis reports U-Pb ages for 8 rock units based on a total of 45 zircon fractions and 2 titanite fractions analyzed. The location of the samples is shown in Fig. 2.2. and also given in Appendix A, together with sample descriptions, photomicrographs and scanning electron micrographs of the zircons. The analytical results are given in Tables 5.1 and 5.2 and shown as concordia plots (conventional and others) in Figures 5.1 to 5.14, all of which have been put at the end of this chapter.

The rock units dated are as follows :

**Lac du Bonnet batholith (MA-17) — 2660.1 ± 3.1 Ma**

**Pointe du Bois batholith (MA-21) — 2729 ± 8.7 Ma**

**Maskwa Lake batholith I (MA-10) — 2725.1 ± 5.5 Ma**

**Maskwa Lake batholith II (MA-23) — 2782 ± 11 Ma**

**Bird River sill (MA-3) — 2744.7 ± 5.2 Ma**

**Diorite stock (MA-6) — 2715 Ma (metamorphic age)**

**Gabbro/Diorite (MA-26) — 2844 ± 12 Ma**

**Peterson Creek volcanic tuff (MA-4) — 2740.2 ± 3.6 Ma**

## Lac du Bonnet batholith (MA-17)

The sample collected from this body is a quartz monzonite. The zircons in this rock are of good quality, euhedral to sub-euhedral, elongate (length:width, 4:1), transparent. Colour ranges from colourless through white to brown. Five fractions were selected (Table

5.1 and 5.2, Fig.5.1). Fraction B is brown in colour, the other fractions are light coloured and transparent, fractions D and E were strongly abraded. Four of the 5 fractions are collinear and define a discordia with intercepts of 2660.1 ± 3.1 Ma and 91 ± 22 Ma which is interpreted as the age of the rock. It is a model 1 regression with a probability of fit of 15%, hence it is within experimental error. The data points are 11% to 39% discordant. The minimum $^{207}Pb/^{206}Pb$ age is 2654 Ma.

Point B lies to the right of the discordia which implies an older component age, its $^{207}Pb/^{206}Pb$ age is 2672 Ma. This fraction is brown in colour and also has a low $^{208}Pb/^{206}Pb$ ratio (Table 5.1) relative to the other 4 fractions, and has been excluded from the regression.

### Pointe du Bois batholith (MA-21)

This sample collected is a foliated tonalite. Zircons separated from this rock are pastel brown in colour, transparent, euhedual, and are elongate (length:width, 6:1) with short pyramid terminations. There are very few fractures present and they tend to be transverse. One of the fractions, D, was strongly abraded. All 4 fractions plot on a straight line within experimental error (Table 5.2 and Fig. 5.2). They are 12% to 21% discordant. The indicated age is 2729 ± 8.7 Ma with a lower intercept of 829 Ma. It is a model 1 age with a probability of fit of 51%.

### Maskwa Lake batholith I (MA-10)

Zircons separated from a quartz monzonite from this batholith were very impure with strongly adhering feldspar and other mineral coatings. They were crushed by hand in an agate mortar then abraded, sieved, and reprocessed using methylene iodode and the Frantz

magnetic separator to obtain a clean separate. Nevertheless the quality of the zircons isolated is poor, they are clear to brown, subhedral, short crystals (length:width, 2:1). Fraction D, F, G, K were in addition strongly abraded. The 5 fractions analyzed are 17% to 33% discordant (Table 5.1 and 5.2, Fig. 5.3), but they do define a discordia within experimental error, the fit is a model 1 age with a probability of fit of 60%. The concordia intercepts are 2725.1 $\pm$ 5.5 Ma and 405 Ma. The minimum $^{207}Pb/^{206}Pb$ age is 2695 Ma.

### Maskwa Lake batholith II (MA-23)

This is a granodiorite from the northern part of the Maskwa Lake batholith. Five zircon fractions were selected from this sample (Table 5.1 and 5.2, Fig 5.4). A model 1 age of 2782 $\pm$ 11 Ma with a lower intercept of 709 Ma and probability of 33% is given by the five zircon fractions. The zircons from this sample are of good quality. They are brown to colourless, euhedual to sub-euhedual, most of the zircon grains are short (length:width, 2:1). Fraction C is abraded. Fraction E is handpicked. The discordance is 19% to 33%. The minimum $^{207}Pb/^{206}Pb$ age is 2727 Ma.

### Bird River sill (MA-3)

A gabbro sample from the chromite bearing band in this sill was found to contain good quality zircons. These zircons are clear and euhedual, slightly pink to light brown in colour. The fine (-325) grains tend to be pink while the large (>100) grains tend to be brown and show minor zoning. The three fractions, all handpicked, are 1% to 6% discordant. The indicated concordia age is 2744.7 $\pm$ 5.2 Ma with a lower intercept age of 452 Ma. The minimum $^{207}Pb/^{206}Pb$ age is 2743 Ma (Table 5.1 and 5.2, Fig.5.5).

### Diorite stock (MA-6)

This small stock, that is thought to be a subvolcanic unit, was found to contain a light brown euhedral sphene. Two fractions analyzed have $^{207}Pb/^{206}Pb$ ages of 2698 Ma and 2715 Ma. The latter is concordant, and is interpreted as metamorphic age (Table 5.1 and 5.2, Fig. 5.6).

### Gabbro/Diorite (MA-26)

Geological maps of the area by Davies (1952) and Kowerchuk and Weber (1987) but not Springer (1948) show a 6 × 2 km east-west gabbroic band to the west of Lake Oiseau as an offset of the Bird River sill. Sample collected from this unit, based on thin section examination is a granodiorite. Zircons separated from this sample are of good quality, euhedral to subhedral, elongate (length:width, 4:1), clear, amber, brown in colour, transparent to translucent. Seven fractions were analyzed, two were strongly abraded. The discordance is 17% to 28%. The data (Table 5.1 and 5.2, Fig. 5.7) show scatter.

The minimum $^{207}Pb/^{206}Pb$ age is 2832 Ma, and the average of the $^{207}Pb/^{206}Pb$ ages of the 7 fractions is 2813 Ma. Several judicious selections of data points were considered based on various morphological similarities or other group features. But some attempts produced negative lower intercepts or too young an age. The following are three of the attempts:

a) Regression of all 7 data points gives intercepts of 2779 ± 61 Ma and -445 ± 844 Ma (Fig.5.7).

b) Regression of points B, C, G gives intercepts of 2759 ± 11 Ma and -718 ± 182 Ma; the excluded 4 points plot above and below the discordia (Fig.5.8).

c) Regression of points A, D, B, E gives concordia intercepts of 2844 ± 12 Ma and 385 ± 100 Ma; the excluded 3 points are to the right of the discordia implying existence of an older component (Fig. 5.9).

At this stage perhaps the most logical interpretation is that the rock is certainly older than 2813 Ma, the average of the $^{207}Pb/^{206}Pb$ ages; and the scatter is due to an inherited older component. Hence, the 2844 ± 12 Ma, regression of 4 points (as above) is the best interpretation of the concordia plot; the other two interpretations can not be valid as they have negative lower intercepts.

There are still other possible explanations for the observed scatter. Such as radon loss or multiple loss of Pb. These are very rare occurrences and are not well documented, and are not considered likely in view of the good quality of the zircons.

A plot of $^{207}Pb/^{206}Pb$ vs $^{238}U/^{206}Pb$, the Tera-Wasserburg concordia diagram (Fig. 5.10) shows the points plotting on an almost horizontal line which can indicate a modern loss of Pb (or gain of U), as well as presence of an older component (Geyh and Schleicher, 1990).

### Peterson Creek volcanic tuff (MA-4)

The sample collected is a lapilli tuff. The zircons separated are of poor quality with extensive alteration. Again the zircons were reprocessed (cf. MA-10) by hand crushing in an agate mortar, abrasion, sieving, and heavy liquid separation. The zircons are generally euhedual, they are pink, white, brown, transparent to opaque. Under polarizing microscope alteration is very pronounced. A total of 12 fractions was analyzed (Table 5.1 and 5.2) and as is evident from the concordia plot (Fig. 5.11 to 5.14) the data points scatter. They are

from 3% to 30% discordant. Point AA is almost within error of the concordia and has a $^{207}Pb/^{206}Pb$ age of 2740 Ma. An error on a single fraction analysis can be calculated as ± 3 Ma ($2\sigma$). The only discordia that can be drawn within experimental error to give an age about 2740 Ma is through points AA and E, which would give intercepts 2740.2 ± 3.6 Ma and 134 ± 54 Ma. The remaining 10 points all plot above the discordia (Fig. 5.11). The failure of the 10 points can be attributed to effects of alteration. Other possible interpretations of the data are :

a) Regression of points AA, B, A, I, K, J, E, F gives intercepts of 2734 ± 15 Ma and 234 ± 229 Ma. Points C, D, H, G plot above the regression line, which can be caused by alteration (Fig. 5.12). This age of 2734 ± 15 Ma is not significantly different from the minimum age of 2740.2 ± 3.6 Ma at the 5% level of significance..

b) Regression of points AA, C, D, G, H gives intercepts of 2753 ± 11 Ma and 1189 ± 126 Ma. Points A, B, I, J, K plot below the regression line (Fig. 5.13). This implies presence of an older component, which is difficult to envisage for a volcanic rock. It also produces a high lower intercept which too is also difficult to accept. Loss of radon can not be invoked as the mechanism for the points falling below the line as this would produce older than 2740 Ma $^{207}Pb/^{206}Pb$ ages.

The interpretation of 2734 ± 15 Ma age as per a) above is a strong possibility. But seeing point AA is virtually concordant and alteration of the zircons is present, I feel the age of 2740.2 ± 3.6 Ma for this rock is the best interpretation of the current data.

Similar to MA-26, the Tera-Wasserburg concordia diagram for this sample (Fig. 5.14) shows an approximately horizontal linear distribution which in this case can indicate a modern Pb-loss or U gain (Geyh and Schleicher, 1990).

Table 5.1. Analytical data for zircons from the Bird River greenstone belt, southeastern Manitoba

| Sample detail | | | | Concentration (ppm) | | Atomic ratios | | | | |
|---|---|---|---|---|---|---|---|---|---|---|
| Sample No. | Magnetism[1] | Tyler mesh grain size | Weight (mg) | U | Pb | $^{204}Pb/^{206}Pb$[2] | $^{208}Pb/^{206}Pb$[3] | $^{207}Pb/^{206}Pb$[3] | $^{207}Pb/^{235}U$[4] | $^{206}Pb/^{238}U$[4] |
| MA-17 | | | | | | | | | | |
| A | NM1°+M1°,Tr,Hp | -100 +200 | 1.0 | 1495 | 724 | 0.00031 | 0.14997 | 0.18338 | 10.421 | 0.4200 |
| B | NM1°+M1°,Br,Hp | -100 +200 | 0.7 | 1159 | 529 | 0.00022 | 0.08847 | 0.18418 | 10.428 | 0.4154 |
| C | NM3° | -325 | 0.4 | 1462 | 565 | 0.00059 | 0.22283 | 0.18462 | 7.787 | 0.3166 |
| D | M1°,Ab | -200 +325 | 1.8 | 1541 | 820 | 0.00042 | 0.16188 | 0.18508 | 11.327 | 0.4561 |
| E | NM2°,Ab | -200 +325 | 1.4 | 1713 | 827 | 0.00031 | 0.16373 | 0.18376 | 10.300 | 0.4146 |
| MA-21 | | | | | | | | | | |
| A | M1°,Tr | -100 +200 | 0.4 | 1016 | 504 | 0.00026 | 0.08314 | 0.18375 | 11.364 | 0.4539 |
| B | M1°,Br | -100 +200 | 0.6 | 1170 | 599 | 0.00022 | 0.07792 | 0.18562 | 11.882 | 0.4696 |
| C | NM0°+M0° | -100 +325 | 1.3 | 984 | 514 | 0.00006 | 0.07996 | 0.18445 | 12.177 | 0.4799 |
| D | M3°,Ab | -200 +325 | 1.6 | 1462 | 653 | 0.00006 | 0.07870 | 0.17714 | 10.054 | 0.4129 |
| MA-10 | | | | | | | | | | |
| A | NM7°,Cl | -100 +325 | 0.5 | 384 | 187 | 0.00046 | 0.16131 | 0.19053 | 10.641 | 0.4159 |
| B | NM7°,Br | -100 +325 | 5.2 | 527 | 249 | 0.00011 | 0.15264 | 0.18554 | 10.417 | 0.4099 |
| C | NM7°,Br | - 70 +100 | 2.5 | 556 | 256 | 0.00034 | 0.16675 | 0.18729 | 9.949 | 0.3939 |
| D | NM0°+M0°,Ab | -100 +200 | 6.9 | 489 | 244 | 0.00006 | 0.15026 | 0.18470 | 10.986 | 0.4328 |
| E | NM0°+M0° | -200 +325 | 3.2 | 526 | 271 | 0.00014 | 0.15349 | 0.18609 | 11.366 | 0.4465 |
| F | M1°,Ab | -100 +200 | 4.6 | 716 | 316 | 0.00009 | 0.16833 | 0.18153 | 9.458 | 0.3798 |
| G | NM0°,Ab | -100 +200 | 2.6 | 418 | 213 | 0.00007 | 0.15470 | 0.18497 | 11.230 | 0.4415 |
| K | M1°,Ab | -100 +200 | 1.7 | 718 | 310 | 0.00012 | 0.16349 | 0.18158 | 9.280 | 0.3728 |
| MA-23 | | | | | | | | | | |
| A | M0° | -100 +200 | 1.0 | 259 | 136 | 0.00048 | 0.16557 | 0.19111 | 11.534 | 0.4476 |
| B | M0° | -200 +325 | 0.9 | 384 | 208 | 0.00042 | 0.17815 | 0.19210 | 11.893 | 0.4583 |
| C | M1°,Ab | -100 +200 | 1.7 | 569 | 261 | 0.00014 | 0.15251 | 0.18312 | 10.000 | 0.3987 |
| D | NM0° | -100 +200 | 2.2 | 365 | 183 | 0.00016 | 0.14458 | 0.18794 | 11.230 | 0.4366 |
| E | NM0°,Hp | -100 +200 | 1.8 | 443 | 210 | 0.00006 | 0.14408 | 0.18378 | 10.489 | 0.4144 |

Table 5.1. (continued)

| Sample detail | | | | Concentration (ppm) | | Atomic ratios | | | | |
|---|---|---|---|---|---|---|---|---|---|---|
| Sample No. | Magnetism[1] | Tyler mesh grain size | Weight (mg) | U | Pb | $^{204}Pb/^{206}Pb$[2] | $^{208}Pb/^{206}Pb$[3] | $^{207}Pb/^{206}Pb$[3] | $^{207}Pb/^{235}U$[4] | $^{206}Pb/^{238}U$[4] |
| MA-3 | | | | | | | | | | |
| A | NM0°,Hp | -200 +325 | 1.2 | 173 | 138 | 0.00065 | 0.56568 | 0.19048 | 13.752 | 0.5247 |
| B | NM0°,Cl | -200 +325 | 0.8 | 225 | 167 | 0.00009 | 0.48797 | 0.19007 | 13.375 | 0.5121 |
| C | NM0°,Cl | -200 +325 | 1.5 | 266 | 192 | 0.00014 | 0.47249 | 0.19058 | 13.091 | 0.5020 |
| MA-6 | | | | | | | | | | |
| A | NM3°,Cl | -200 +325 | 4.4 | 141 | 86 | 0.00014 | 0.17614 | 0.18846 | 13.326 | 0.5170 |
| B | NM5°,Br | -325 | 3.3 | 46 | 29 | 0.00221 | 0.21295 | 0.20951 | 12.940 | 0.5073 |
| MA-26 | | | | | | | | | | |
| A | NM0°,Br | -100 +200 | 0.9 | 291 | 155 | 0.00029 | 0.12974 | 0.20036 | 12.696 | 0.4641 |
| B | NM0°,Br | -100 +200 | 0.7 | 280 | 141 | 0.00036 | 0.11884 | 0.19961 | 12.007 | 0.4411 |
| C | M0° | -325 | 2.0 | 384 | 190 | 0.00013 | 0.15516 | 0.19964 | 11.639 | 0.4249 |
| D | NM0°,Ab | -200 +325 | 3.2 | 345 | 177 | 0.00017 | 0.12647 | 0.19839 | 12.255 | 0.4490 |
| E | M0°,Ab,Cr | -100 +200 | 1.5 | 304 | 144 | 0.00011 | 0.10119 | 0.19663 | 11.411 | 0.4217 |
| F | M1° | -100 +200 | 1.3 | 199 | 99 | 0.00024 | 0.13871 | 0.20183 | 11.990 | 0.4335 |
| G | M0°,Cl | -200 +325 | 0.5 | 276 | 127 | 0.00024 | 0.14345 | 0.20074 | 11.048 | 0.3992 |
| MA-4 | | | | | | | | | | |
| AA | NM0°-M1°,Ab,Cl | -100 +200 | 3.9 | 63 | 38 | 0.00006 | 0.13914 | 0.19001 | 13.609 | 0.5204 |
| A | NM0°-M1° | -100 +200 | 2.3 | 93 | 53 | 0.00048 | 0.15897 | 0.19410 | 12.598 | 0.4840 |
| B | NM0°-M1°,Cl,Cr | - 70 +100 | 5.6 | 174 | 99 | 0.00033 | 0.16363 | 0.19186 | 12.636 | 0.4876 |
| C | M1°-M2°,Op,Br | - 70 +100 | 5.2 | 932 | 534 | 0.00016 | 0.15857 | 0.18769 | 12.642 | 0.4935 |
| D | M1°-M2°,Op,Wh | - 70 +100 | 6.7 | 1654 | 941 | 0.00016 | 0.15999 | 0.18709 | 12.506 | 0.4898 |
| E | NM0°,Cl | -100 +200 | 1.4 | 142 | 71 | 0.00052 | 0.16131 | 0.19244 | 11.082 | 0.4267 |
| F | M1°,Cl | -200 +325 | 0.7 | 305 | 144 | 0.00025 | 0.15994 | 0.18634 | 10.434 | 0.4080 |
| G | M1°,Ab | -200 +325 | 15.8 | 644 | 350 | 0.00018 | 0.16295 | 0.18405 | 11.737 | 0.4680 |
| H | NM0°+M0°,Hp | -100 +200 | 1.8 | 606 | 342 | 0.00019 | 0.16035 | 0.18651 | 12.373 | 0.4863 |

Table 5.1. (continued)

| Sample detail | | | | Concentration (ppm) | | Atomic ratios | | | | |
|---|---|---|---|---|---|---|---|---|---|---|
| Sample No. | Magnetism[1] | Tyler mesh grain size | Weight (mg) | U | Pb | $^{204}Pb/^{206}Pb$[2] | $^{208}Pb/^{206}Pb$[3] | $^{207}Pb/^{206}Pb$[3] | $^{207}Pb/^{235}U$[4] | $^{206}Pb/^{238}U$[4] |
| I | NM0°+M0°,Hp | -100 +200 | 2.6 | 697 | 390 | 0.00017 | 0.15651 | 0.18882 | 12.454 | 0.4831 |
| J | NM2° | -325 | 3.3 | 443 | 246 | 0.00030 | 0.16713 | 0.19041 | 12.193 | 0.4728 |
| K | NM0° | -200 +325 | 8.3 | 565 | 314 | 0.00015 | 0.16088 | 0.18916 | 12.362 | 0.4784 |

[1]Relative magnetic susceptibility of zircons is reported as M (magnetic) and NM (nonmagnetic) at the indicated inclination of the Frantz isodynamic separator using maximum current of 2 A. Ab, abraded; Hp, hand-picked; Br, brown; Cl, clear; Cr, cracked; Op, opaque; Tr, transparent.

[2]Measured ratio.

[3]Blank corrected.

[4]Blank and nonradiogenic Pb corrected.

Table 5.2. U-Pb age data for zircons from the Bird River greenstone belt, southeastern Manitoba

| Sample No. | Measured ages (Ma) $^{206}Pb/^{238}U$ | Measured ages (Ma) $^{207}Pb/^{235}U$ | Measured ages (Ma) $^{207}Pb/^{206}Pb$ | Concordia ages (Ma) Upper intercept | Concordia ages (Ma) Lower intercept | Remarks[1] |
|---|---|---|---|---|---|---|
| MA-17 Lac du Bonnet batholith | | | | | | |
| A Tr Hp | 2261 | 2473 | 2652 | | | |
| B Br Hp | 2240 | 2474 | 2672 | | | |
| C | 1773 | 2207 | 2638 | | | |
| D Ab | 2423 | 2550 | 2654 | 2660.1±3.1 | 9i±22 | Model 1, P=15% |
| E Ab | 2236 | 2462 | 2654 | | | (Point B is excluded) |
| MA-21 Pointe du Bois batholith | | | | | | |
| A Tr | 2412 | 2554 | 2668 | | | |
| B Br | 2482 | 2595 | 2685 | | | |
| C | 2527 | 2618 | 2690 | 2729±8.7 | 829±71 | Model 1, P=51% |
| D Ab | 2228 | 2440 | 2621 | | | |
| MA-10 Maskwa Lake batholith I | | | | | | |
| A Cl | 2242 | 2492 | 2704 | | | |
| B Br | 2215 | 2473 | 2692 | 2779±64 | 615±325 | Timmins (1985) |
| C Br | 2141 | 2430 | 2682 | | | (Point A,B,and C) |
| D Ab | 2318 | 2522 | 2690 | | | |
| E | 2379 | 2554 | 2695 | | | |
| F Ab | 2076 | 2383 | 2658 | 2725.1±5.5 | 404±38 | Model 1, P=60% |
| G Ab | 2358 | 2543 | 2693 | | | |
| K Ab | 2043 | 2366 | 2658 | | | |

Table 5.2. (continued)

| Sample No. | Measured ages (Ma) $^{206}Pb/^{238}U$ | Measured ages (Ma) $^{207}Pb/^{235}U$ | Measured ages (Ma) $^{207}Pb/^{204}Pb$ | Concordia ages (Ma) Upper intercept | Concordia ages (Ma) Lower intercept | Remarks[1] |
|---|---|---|---|---|---|---|
| MA-23 Maskwa Lake batholith II | | | | | | |
| A | 2384 | 2567 | 2715 | | | |
| B | 2432 | 2596 | 2727 | | | |
| C Ab | 2163 | 2435 | 2670 | 2782±11 | 709±65 | Model 1, P=33% |
| D | 2336 | 2542 | 2712 | | | |
| E Hp | 2235 | 2479 | 2689 | | | |
| MA-3 Bird River sill | | | | | | |
| A Hp | 2719 | 2733 | 2743 | | | |
| B Cl | 2666 | 2707 | 2737 | 2744.7±5.2 | 459±263 | Model 1, P=61% |
| C Cl | 2623 | 2686 | 2735 | | | |
| MA-6 Diorite stock | | | | | | |
| A Cl | 2687 | 2703 | 2715 | | | 2715 Ma Min Age |
| B Br | 2645 | 2675 | 2698 | | | |
| MA-26 Gabbro/Diorite | | | | | | |
| A Br | 2458 | 2657 | 2813 | | | |
| B Br | 2355 | 2605 | 2805 | | | |
| C | 2283 | 2576 | 2815 | | | |
| D Ab | 2388 | 2617 | 2799 | 2844±12 | 385±100 | Model 1, P=65% |
| E Ab Cr | 2268 | 2557 | 2796 | | | |
| F | 2321 | 2604 | 2831 | | | |
| G Cl | 2165 | 2527 | 2832 | | | |

Table 5.2. (continued)

| Sample No. | Measured ages (Ma) $^{206}Pb/^{238}U$ | $^{207}Pb/^{235}U$ | $^{207}Pb/^{206}Pb$ | Concordia ages (Ma) Upper intercept | Lower intercept | Remarks[1] |
|---|---|---|---|---|---|---|
| MA-4 Peterson Creek volcanic tuff | | | | | | |
| AA | 2701 | 2723 | 2740 | | | |
| A | 2545 | 2650 | 2732 | | | |
| B Cl Cr | 2560 | 2653 | 2724 | | | |
| C Op Br | 2586 | 2653 | 2706 | | | |
| D Op Wh | 2570 | 2643 | 2700 | | | |
| E Cl | 2291 | 2530 | 2727 | | | |
| F Cl | 2206 | 2474 | 2702 | 2740.2±3.6 | 134±54 | Regression through point AA and E |
| G Ab | 2475 | 2584 | 2670 | | | |
| H Hp | 2554 | 2633 | 2694 | | | |
| I Hp | 2540 | 2639 | 2716 | | | |
| J | 2496 | 2619 | 2716 | | | |
| K | 2520 | 2632 | 2720 | | | |

NOTES: Decay constants used: $\lambda^{238}U = 1.55125 \times 10^{10}$ year$^{-1}$-1 and $^{235}U = 9.8485$ $10^{10}$ year$^{1}$ (Steiger and Jäger 1977). Error terms of concordia ages are 95 CI.

[1]P is probability of fit as defined by Ludwig (1992).

Refer to Table 5.1 for sample detail.

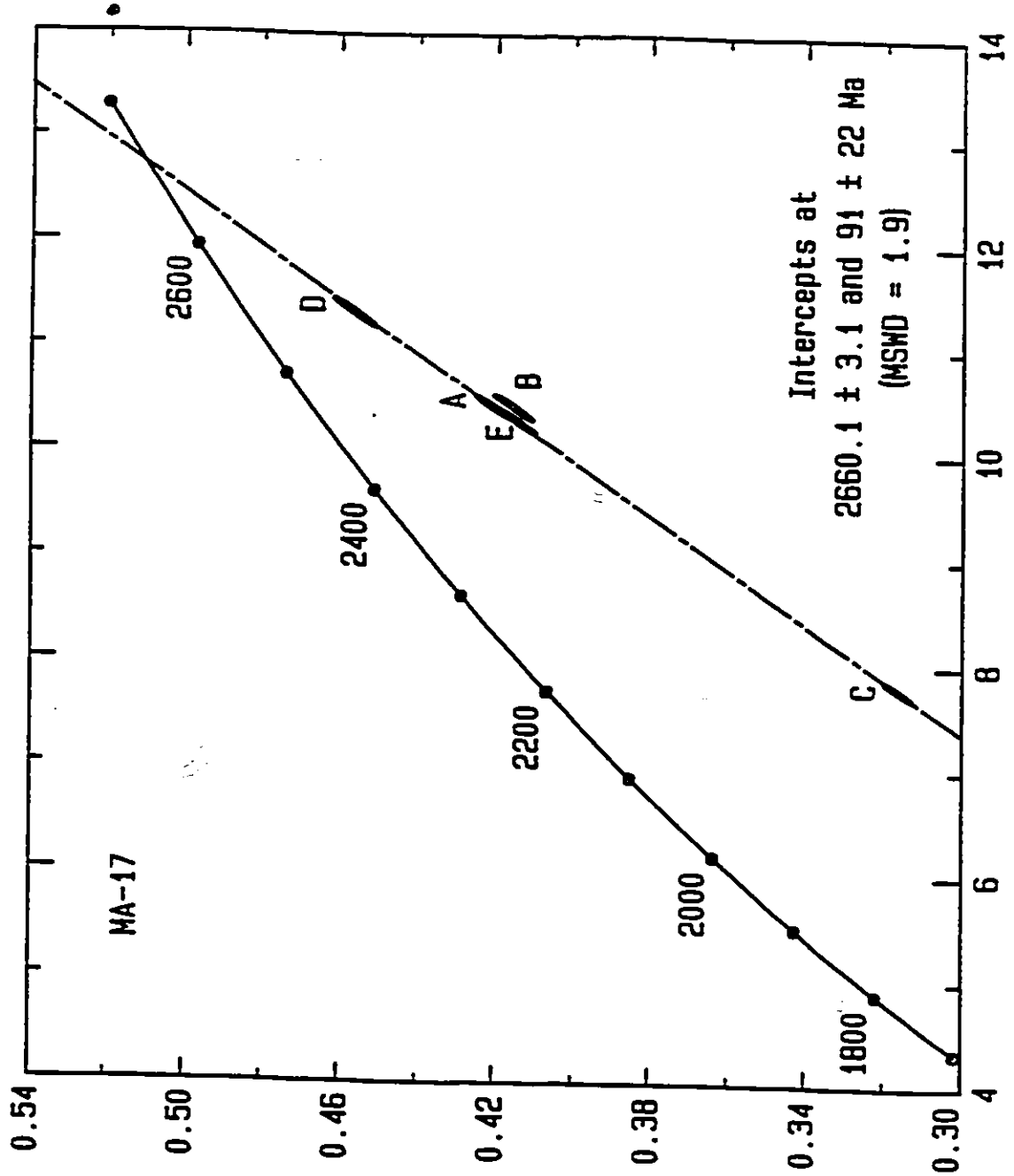


Fig. 5.1. Concordia diagram for Lac du Bonnet quartz monzonite (MA-17).

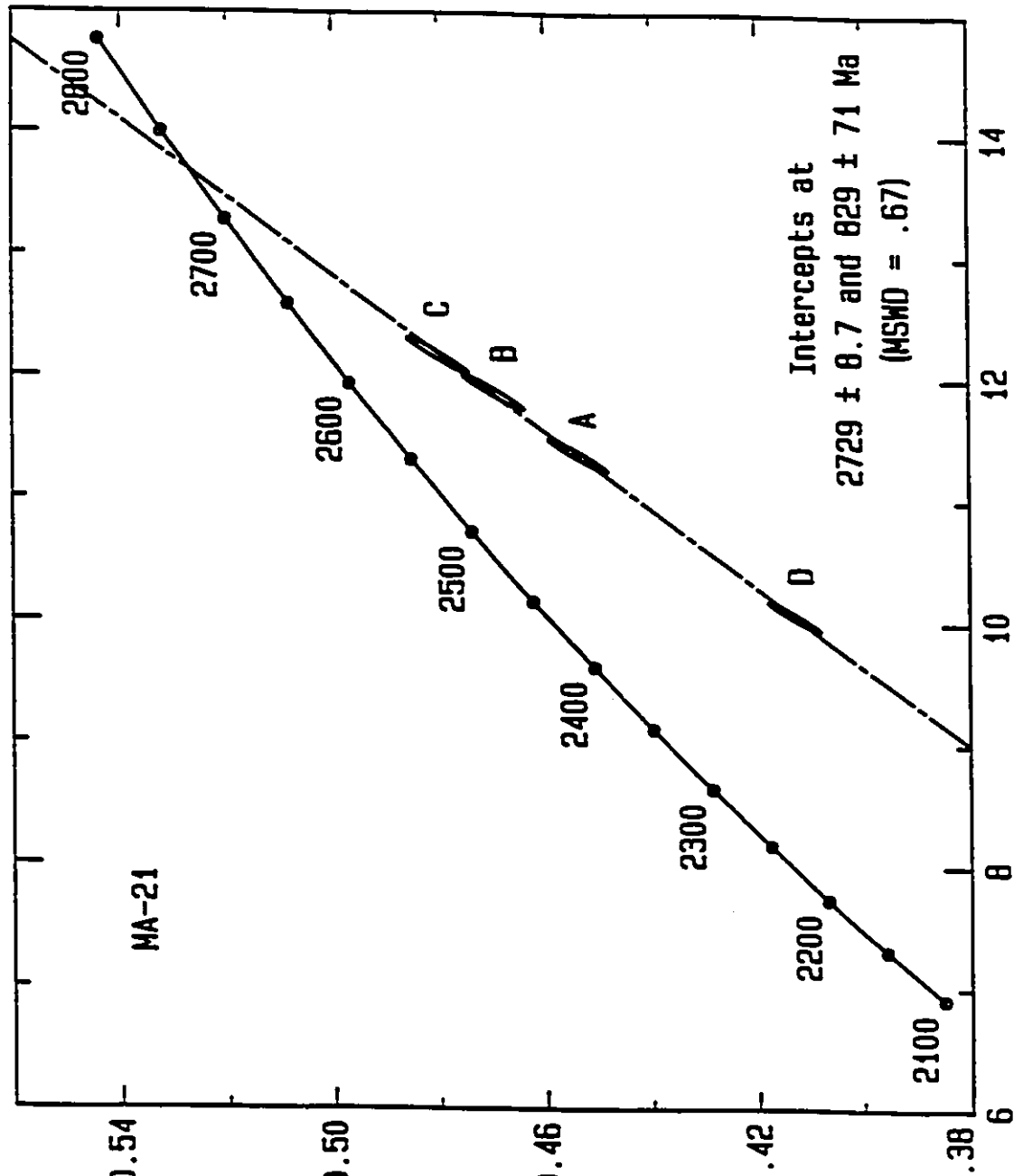


Fig. 5.2. Concordia diagram for Pointe du Bois tonalite (MA-21).

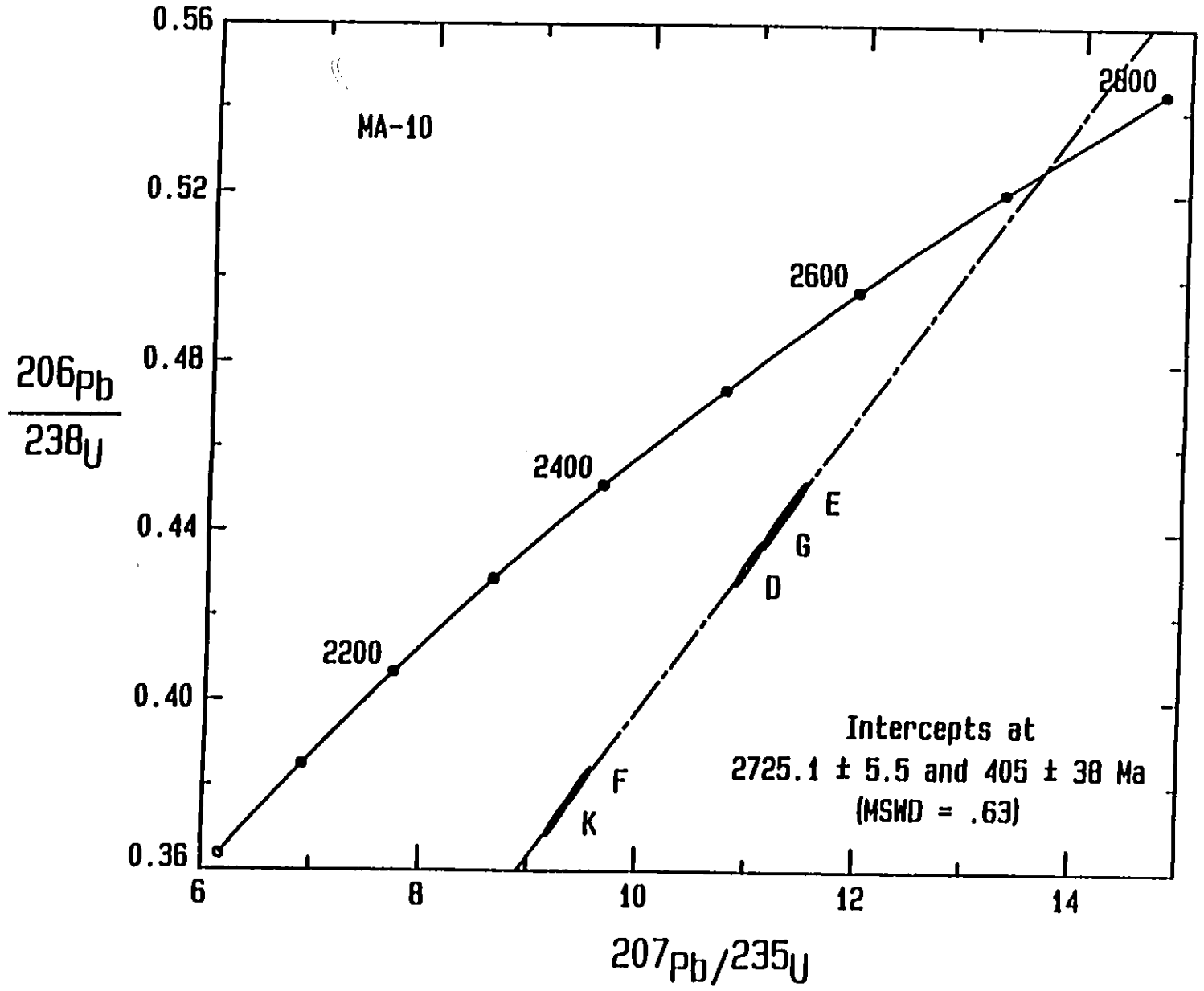


Fig. 5.3. Concordia diagram for Maskwa Lake quartz monzonite (MA-10).

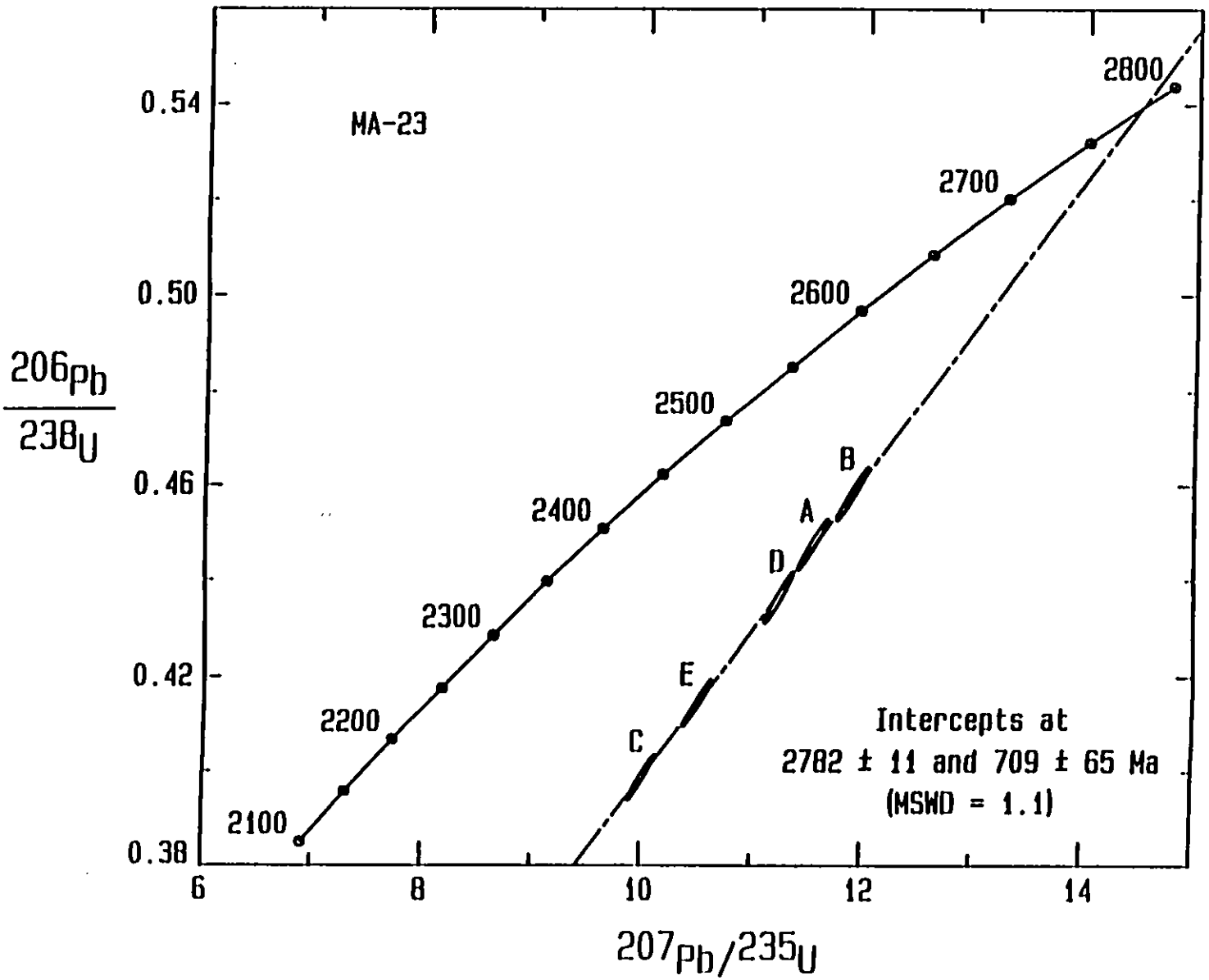


Fig. 5.4. Concordia diagram for Maskwa Lake granodiorite (MA-23).

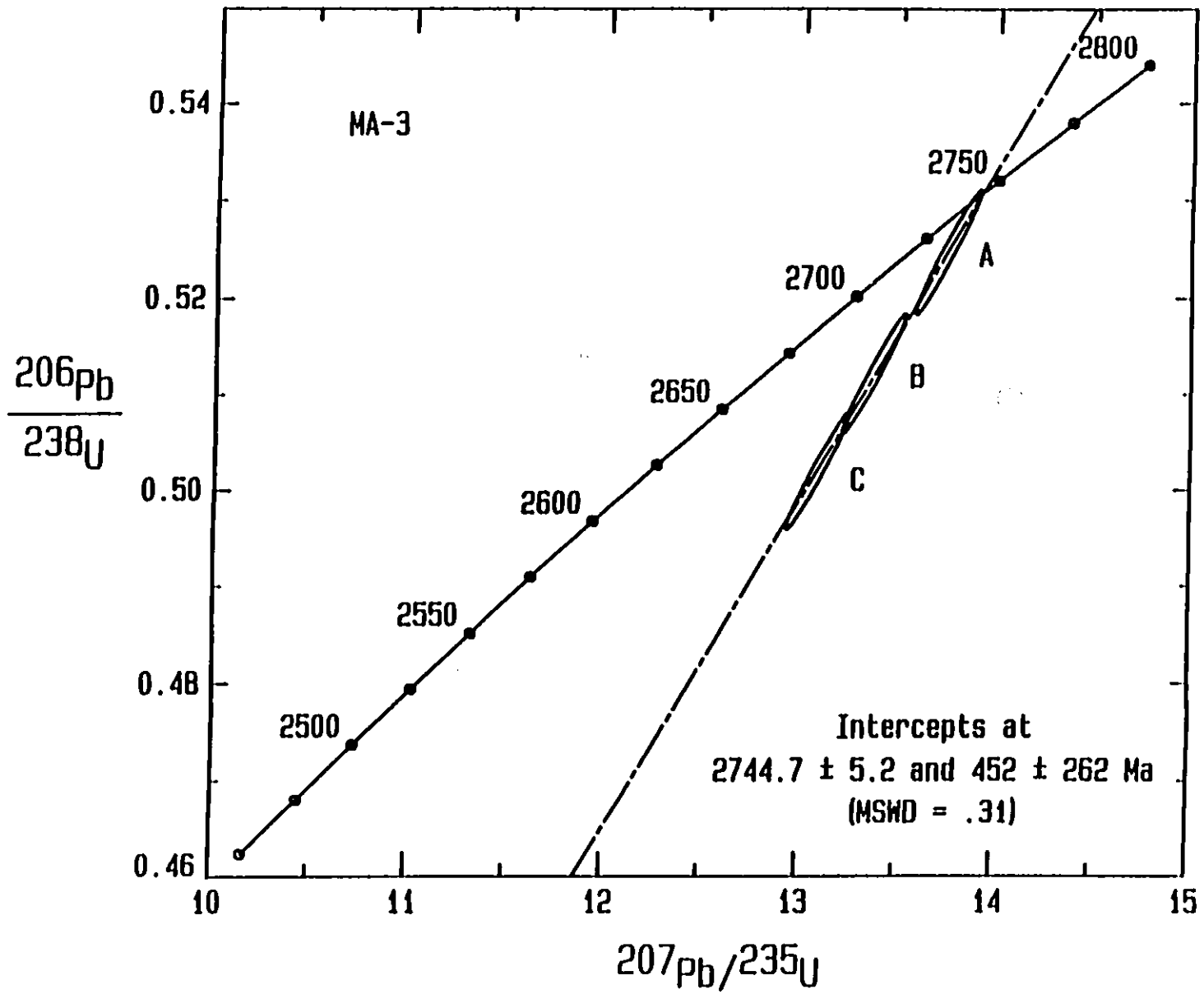


Fig. 5.5. Concordia diagram for Bird River gabbro (MA-3).

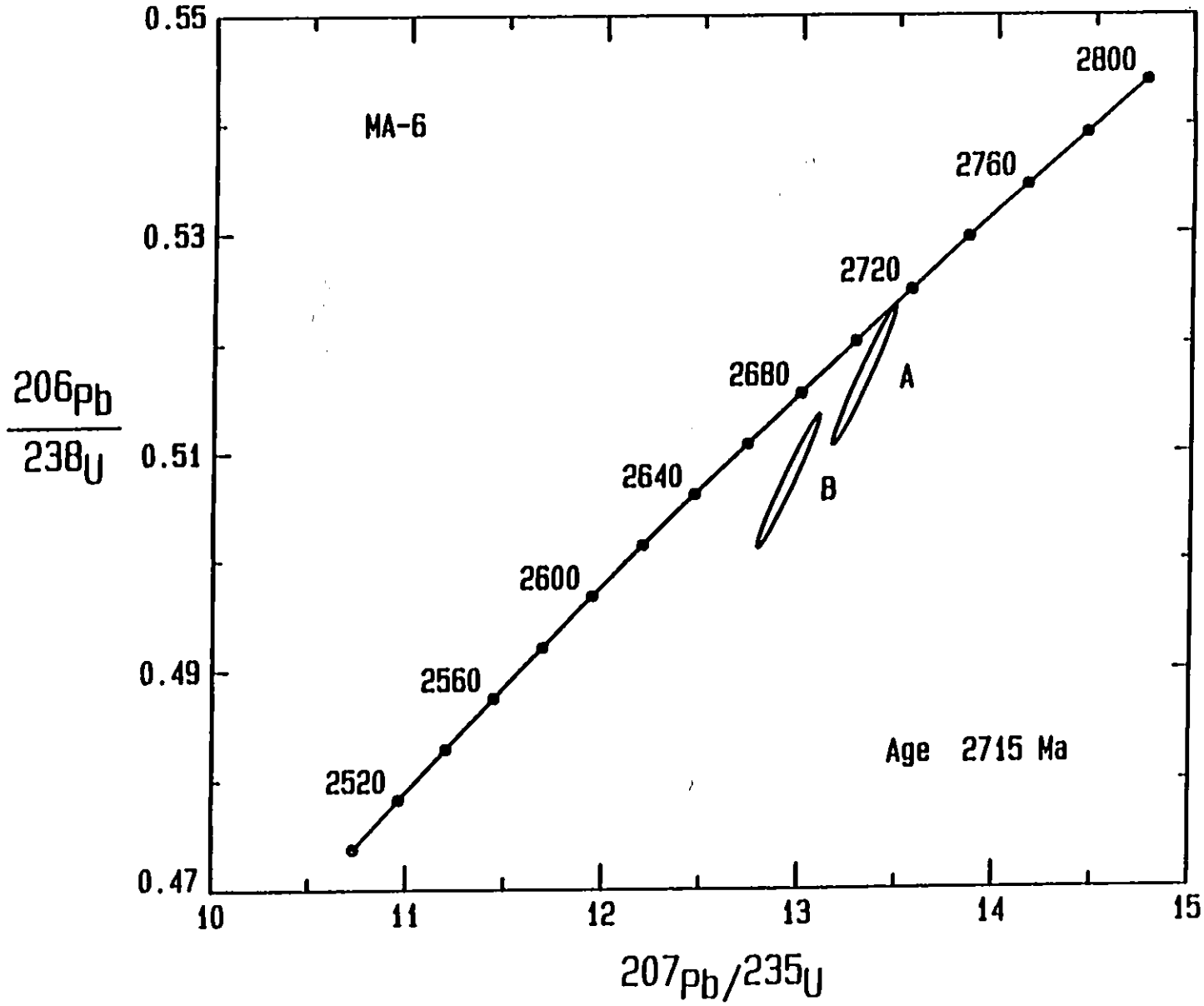


Fig. 5.6. Concordia diagram for Bird River diorite (MA-6).

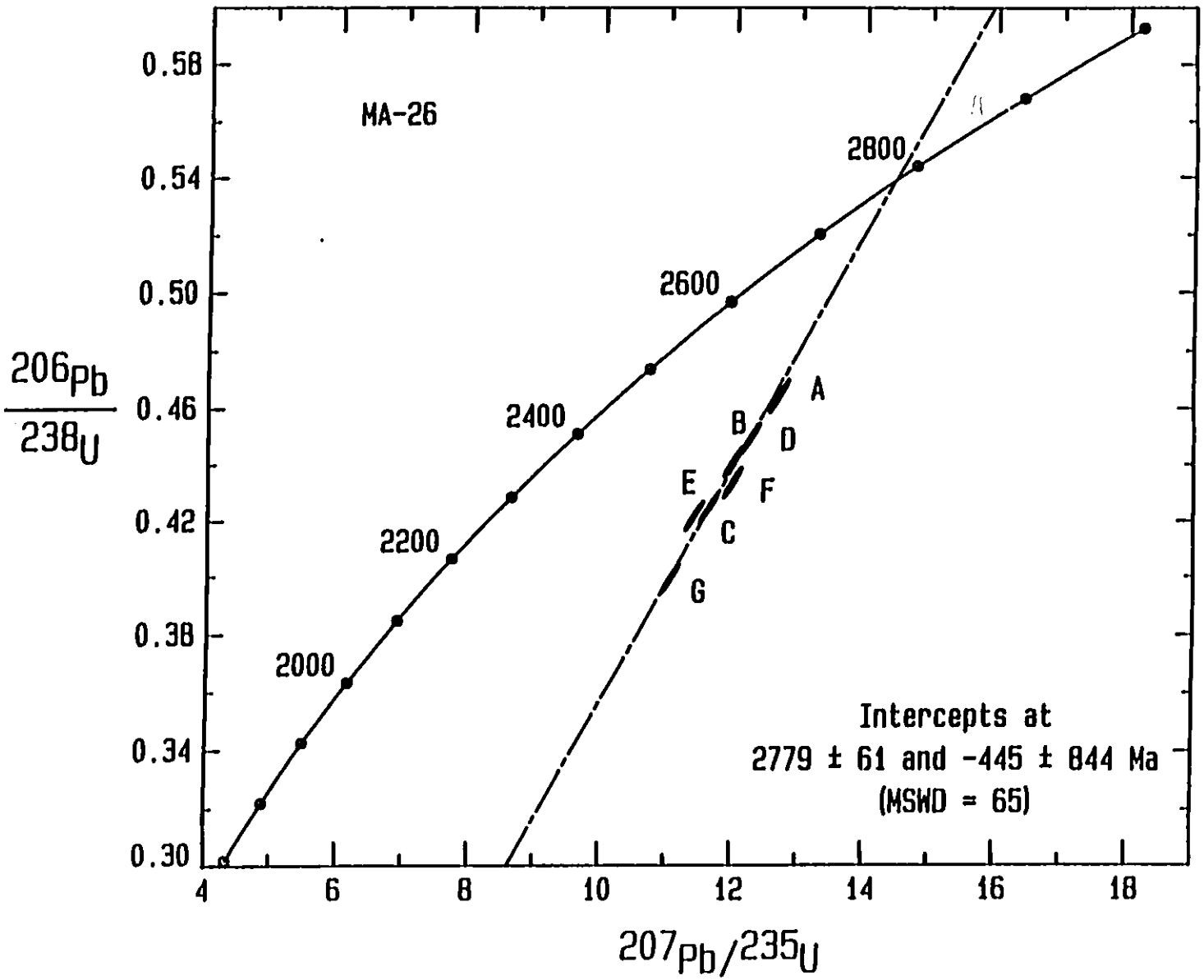


Fig. 5.7. Concordia diagram I for Bird River gabbro/diorite (MA-26).

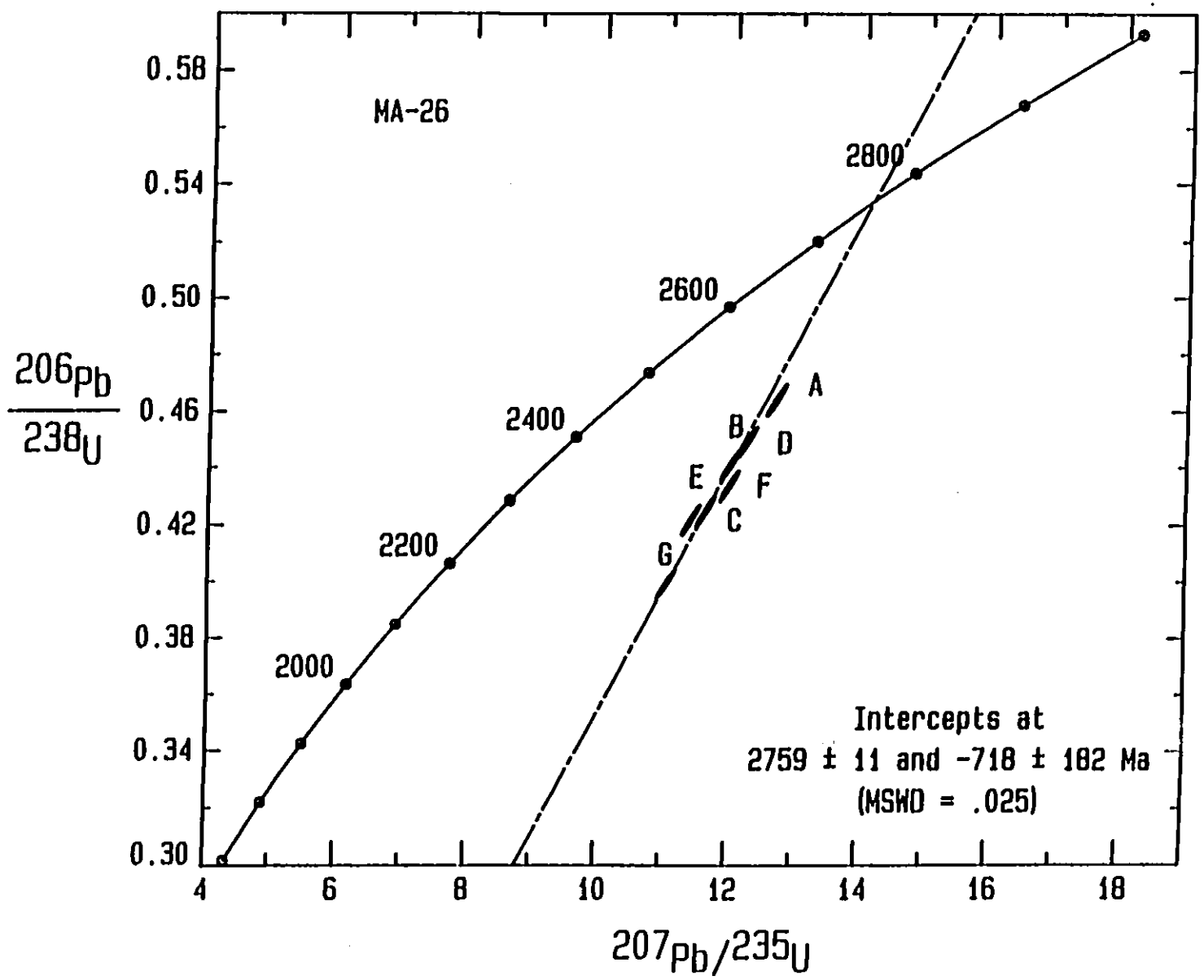


Fig. 5.8. Concordia diagram II for Bird River gabbro/diorite (MA-26).

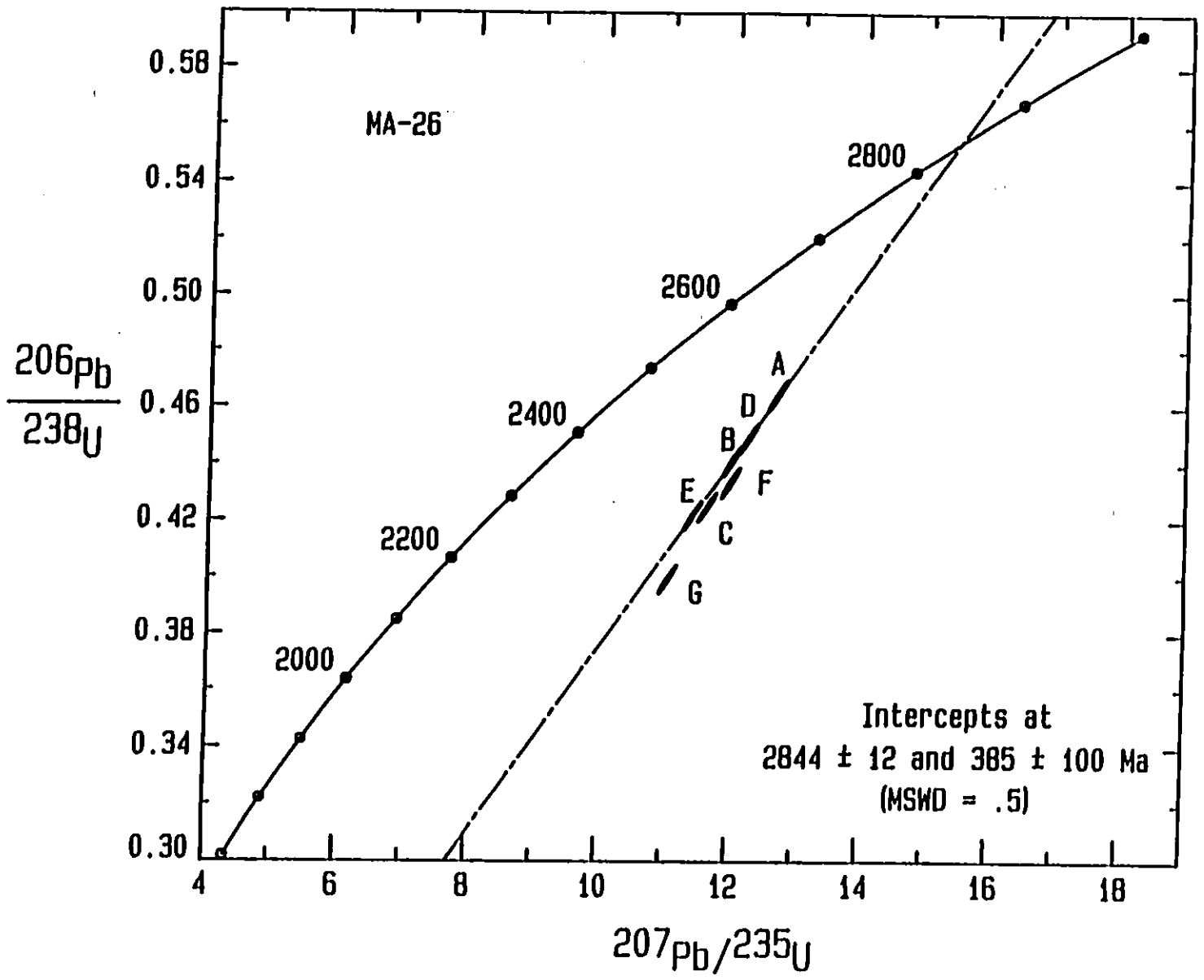


Fig. 5.9. Concordia diagram III for Bird River gabbro/diorite (MA-26).

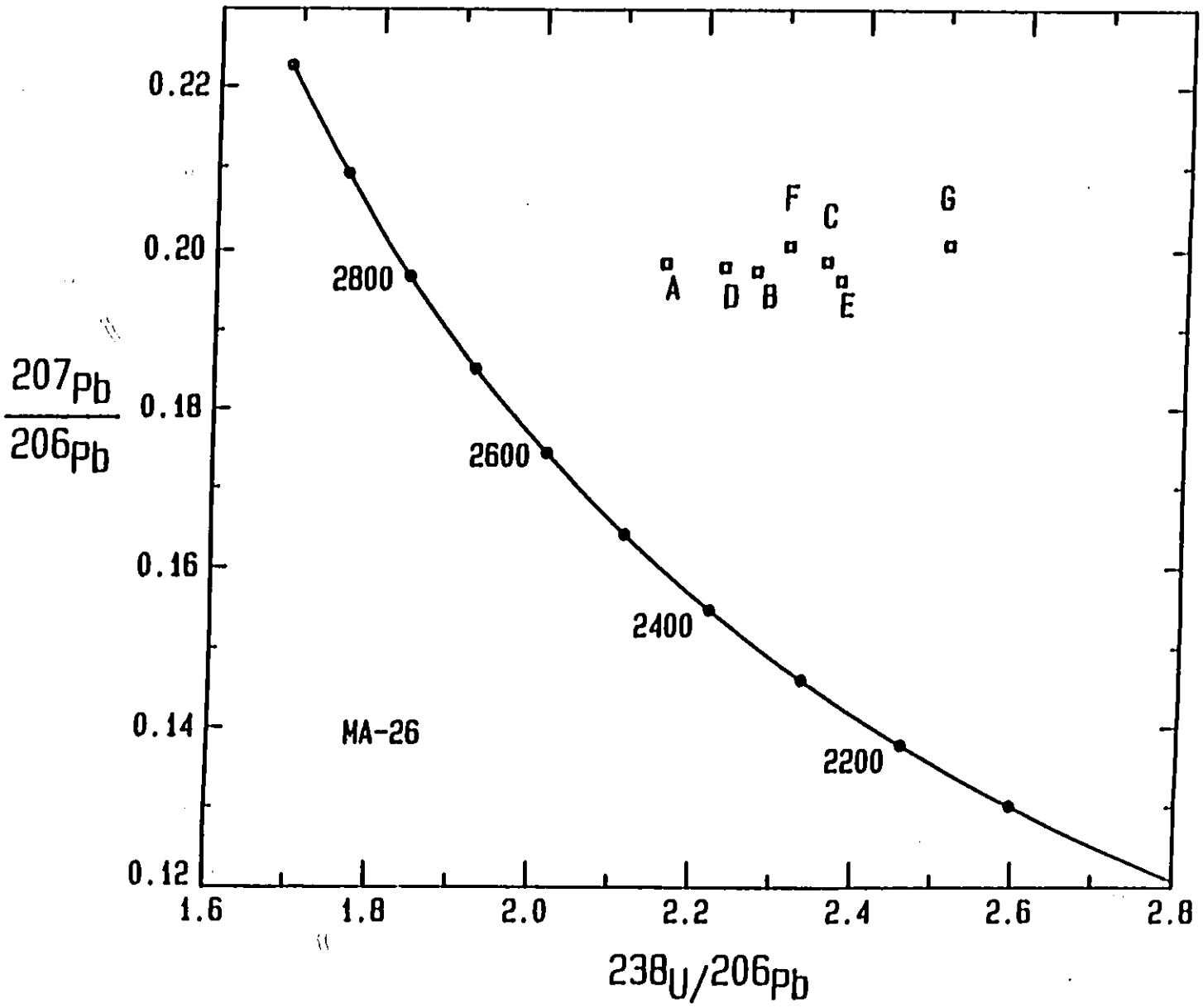


Fig. 5.10. Tera-Wasserburg concordia diagram for Bird River gabbro/diorite (MA-26).

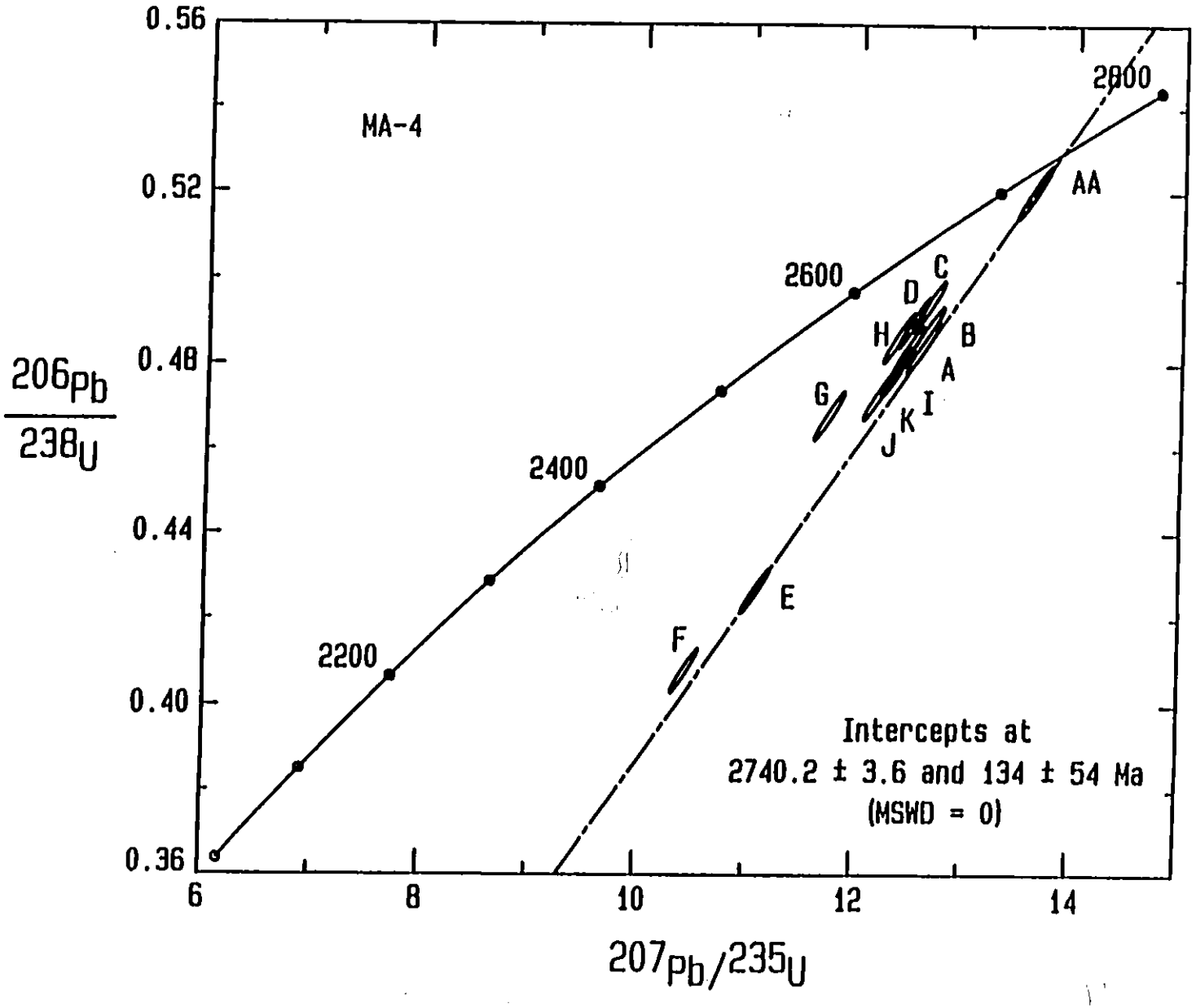


Fig. 5.11. Concordia diagram I for Peterson Creek volcanic tuff (MA-4).

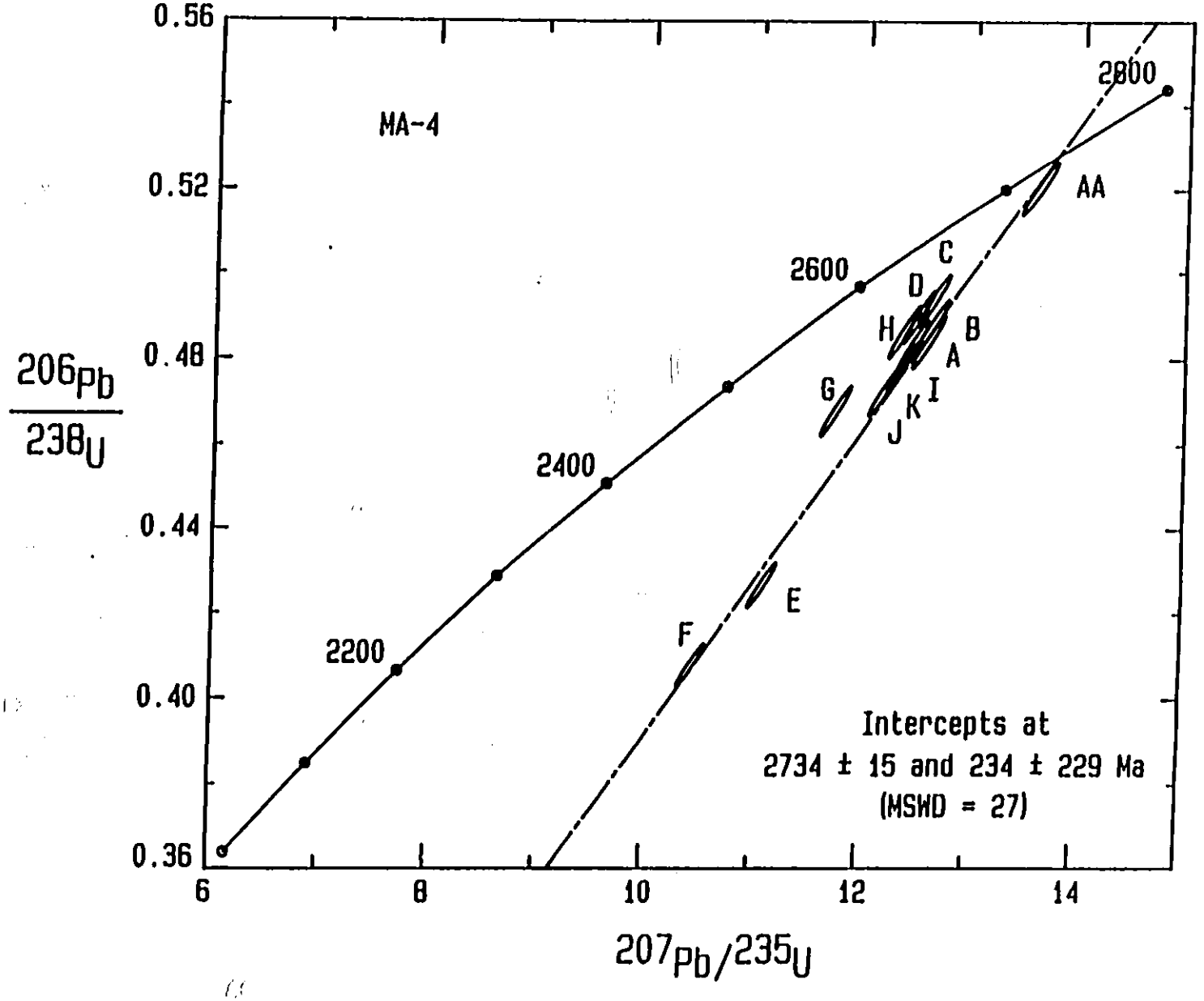


Fig. 5.12. Concordia diagram II for Peterson Creek volcanic tuff (MA-4).

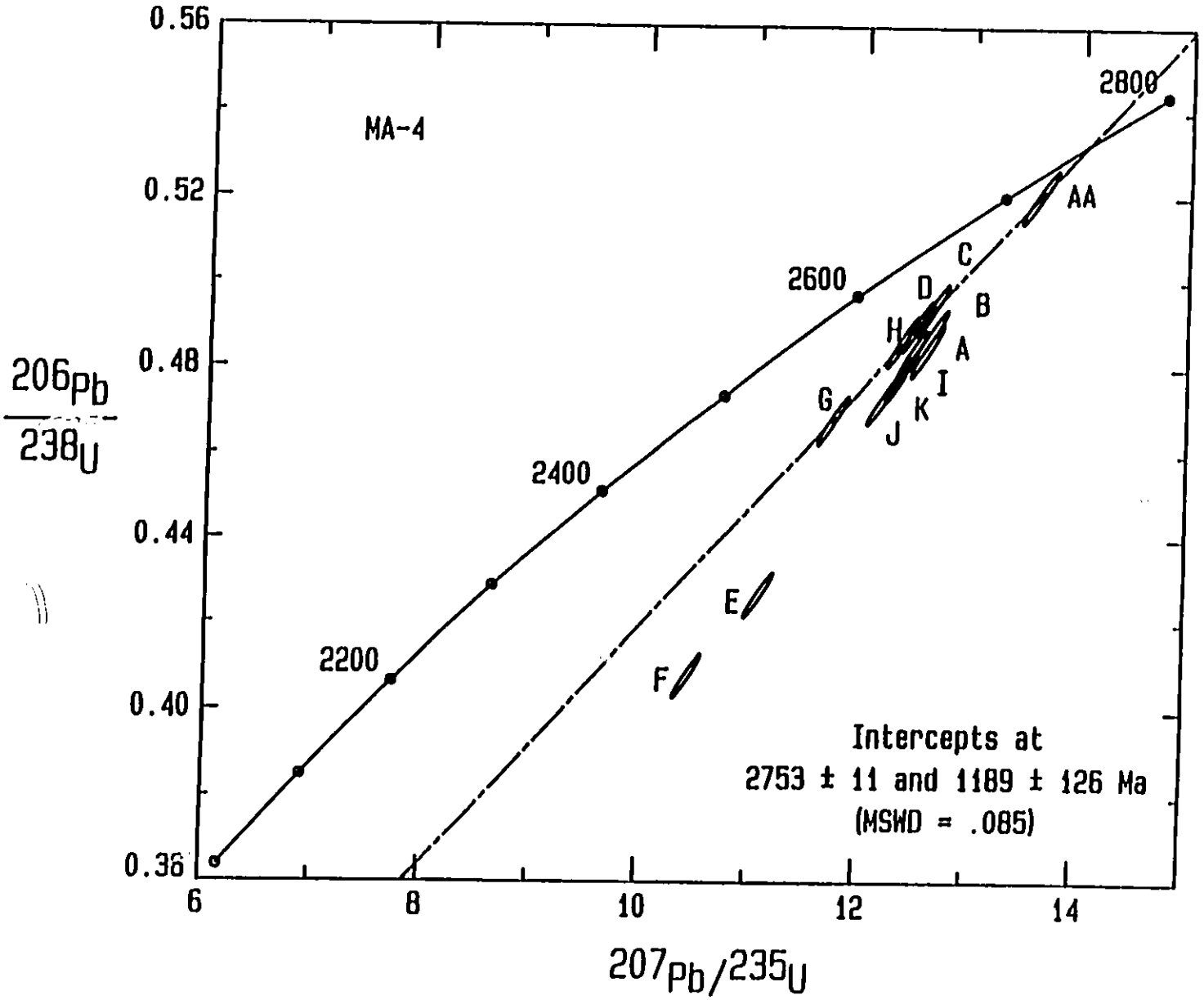


Fig. 5.13. Concordia diagram III for Peterson Creek volcanic tuff (MA-4).

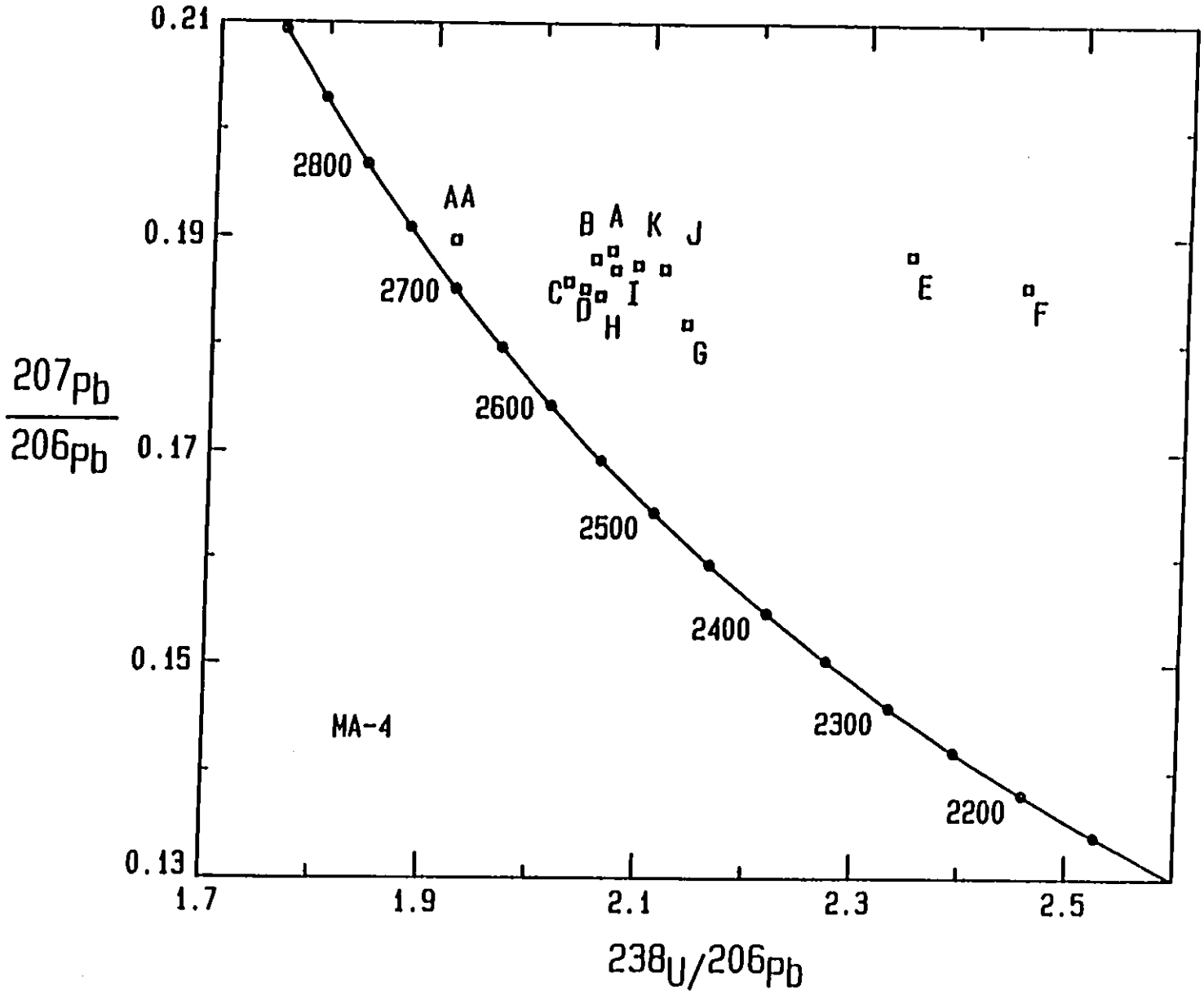


Fig. 5.14. Tera-Wasserburg concordia diagram for Peterson Creek volcanic tuff (MA-4).

# CHAPTER VI

# DISCUSSION OF RESULTS

Eight rock units were dated in this study. Six of these define ages within experimental error with little need for interpretation of results. However, data for two units (Gabbro/diorite MA-26 and Peterson Creek volcanic tuff MA-4) are not clear and require interpretation. The detailed discussion is as follows :

## Lac du Bonnet batholith (MA-17)

The age determined for a granite sample from this batholith is 2660.1 ± 3.1 Ma, based on 4 zircon fractions. A fifth fraction, excluded from the above age calculation is showing a slightly older age, which is probably due to existence of an older component, though no cores have been positively identified under the microscope. This batholith is non-foliated and is late-tectonic, and the 2660 Ma age is geologically very appropriate. It is similar to the age of the Black Lake granite to the north of the Bird River belt in the Manigotagan gneissic belt, which is also post-tectonic and dated at 2663 ± 7.3 Ma by Turek et al. (1989).

## Pointe du Bois batholith (MA-21)

An age of 2729 ± 8.7 Ma has been obtained for a gneissic tonalite from this body based on 4 points that are collinear within experimental error. The compilation map of Kowerchuk and Weber (1987) shows this batholith as a member of the so called "Older basement gneiss complex" and older than the greenstone belt. It is clearly not the case and age-wise this body falls into a well proven ca. 2730 Ma age of several volcanic plutonic

rocks of this belt as well as to the north in the Rice Lake belt (Turek et al., 1989) and the Red Lake belt (Corfu and Andrews, 1987). Hence, a revision of the stratigraphy sequence as shown on the map of Kowerchuk and Weber (1987) is required, and is shown in Table 6.1. This major modification of the stratigraphic sequence dose not conflict with any observed field relations. Past field mapping placed this rock as "old", essentially basement complex, simply because it was very gneissic.

An age of ca. 2730 Ma is well established throughout the Superior Province as a major igneous event. In this area 2730 Ma is an age of volcanism and plutonism in both the Rice Lake belt and the Red Lake belt. In the Rice Lake area the following units belong to this event: Narrows dacite (2731 Ma), Ross River quartz diorite (2728 Ma), Gunnar porphyry (2733 Ma) and Northern granite I at Wallance Lake (2731 Ma) (Turek et al., 1989). In the Red Lake area, similar ages are for the following units: Little Vermilion Lake granodiorite (2731 Ma), and porphyritic quartz diorite at small Red Crest stock (2729 Ma) (Corfu and Andrews, 1987); Okanse Lake quartz monzonite (2730 Ma), Cycle III felsic porphyritic flow (2738 Ma), and a granodiorite (2734 Ma)(Nunes and Thurston, 1980).

### Maskwa Lake batholith I (MA-10)

Zircons from a quartz monzonite in this batholith were found to be very discordant, but all 5 fractions define an age of 2725.1 $\pm$ 5.5 Ma within experimental error. Presumably this age belongs to the wanning stage of the 2730 Ma igneous event.

### Maskwa Lake batholith II (MA-23)

Five zircon fractions from a granodiorite to the north of the previous sample define an age of 2782 ± 11 Ma. This is a model 1 age, in spite of the 19% to 33% of discordance. It is clearly an older granitic rock than the 2725 Ma of Maskwa I sample (MA-10) above. Thus the Maskwa Lake batholith must be either a complex mosaic of granitoid plutons of different ages or essentially a batholith of 2782 Ma age that has been intruded by 2725 Ma pluton near its contact within the greenstone belt. The granite terrain between the Bird River belt and the Rice Lake belt is not very well mapped.

### Bird River sill (MA-3)

The Bird River sill is thought to be a feeder to some of the mafic volcanic rocks. The age of 2745 ± 5 Ma is well defined by the data. The sample is a gabbro.

### Diorite stock (MA-6)

Several mafic to intermediate stocks in the supracrustal pile are thought to be feeded pipes related to the mafic/felsic volcanism (Trueman, 1980). From this sample a titanite was dated, the age of 2715 Ma is possibly a metamorphic age, as titanites update easily, but it could very well be a true igneous age in which case it would indicate a volcanic event at ca. 2715 Ma. This stock is mapped by Trueman (1980) as related to the Bernic Lake formation. In the Red Lake area, there is a subvolcanic porphyry dated at 2714 Ma, hence 2715 Ma volcanic episode may be a widespread volcanic event.

## Gabbro/Diorite (MA-26)

This sample was collected in the belief that this was part of the Bird River sill as shown on the maps of Davies (1952) and Kowerchuk and Weber (1987). It was believed that the sample would have an age of 2745 Ma as determined for the Bird River sill on a sample from the Chrome property. The 7 zircon fractions measured all indicate an old age, older than 2813 Ma. The interpreted age is 2844 $\pm$ 12 Ma and there must be older components present as evident from the scatter of the data.

Clearly this rock is not related to the Bird River sill. It may be related to volcanic activity at that time and thus related to the supracrustal rocks. But, it may also be related to the Maskwa Lake batholith to which it is adjacent. If the Maskwa Lake terrain is a plutonic complex, then this is an older pluton in it. On the other hand, this could be an amalgamated supracrustal block in a 2870 Ma or 2730 Ma pluton.

Until this whole granite terrain to the north of the Bird River belt is mapped in some detail the chronology and evolution of this area has to be highly speculative. Based on thin section examination, the sample collected (MA-26) is a granodiorite and not gabbro/diorite as mapped (Kowerchuk, D., and Weber, W., 1987). The modal analysis is: quartz 32.61%, plagioclase ($An_{28}$-$An_{25}$) 40.09%, biotite 12.65%, microcline 5.30%, zircon 0.6%, magnetite 1.78%, sphere 0.2%, rest are epidote, sericite and chlorite.

## Peterson Creek volcanic tuff (MA-4)

It was very difficult to find zircons in felsic volcanic rocks in this belt. This was the only one sample that had zircons but simply not very good ones. The zircons are highly altered, and neither abrasion or single crystal analysis would be helpful. A total of 12

fractions was analyzed, the interpreted age is 2740 Ma, based essentially on one almost concordant point. This interpretation makes all remaining 11 points plot above the concordia which would result from alteration or from multiple stage Pb loss (see the related theory in Chapter III).

From the geological field relations, this felsic volcanic rock is younger than the Bird River sill (i.e. 2745 Ma), hence it could be 2730 Ma which is a well established age of volcanism in the Rice Lake belt (Turek et al., 1989), while 2740 Ma is a well determined age of volcanism in the Red Lake area (Corfu and Andrews, 1987). In view of the severe alteration (see the picture in Appendix A), the most concordant point is thought to be most reliable, hence the suggested age is 2740 Ma.

## Revised stratigraphy

As a result of the age determinations reported here, a revision of the stratigraphic sequence is necessary. Table 6.1 shows the changes being suggested. It is important to note that these changes do not contradict any geological observations. The idea of volcanic cycles is also being introduced here for this greenstone belt. The Eaglenest formation is a volcanic wacke. It is assumed that the volcanics from which it is derived are not exposed. Hence the base of the volcanics is not known. The granitoid dated at 2782 Ma (MA-23) and 2844 Ma (MA-26) may be a granite basement to the volcanic sequence here, but as the basal volcanics are not dated and not exposed, this is still an unknown.

## Regional Correlation

Ages obtained in this study together with those published for the adjacent areas of Rice Lake and Red Lake greenstone belts are given in Table 6.2 and Table 6.3. They are also plotted as a frequency diagram (Fig. 6.1). There are several definable apparent events in these areas. In Table 6.2 and Table 6.3, seven such plutonic or volcanic/plutonic events are suggested. These are as follows :

(a) 2840 - 3010 Ma plutonic and volcanic event: widespread granite rocks and felsic tuff (Bird River, Red Lake and Rice Lake areas).

(b) 2790 Ma volcanic and plutonic event: rhyolite and granodiorite (Bird River and Red Lake areas).

(c) 2740 Ma volcanic and plutonic event: mainly rhyolite and gabbro (Bird River and Red Lake areas).

(d) 2730 Ma plutonic and volcanic event: widespread igneous activity, granitoid, rhyolite, dacite and porphyry (Bird River, Red Lake and Rice Lake areas).

(e) 2715 Ma plutonic and volcanic event: granitoid and porphyry (Bird River and Red Lake areas).

(f) 2700 Ma plutonic event: granodiorite (Red Lake area).

(g) 2660 Ma plutonic event: granite and similar rocks, post tectonic intrusive rocks (Bird River and Rice Lake areas).

Table 6.4 is a summary of the igneous activities from 2660 Ma to 3010 Ma in the Bird River, Rice Lake, and Red Lake areas. Clearly, there was a major and widespread volcanic and plutonic event in the period of 2730-2740 Ma. Also crustal creation was taking

**Table 6.1.** Table of formations for the Archean rocks of the Bird River greenstone belt, Manitoba.

| Orginal Rock units and sequence (Kowerchuk & Weber, 1987) | Age ( Ma ) | Revised sequence ( based on this study ) |
|---|---|---|
| Younger Plutonic rocks (Lac du Bonnet batholith) | 2660±3 | 2660 event |
| Booster Lake Formation | | |
| Flanders Lake Formation | | |
| Great Falls pluton (Maskwa Lake complex) | 2725±6<br>2782±11<br>2844±12 | |
| Granodiorite | | |
| Diorite | 2715 (min. age) | → Cycle III volcanics (2730 event) |
| Gabbro | | |
| Bernic Lake Formation | | |
| Peterson Creek Formation | 2740±4 | |
| Bird River sill (gabbro, peridotite) | 2745±5 | → Cycle II volcanics (2740 event) |
| Lamprey Falls formation | | |
| Eaglenest Lake formation (1) | | → Cycle I volcanics (2780-? event) |
| Plutonic rocks of intermediate age: | | |
| Winnipeg River complex | | |
| Older gneiss complex | 2729±9 | |
| | | (2) |

(1) Exposed is a volcanic wacke, hence volcanic rocks are assumed to exist but are not exposed.

(2) Granitoid rocks older than 2782 Ma.

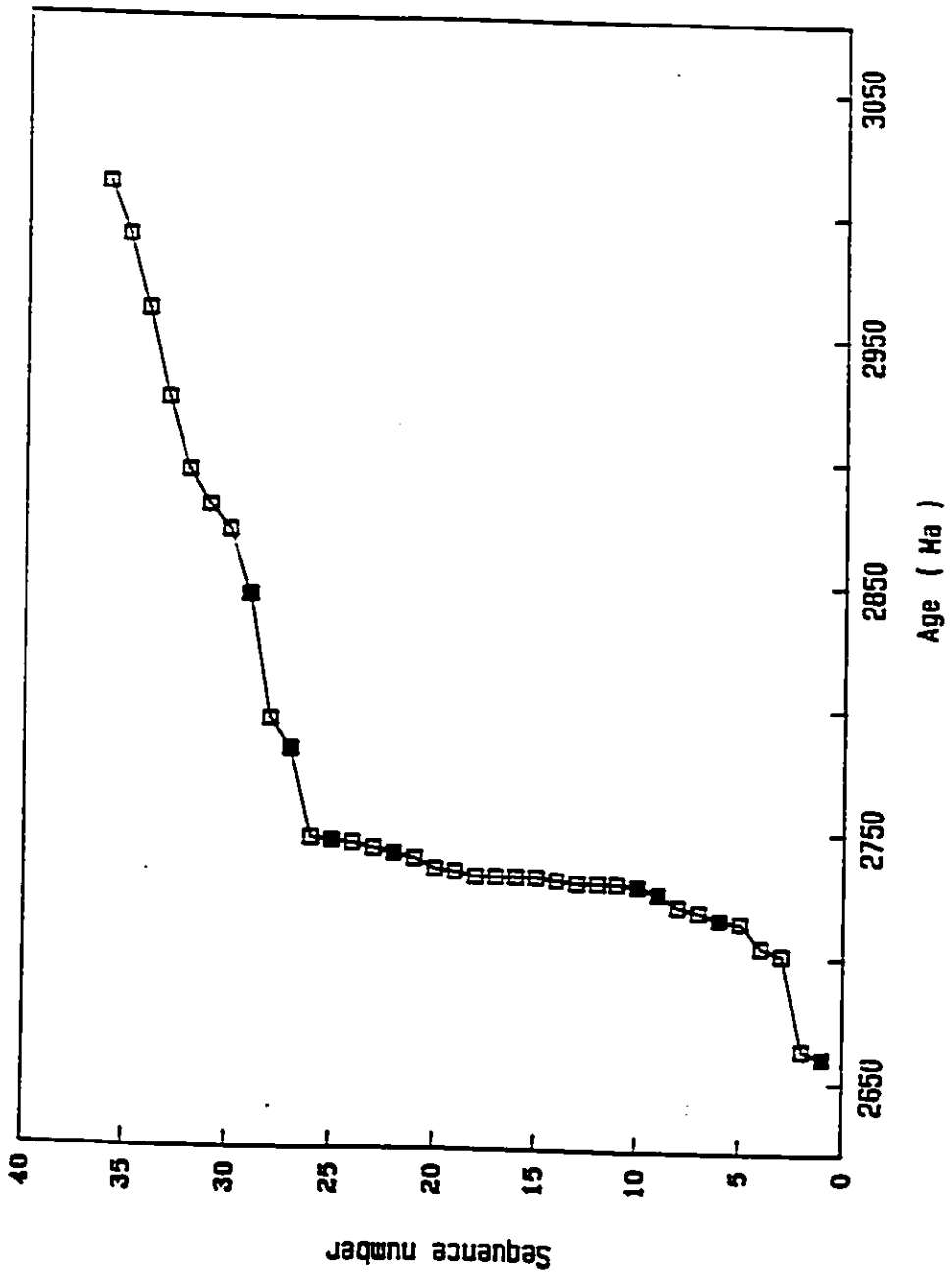


Fig. 6.1. Frequence plot of U-Pb zircon ages from the Bird River area (shaded squares), the Rice Lake and Red Lake areas. This is a plot of ages (X axis) arranged in ascending order (Y axis), so each age has a frequence of one.

Table 6.2. Summary of U-Pb zircon ages for the Bird River, Rice Lake and Red Lake areas.

| Sample no. | Location | Sample detail | Event (Ma) [1] | Concordia Intercept Ages (Ma) Upper | Lower | Reference |
|---|---|---|---|---|---|---|
| MA-17 | Bird River | quartz monzonite | (g) 2660 | 2660 ± 3 | 91 | This study |
| M710 | Rice Lake | granite | | 2663 ± 7 | 120 | Turek et al. (1989) |
| G | Red Lake | granodiorite | (f) 2700 | 2701 ± 1.5 | 430 | Corfu and Andrews (1987) |
| K | Red Lake | granodiorite | | 2704 ± 1.5 | 370 | Corfu and Andrews (1987) |
| H | Red Lake | quartz-fledspar porphyry | (e) 2715 | 2714 ± 4 | | Corfu and Andrews (1987) |
| MA-6 | Bird River | diorite | | 2715 (Min. age) | | This study |
| F | Red Lake | granodiorite | | 2718 ± 6 | 1270 | Corfu and Andrews (1987) |
| E | Red Lake | granodiorite | | 2720 ± 2 | 250 | Corfu and Andrews (1987) |
| MA-10 | Bird River | quartz monzonite | (d) 2730 | 2725 ± 6 | 404 | This study |
| M702 | Rice Lake | quartz diorite | | 2728 ± 8 | 191 | Turek et al. (1989) |
| MA-21 | Bird River | foliated biotite granite | | 2729 ± 9 | 829 | This study |
| M716 | Rice Lake | rhyolite | | 2729 ± 3.2 | 64 | Turek et al. (1989) |
| N | Red Lake | porphyritic quartz diorite | | 2729 ± 1.5 | 320 | Corfu and Andrews (1987) |
| N77-8 | Red Lake | quartz monzonite | | 2730 ± 1.3 | | Nunes and Thurston (1980) |
| M711 | Rice Lake | quartz fledspar porphyry | | 2731 ± 13 | 246 | Turek et al. (1989) |
| M705 | Rice Lake | granitoid gneiss | | 2731 ± 10 | 49 | Turek et al. (1989) |
| M | Red Lake | granodiorite | | 2731 ± 3 | 1090 | Corfu and Andrews (1987) |
| M703 | Rice Lake | dacite | | 2731 ± 3.2 | 519 | Turek et al. (1989) |
| 89-21 | Rice Lake | porphyry | | 2733 ± 6 | 232 | Turek and Weber (1991) |
| N76-11 | Red Lake | granodiorite | | 2734 ± 8 | | Nunes and Thurston (1980) |
| N76-7 | Red Lake | rhyolite | (c) 2740 | 2738 ± 4 | | Nunes and Thurston (1980) |
| MA-4 | Bird River | meta-rhyolite | | 2740 ± 4 | 134 | This study |
| D | Red Lake | fledspar porphyry | | 2742 ± 3 | 820 | Corfu and Andrews (1987) |
| I | Red Lake | crystal tuff | | 2744 ± 1 | 180 | Corfu and Andrews (1987) |
| MA-3 | Bird River | meta-grabbro | | 2745 ± 5 | 452 | Timmins (1985) |
| J | Red Lake | Spherulitic felsic flow | | 2746 ± 26 | 1340 | Corfu and Andrews (1987) |

Table 6.2. (Continued)

| Sample no. | Location | Sample detail | Event (Ma) [1] | Concordia Intercept Ages (Ma) Upper | Lower | Reference |
|---|---|---|---|---|---|---|
| MA-23 | Bird River | granodiorite | (b) 2790 | 2782 ± 11 | 709 | This study |
| N76-8 | Red Lake | rhyolite | | 2794 ± 6 | 136 | Nunes and Thurston (1980) |
| MA-26 | Bird River | granodiorite | (a) 2840-3010 | 2844 ± 12 | 385 | This study |
| C | Red Lake | quartz gabbro | | 2870 ± 15 | | Corfu and Andrews (1987) |
| M708 | Rice Lake | porphyoclastic granodiorite | | 2880 ± 9 | 148 | Turek et al. (1989) |
| B | Red Lake | felsic tuff | | 2894 ± 2 | 1070 | Corfu and Andrews (1987) |
| M708 | Rice Lake | porphyoclastic granodiorite | | 2923 ± 16 | 610 | Turek et al. (1989) |
| N76-9 | Red Lake | felsic lapilli tuff | | 2959 ± 1.7 | | Nunes and Thurston (1980) |
| A | Red Lake | rhyolite | | 2989 ± 3 | | Corfu and Andrews (1987) |
| 89-9 | Rice Lake | tonalite | | 3010 ± 13 | 63 | Turek and Weber (1991) |

NOTE: [1]Refer to text for discussion of event. Errors for the ages are as published, either 2σ or 95% CL.

**Table 6.3.** Comparison of the revised stratigraphic sequence in the the Rice Lake and the Red Lake areas.

| Revised sequence in Bird River area (1) | Age ( Ma ) | Sequence in Rice Lake area (2) | Age ( Ma ) |
|---|---|---|---|
| Lac du Bonnet batholith | 2660±3 | Black Lake quartz monzonite | 2663±7 |
| | | Ultramafic rocks | |
| Booster Lake formation<br>Flanders Lake formation | | San Antonic formation | |
| | | Edmunds Lake formation | |
| Maskwa Lake batholith | 2725±6 | Ross River quartz diorite | 2728±8 |
| Winnipeg River complex (?) | | Gunnar porphyry | 2731±13 |
| "Older" gneiss complex (Pointe du Bois batholith) | 2729±9 | | |
| Granodiorite | | Wallace Lake granite | 2731±10 |
| Diorite /gabbro | 2715 (min. age) | Anorthositic gabbro /gabbro | |
| | | Manigotagan River formation | |
| Bernic Lake formation | | Narrows formation | 2729±3<br>2731±2<br>2733±6 |
| Peterson Creek formation<br>Bird River sill<br>Lamprey Falls formation | 2740±4<br>2745±5 | Stormy Lake formation | |
| | | Stovel Lake formation<br>Dove Lake formation | |
| Eaglenest Lake formation | | Tinney Lake formation<br>Gunnar formation | |
| Granitoid basement(?) | 2782±11 | | |
| Granitoid basement(?) | 2844±12 | Granitoid basement(?) | 2880±9<br>3010±13 |

(1) This study.
(2) Kowerchuk and Weber (1987), Turek et al.(1989), and Turek and W
(3) Corfu and Andrews (1987), Corfu and Wallace (1986), and Nunes a

quence in the Bird River area with the sequences in

| Age ( Ma ) | Sequence in Red Lake area (3) | Age ( Ma ) | Igneous event (- Ma) |
|---|---|---|---|
| 2663±7 | | | 2660 |
| | Wilmar granodiorite | 2701±2 | |
| | Killala-Baird granodiorite | 2704±2 | 2700 |
| | White Mine porphyry dyke | 2714±4 | |
| | Abino granodiorite | 2718±6 | 2715 |
| | McKenzie granodiorite | 2720±2 | |
| 2728±8 | Little Vermilion Lake granodiorite | 2731±3 | |
| 2731±13 | Northwestern porphyritic quartz diorite | 2729±2 | 2730 |
| | Northeastern quartz monzonite | 2730±1 | |
| | Northeastern granodiorite | 2734±8 | |
| 2731±10 | | | |
| | Northeastern rhyolite | 2738±4 | |
| | Eastern Red Lake quartz-feldspar porphyry | 2742±3 | 2740 |
| | Central Red Lake : | | |
| 2729±3 | lapilli-crystal tuff | 2744±1 | |
| 2731±2 | Spherulitic felsic flow | 2746±26 | |
| 2733±6 | | | |
| | Northeastern rhyolite | 2794±6 | 2790 |
| | Eastern Red Lake : | | |
| | Quartz gabbro | 2870±15 | 2840 |
| | Intermediate-felsic tuff | 2894±2 | to |
| | Rhyolite | 2989±3 | 3010 |
| | Northeastern felsic lapilite tuff | 2959±2 | |
| 2880±9 | | | |
| 3010±13 | | | |

nd Turek and Weber (1991).
), and Nunes and Thurston (1980).

**Table 6.4.** Igneous activity from 2660 to 3000 Ma in the Bird River, Rice Lake, and Red Lake areas.

| Event (- Ma ) | Area | | |
|---|---|---|---|
| | Bird River | Rice Lake | Red Lake |
| 2660 Plutonism | P | P | |
| 2700 Plutonism | | | P |
| 2715 Plutonism /Volcanism | | | P & V |
| 2730 Plutonism /Volcanism | P & V | P & V | P & V |
| 2740 Volcanism /Plutonism | V & P | V | V |
| 2790 Plutonism /Volcanism | P & V | | P & V |
| 2840 Plutonism -3010 /Volcanism | P & V | P & V | P & V |

Note: P is plutonism, V is volcanism.

place from 2730 to 3010 Ma in all the three greenstone belts, and all these three belts had evolved over a time span of 2660-3010 Ma. Fig 6.1, plot of ages for the three belts, clearly shows igneous activities from 2660 to 3010 Ma, and also shows the extensive igneous activity of the 2630-2640 Ma time.

## Tectonic Implications

### Background

This study is a highly focused age dating project confined to one greenstone belt. Studies like this are fundamental to our understanding of the formation of Archean greenstone belts. Geochronology is only one of numerous geological specialties that are continuously evaluated and combined with other data into comprehensive models for early crust formation by specialists in that field. In the last 25 years, significant contributions towards this goal have been made by advances in field mapping, petrology, petrochemistry, volcanology, thermodynamics, plate tectonics, trace element geochemistry, isotope geology, and most importantly by geochronology. Nevertheless, the emerging picture is becoming more and more complex as the basic database becomes larger. The most basic question which still has not been answered is that of the composition of the early crust.

The nature of the basement beneath the Archean supracrustal sequences has been subject of much debate. Proposed basement ranges in composition from komaittitic to baseltic to sialic. According to Beakhouse (1985) and Easton (1985), the early recognizable basement is generally sialic, largely composed of granitoid plutons partly converted to orthogneisses, but plutons were intruded into and possibly derived from older volcanic-sedimentary sequences (Persival and Card, 1983). On the other hand, Glikson (1972),

Glikson and Jahn (1985) argue for a mafic to ultramafic basement. Goodwin (1977) declares that the prefered Archean tectonic model involves interaction of small sialic nuclei (protocontinents) and oceanic type crust.

The oldest zircons, 4.2 Ga (Froude et al., 1983), are detrital which means that in the first 300 Ma of earth's history a sialic source, a protocrust, existed. Hill and Campbell (1992) see mantle plumes as an important tectonic force in contrast to ridge and island arc plate tectonics. Turek and Smith (1984) pointed out that there is a progression in zircon ages from younger to older, from east to west in parts of the Superior Province and attribute this to migrating plumes. Hill et al. (1992) see cratonization process being produced by mantle plumes and support their model by fluid dynamic and thermodynamic theories. A mantle plume originating at core mantle boundary would ascend up to the solid crustal surface and build up into a major magmatic chamber. The resulting volcanic outpouring of lava would build up a large quantity of volcanic rocks and the early formed rocks would then melt and fractionate due to heat from the plume head and produce felsic volcanism and plutonism, and in this way produce the Archean greenstone terrains, including the granitoid terrains.

Wilson (1977) points to similarities between Archean shields on three continents and postulates similar development history related to meteorite impacts analogues to those observed on the Moon, Mars, and Mercury. Such impact activity would produce volcanism and the reprocessing of these volcanic rocks would produce diapiric felsic plutonism resulting in the greenstone belt-granitoid diapiric type of tectonic style.

The Bird River greenstone belt and Separation Lake greenstone belt are called internal belts by Beakhouse (1985) as they are internal to the English River subprovince, a terrane of

orthogneisses and batholithic plutons (Beakhouse, 1977). The Separation Lake belt is 20 km east of the Bird River belt in Ontario and is very likely the extension of the Bird River belt, although there are no isotopic ages to prove that. Beakhouse (1985) proposes that the orthogneisses of the Winnpeg River Complex are older than these two belts and are the remains of the sialic basement. The Pointe du Bois tonalite dated in this study at 2729 Ma was thought to be older than rocks labelled as Winnipeg River Complex in that area (Kowerchuk and Weber, 1987). Clearly this tonalite belongs to the Kenoran orgeny which in literature is variously assigned an age of 2660-2760, 2730 or 2710-2760 Ma. It is possible that the orthgneisses exposed along the Winnepeg River between the Bird River and Rice Lake greenstone belt may be the basement rocks. Zircon ages by Krogh et al. (1974) are ca. 3 Ga for rocks in that region. Also Turek and Weber (1991) report an age of 3 Ga for a granitoid boulder in a conglomerate in the Rice Lake greenstone belt. Hence there is evidence for the existence of a felsic granitoids at 3 Ga which could be the sialic basement. The next question is the thickness of such a basement. Beakhouse (1985) postulates a thick sialic crust while Easton (1985) sees a thin sialic crust.

The oldest supracrustal rocks in the Bird River greenstone belt are a metavolcanic wacke (Eaglenest formation). The source of these must have been mafic volcanics that are not exposed or have been consumed and possibly recycled subsequently as felsic lavas and plutons. The mafic to felsic volcanics in the belt are accompanied by sedimentary rocks of the Resedimented Facies Association of greywacke, mudstone siltstone and conglomerate. Deposition was generally on submarine facies (upper to middle fan). Such sediments have been shown to be a facies change of the volcanic rocks by Sage (1992) in the Wawa belt in

Ontario. The occurence of the Alluvial Fan-Fluvial Facies Association of cross banded sanstone and associated conglomates in the Archean is rare (Ojakangas, 1985). However, they are well developed here in the Bird River belt. These are the Flanders Lake and Booster Lake Formations. Also in the Rice Lake belt, similar to these, is the San Antonio Formation. This implies the existence of a well evolved platform of Archean rocks including felsic plutonic rocks, which would be the major source of this detritus.

Proposed model

A thin felsic crust is thought to have existed and was the basement for the supracrustal rocks. Volcanism was produced by a mantle plume that formed a magma chamber under this crust. The age of this crust would be about 3 Ga. Volcanism was produced by the ascent of a mantle plume that formed a magma ocean under this thin crust. Once a high volcanic edifice was formed the early formed volcanic rocks would melt to produce a felsic magma which erupted as a lava and intruded the edifice producing plutonic rocks. This mechanism would lead to a thining and extension of the crust. Thus there would be very little difference in age between felsic volcanic and felsic plutonic rocks as has been observed by Turek et al. (1984, 1992) for the Wawa area in Ontario and Campbell and Hill (1988) for the Kalgoorlie-Norsemen area in Western Australia.

This hypothesis is in keeping with Sutton (1971) who favours a sialic crust and contrary to the views of Glikson (1972) who subscribes to the simatic model. The igneous and plutonic activity was accompanied by sedimentation of the Resediment Facies Association. Time span for this would be from 3000 Ma to 2740 Ma; i.e., from the postulated age of the basement to the age of felsic volcanics of the Peterson Creek Formation. This

was followed by a major plutonism at 2730 Ma when parts of the Maskwa complex and the Pointe du Bois plutonic rocks were emplaced. The next series of rocks to form would be Alluvial Fan-Fluvial Facies, the Flanders Lake and Booster Lakes Formations in this area and the San Antonio Formation in the Rice Lake area. There are no equivialents to these in the Red Lake area. This sedimentary association means that the granitoid terranes were all formed and were being erroded. This platform sedimention would be between 2730 and 2660 Ma. At 2660 Ma, post tectonic potassic plutons such as the Lac du Bonnett batholith were emplaced. This plutonism would be the termination of the Kenoran orgeny, which peaked at 2730 Ma.

# CHAPTER VII

## SUMMARY AND CONCLUSION

The evolution of the Bird River greenstone belt and the adjacent areas occurred over a time span of ca. 350 Ma, between 3010 Ma and 2660 Ma. Crustal creation in the area was taking place from ca. 3010 to 2730 Ma. There was a major and widespread volcanic/plutonic event in the area in the period of 2740-2730 Ma. No obvious volcanic activities existed in the period between 2700 Ma and 2660 Ma, and plutonism was the major event in this period.

Most of the objectives of this study have been met. Eight rock units have been dated, six yield very precise ages. Geological effects such as alterations and inheritance cause problems with the other two ages. To overcome these problems, ion probe mass spectrometry (SHRIMP) determinations would be needed.

The oldest supracrustal rocks in the Bird River greenstone belt are volcanic wacke (Eaglenest formation), derived from an older and unexposed volcanic pile. The Bird River sill is 2745 Ma and dates some of the mafic volcanics here as it is thought to be a feeder sill. The base of the greenstone belt is unknown; it can be ca. 2844 Ma (age for sample MA-26) or even older, depending on the interpretation of the age for the granodiorite MA-26 sample. By correlation with volcanic rocks in the Red Lake and Rice Lake areas, it could possibly be 3 Ga old. The upper limit on the supracrustal rocks is older than the 2725 Ma age obtained from granitoids intruding the greenstone belt.

The Pointe du Bois batholith which was thought to be an "older basement gneiss complex" and older than the Bird River greenstone belt, is actually not very old. Its age

falls into the well proven ca. 2730 Ma igneous event in the area. Therefore, the Winnipeg River complex which intrudes this "older gneiss complex", must also be young.

The Maskwa Lake batholith must be a granitoid complex incorporating rafters of older material. Two ages obtained for this complex are 2725 Ma and 2782 Ma, presumably the latter is a rafter. A gabbro/diorite that was believed to be part of the Bird River sill is significantly older, it is older than 2813 Ma. This terrain borders the Maskwa Lake batholith, it is probably another rafter of older material in this Maskwa Lake batholith. If this is not the case, then it must be related to volcanism in the supracrustal belt, and therefore an age ca. 2840 Ma for this rock would indicate that the supracrustal rocks must be at least that old. The nature of the basement, granitoid or mafic volcanic, is of course unknown.

The age determinations reported in this study augment the previous geochronology concepts of the Bird River greenstone belt, and have indicated revisions to the chrono-stratigraphy of the area. A detailed geochronological comparison of Archean evolutionary history for the Bird River, Rice Lake, and Red Lake areas demonstrates that these three greenstone belts are very similar, even though they are in two different tectonic domains.

## REFERENCES

Ahrens, L.H., 1955. Oldest rocks exposed in crust of the earth. Ed. by A. Poldervaart, Geological Society of American Special Paper 62: 155-168.

Aldrich, L.T., Wetherill, G.W., and Davis, G.L., 1956. Determination of radiogenic $Sr^{87}$ of an interlaboratory series of lepidolites. Geochem Cosochem Acta 10: 238-240.

Bannatyne, B.B., and Trueman, D.L., 1982. Chromite reserves and geology of the Bird River sill, Manitoba. Dept. of Energy and Mines Resource Division Open File Report Of-82-1.

Beakhouse, G.P., 1977. A subdivision of the western English River subprovince. Can. J. Earth Sc., 14: 1481-1489.

Beakhouse, G.P., 1985. The relationship of supracrustal sequences to a basement complex in the western English River subprovince. The Geological Associaticn of Canada Special Paper, 28:169-178.

Campbell, I.H., and Hill, R.I., 1988. A two-stage model for formation of the granite-greenstone terrains of the Kalgoorlie-Norseman area, Western Australia. Earth and Planetary Science Letters. 90: 11-25.

Card, K.D., and Ciesielski, A., 1987. Subdivisions of the Superior Province of the Canadian Shield. Geoscience Canada, 13-1: 5-13.

Carlson, H.D., 1958. Geology of the Werner Lake - Rex Lake area. Ont. Dept. Mines, V. LXVI, pt. 4.

Cerny, P., Trueman, D.L., Ziehlke, D.V, Good, B.E., and Paul, B.J., 1981. The Cat Lake-Winnipeg River and the Wekusko Lake pegmatite fields. Manitoba Mineral Resources Division, Economoc Geology Report ER. 80-1.

Corfu, F., and Andrews, A.J., 1987. Geochronological constraints on the timing of magmatism, deformation, and gold mineralization in the Red Lake greenstone belt, northwestern Ontario. Can. J. Earth Sc., 24: 1302-1320.

Corfu, F., and Wallace, H., 1986. U-Pb zircon ages for magmatism in the Red Lake greenstone belt, northwastern Ontario. Can. J. Earth Sc., 23: 27-42.

Cummings, G.L., Wilson, J.T., Farquhar, R.M., and Russell, R.D., 1955. Some dates and subdivisions of the Canadian Shield. Geological Association of Canada Proceedings 7: 27-49.

Davies, J.F., 1951. Bird River area, Lac du Bonnet mining division, southeastern Manitoba, map 51-3, scale 2 inches to 1 mile, 1:31,680. Mines and Surveys Branch, Manitoba.

Davies, J.F., 1952. Geology of the Oiseau (Bird) River area, Lac du Bonnet mining division. Manitoba Mines Branch, Publication 51-3.

Davies, J.F., 1955. Geology and mineral deposits of the Bird River Lake area. Manitoba Mines Branch, Publication 54-1.

Davies, J.F., 1956. Geology of the Booster Lake area, Lac du Bonnet mining division. Manitoba Mines Branch, Publication 55-1.

Davies, J.F., 1957. Geology of the Winnipeg River area (Shatford Lake-Ryerson Lake), Lac du Bonnet mining division, Manitoba. Manitoba Mines Branch, Publication 56-1.

Davies, J.F., Bannatyne, B.B., Barry, G.S., and McCabe, H.R., 1962. Geology and mineral resources of Manitoba. Manitoba Mines Branch, Publication 62-1: 30-53.

Doe, B.R., 1970. Lead isotopes. Springer-Verlag. New York, Heidelberg, Berlin.

Dwibedi, K., 1966. Petrology of the English River gneissic belt, northwestern Ontario and southeastern Manitoba. ph.D. Thesis, University of Manitoba.

Easton, R.M., 1985. The nature and significance of pre-yellowknife supergroup rocks in the Point Lake area, Slave structural province, Canada. The Geological Association of Canada Special Paper, 28: 153-167.

Eckelmann, P.O., Gast, F.W., 1957. Plutonic history and absolute age: the Huron claim-Johnston Lake area, southeastern Manitoba. Geological Society of America Bulletin, Vol. 68, 1720-1722.

Ermanovics, I.F., McRitchie, W.D., and Houston, W.N., 1979. Petrochemistry and tectonic setting of plutonic rocks of the Superior Province in Manitoba; in: Trondhjemites, Dacites, and Related Rocks. Ed. by F. Barker, Developments in Petrology, Vol. 6, Elsevier, 323-362.

Farquharson, R.B., 1975. Revised Rb-Sr age of the Lac du Bonnet quartz monzonite, southeastern Manitoba. Can. J. Earth Sc., 12: 115-118.

Farquharson, R.B., and Clark, G.S., 1971. Rb-Sr geochronology of some granitic rocks in southeastern Manitoba. Geological Association of Canada, Special Paper 9: 111-117.

Faure, G., 1986. Principles of isotope geology, second edition. John Wiley and Sons.

Froude, D.O., Ireland, T.R., Kinney, P.D., Williams, R.S., Compston, W., Williams, A.R., and Myers, J.S., 1983. Ion microprobe identification of 4100-4200 Myr-old detrital zircons. Nature, 304: 616-618.

Gait, R.I, 1964. The mineralogy of the chrome spinels of the Bird River sill, Manitoba. M.Sc. thesis, University of Manitoba.

Gast, P.W., Kulp, J.L., and Long, L.E., 1958. Absolute age of early Precambrian rocks in the Bighorn Basin of Wyoming and Montana and southeastern Manitoba. Transactions, American Geoghysical Union, Vol. 3, No. 2, 322-334.

Geyh, M.A., and Schleicher, H., 1990. Absolute age determination, physical and chemical dating methods and their application. Springer-Verlag, Berlin, Heidelberg, New York, London, Paris, Tokyo, Hong Kong, Barcelona.

Glikson, A.Y., 1972. Early Precambrian evidence of a primitive ocean crust and island nuclei of sodic granite. Geol. Soc. Am. Bull. 83: 3323-3344.

Glikson, A.Y., and Jahn, B.M., 1985. REE and LIL elements, eastern Kaapvaal Shield, south Africa: evidence of crustal evolution by 3-stage melting. The Geological Association of Canada Special Paper, 28: 303-324.

Goldich, S.S., and Mudrey, M., Jr., 1972. Dilatancy model for discordiant U-Pb zircon ages. In contributions to recent geochemistry and analytical chemistry (A.P.Vinegradov volume). Ed. by A.I. Tugarinov. Nauka, Moscow, 415-418.

Goodwin, A.M., 1977. Archean volcanism in Superior Province, Canadian Shield. The geological Association of Canada Special Paper, 16: 205-241.

Hall, D.H., 1974. Long wavelength aeromagnetic anomalies and deep crustal magnetization in Manitoba and northwestern Ontario, Canada. Geophysics, 40: 403-430.

Hall, D.H., and Hajnal, Z., 1973. Deep seismic crustal studies in Manitoba. Bulletin of the Seismological Society of America, 63: 885-910.

Hill, R.I., Campbell, I.H., Davies, G.F., and Griffiths, R.W., 1992. Mantle plumes and continental tectonics. Science, 256: 186-193.

Jackson, E.D., 1967. Ultramafic cumulates in the stillwater great dike and bushveld intrusions: in ultramafic and related rocks. Ed. by P. J. Wyllic, Wiley and Sons, New York.

Kowerchuk, D., and Weber W., 1987. Bedrock geology and compilation map series. Pointe du Bois NTS 52L. Scale 1:250 000. Manitoba Energy and Mines.

Krough, T.E., Ermanovics, I.F., and Davis, G.L., 1974. Two episodes of metamorphism in the Archean rocks of the Canadian Shield. Carnegie Institution of Washington, Yearbook, 73: 573-575.

Krogh, T.E., 1982. Improved accuracy of U-Pb zircon ages by the creation of more concordant systems using an air abrasion technique. Geochim. Cosmochim. Acta, 46: 637-649.

Ludwig, K.R., 1982. A computer program to convert raw Pb-U-Th isotope ratios to blank-corrected isotope ratios and concentrations, with associated errors and error-correlations. U.S. Geol. Surv., Open-file Report 82-820.

Ludwig, K.R., 1992. A plotting and regression program for radiogenic-isotope data, version 2.57. U.S. Geol. Surv., Open-file Report 91-445.

Mattison, J.M., 1972. Preparation of hydrofluoric, hydrocloric and nitric acids at ultralow lead levels. Analytical Chemistry, 44: 1715-1716.

McRitchie, W.D., and Weber, W., 1971. Geology and geophysics of the Rice Lake region, southeastern Manitoba (project pioneer). Manitoba Mines Branch, Publication 71-1.

Nier, A.O., Thompson, R.W., and Murphey, B.F., 1941. The isotopic composition of lead and the measurement of geological time, III. Physics Review, 60: 112-116.

Nunes, P.D., and Thurston P.C., 1980. Two hundred and twenty million years of Archean evolution: a zircon U-Pb age stratigraphic study of the Uchi-Confederation Lakes greenstone belt, northwestern Ontario. Can. J. Earth Sc., 17: 710-721.

Ojakangas, R.W., 1985. Review of Archean clastic sedimentation, Canadian Shield: major felsic volcanic contributions to turbidite and alluvial fan-fluvial facies associations. The Geological Association of Canada Special Paper, 28: 23-47.

Ontario Geological Survey, 1986. Geological highway map, northern Ontario, map 2506, 1: 1 600 000. Ontario Geological Survey.

Penner, A.P., and Clark, G.S., 1971. Rb-Sr age determinations from the Bird River area, southeastern Manitoba. Geol. Assoc. Canada, Spec. Paper #9, 105-109.

Percival, J.A., and Card, K.D., 1983. Archean Crust as Revealed in the Kapuskasing Uplift, Superior Province, Canada. Geology, 11: 323-326.

Posehn, G., 1976. The metaconglomerate and metagreywacke at Booster Lake, Manitoba. Unpublished M.Sc. Thesis, Department of Earth Sciences, University of Manitoba.

Sage, R.P., 1992. Geology of Michipicootten greenstone belt. Ontario Geological Survey, Report (in press).

Springer, G.D., 1948. Cat Lake-Winnipeg River area, Lac du Bonnet mining division, southeastern Manitoba, map 48-7, scale 2 inches to 1 mile (1:31 680). Mines and Surveys Branch, Manitoba.

Stacey, J.S. and Kramers, J.D., 1975. Approximation of terrestial lead isotope evolution by a two stage model. Earth Planet. Sci. Lett., 26: 207-221.

Steiger, R.H. and Jäger, E., 1977. Subcommission on geochronology: convention on the use of decay constants in geo- and cosmochronology. Earth Planet. Sci. Lett., 28: 359-362.

Stevens, J.R., and Shillibeer, H.A., 1956. Loss of argon from minerals and rocks due to crushing. Geological Association of Canada Proceedings 8: 71-76.

Sutton, J., 1971. Some developments in the crust. Geol. Soc. Aust. Spec. Publ. 3: 1-10.

Tera, F., and G.J. Wasserburg, 1972. U-Th-Pb systematics in three Apollo 14 basalts and the problem of initial Pb in lunar rocks. Earth Planet. Sci. Letters, 14: 281-304.

Tera, F., and Wasserburg, 1974. U-Th-Pb systematics on lunar rocks and inferences about lunar evolution and the age of the moon. Proc. 5th Lunar Conf., Geochim. Cosochim. Acta, Suppl. 5, Vol. 2, 1571-1599.

Tilton, G.R., 1960. Volume diffusion as a mechanism for discordant lead ages. J. Geophys. Res., 65: 2933-2945.

Timmins, E.A., 1985. Paleomagnetism and geochronology of the Bird River greenstone belt. Unpublished M.Sc. Thesis, Department of Geology, University of Windsor.

Timmins, E.A., Turek, A., Symons, D.T.A., and Smith, P.E., 1985. U-Pb zircon geochronology and palemagnetism of the Bird River greenstone belt. Mineralogical Association of Canada, Joint Annual Meeting, Program and Abstracts, 10: A62.

Trueman, D.L., 1971. Petrological, structural, and magnetic studies of a layered basic intrusion, Bird River sill, Manitoba. M.Sc. Thesis, University of Manitoba.

Trueman, D.L., 1975. Geology of the Winnipeg River - Bird River area, southeastern Manitoba. Manitoba Mines Branch, Summary Report of Fieldwork.

Trueman, D.L., 1980. Stratigraphy, structure and metamorphic petrology of the Archean greenstone belt at Bird River, Manitoba. ph.D. Thesis, University of Manitoba.

Turek, A., Keller R., Van Schmus W.R. and Weber W., 1989. U-Pb zircon ages for the Rice Lake area,southeastern Manitoba. Can. J. Earth Sc., 26: 23-30.

Turek, A., and Weber, W., 1991. New U-Pb zircon ages from the Rice Lake area: evidence for 3 Ga crust. Manitoba Energy and Mines, Minerals Division, Report of Activities, 1991: 53-55.

Wendt, I., 1984. A three-dimensional U-Pb discordia plane to evaluate samples with common lead of unknown isotopic composition. Isotope Geoscience, 2: 1-12.

Wetherill, G.W., 1956. Discordant uranium-lead ages. Trans. Amer. Geophys. Union, 37: 320-326.

Wetherill, G.W., 1963. Discordant uranium-lead ages - Part 2: discordant ages resulting from diffusion of lead and uranium. Journal of Geophysical Research, 68: 2957-2965.

Wilson, H.D.B., 1971. The Superior Province in the Precambrian of Manitoba; geoscience studies in Manitoba. The Geological Association of Canada Specical Paper, 9: 41-49.

Wilson, H.D.B., and Morrice, M.G., 1977. The volcanic sequence in Archean Shields. The Geological Association of Canada Special Paper, 16: 355-374.

# APPENDIX A

## SAMPLE LOCATIONS AND DESCRIPTIONS *

| Sample No. | Description | Location |
|---|---|---|
| MA-3 | Gabbro,<br>Bird River sill | 50° 27′ 53"<br>95° 33′ 55" |
| MA-4 | Tuff/rhyolite,<br>Peterson Creek formation | 50° 27′ 40"<br>95° 24′ 50" |
| MA-6 | Diorite,<br>Volcanic plug | 50° 27′ 00"<br>95° 26′ 29" |
| MA-10 | Quartz monzonite,<br>Maskwa Lake batholith | 50° 29′ 47"<br>95° 29′ 07" |
| MA-17 | Granite,<br>Lac du Bonnet batholith | 50° 22′ 40"<br>95° 44′ 55" |
| MA-21 | Tonalite, foliated,<br>Pointe du Bois batholith | 50° 17′ 50"<br>95° 33′ 55" |
| MA-23 | Granodiorite,<br>Maskwa Lake batholith | 50° 31′ 40"<br>95° 27′ 35" |
| MA-26 | Granodiorite | 50° 28′ 00"<br>95° 28′ 50" |

* Rock names based on thin section examination.

**Plate A.** Photomicrograph of sample MA-4, Peterson Creek volcanic tuff, showing very extensive alteration. Crossed nicols, grain size: -100+200, magnification: 50X.

**Plate B.** Photomicrograph of sample MA-23, Maskwa batholith granodiorite, showing sharp prismatic crystals with low amount of alteration. Crossed nicols, grain size: -100+200, magnification: 50X.

**Plate C.** Photomicrograph of sample MA-26, granodiorite, showing variable population of zircons from poor quality altered grains to good quality prismatic zircon grains. Crossed nicols, grain size: -100+200, magnification: 50X.

**Plate D.** SEM photograph of sample MA-23, showing typical prismatic and euhedral shape of zircons. Some exfoliation alteration is noticeable. Grain size: -200+325, magnification: X250.

# APPENDIX B

## U-Pb CHEMISTRY

For mass spectrometer U and Pb analyses of the zircon sample, the sample must be dissolved and U and Pb separated. Three mass spectrometer runs are required. These include Pb isotope composition (IC) analysis and U and Pb isotope dilution (ID) analysis. The concentration of U in the sample is determined by the ID run. The isotope concentrations of Pb in the sample are determined by both ID and IC runs (Faure, 1986; Ludwig, 1982).

This whole chemistry procedure is a microscale operation with a lot of attention paid to cleanliness to minimize contamination. The laboratory procedures of U-Pb chemistry can be divided into three parts : zircon cleaning, zircon dissolution and U-Pb separation.

1. Zircon cleaning procedure :

- Use ultrapure water to wash zircons out of petri dish, and put them into a clean glass beaker.
- Add appropriate amount of 7N $HNO_3$, and heat the beaker at low temperature for about one hour.
- Ultrasound for one hour and decant supernatant.
- Rinse zircons with ultrapure water, heat gently for about 30 minites; then again ultrasound for one hour and decant supernatant.
- Repeat the above steps for several times when necessary

until clean zircons are collected.

- Store the clean zircons in a covered petri dish for weighing and dissolution.

2. Zircon dissolution :

- For each sample, put approximately 1-2 mg clean zircons into a teflon bomb, add 0.5 ml HF and 1 ml 7N $HNO_3$.
- Put bombs in oven at 190°C - 200°C for 5 to 7 days, then cool the bombs to room temperature and open.
- Dry on hot plate for about one hour, then add 1 ml of ultrapure $HNO_3$, when dry, add 0.5 ml 6N HCl.
- Reassemble bombs and put them in oven at 190°C - 200°C for about 10 hours, then remove bombs from oven and cool.
- Quantitatively transfer the solution to two 5 ml teflon beakers , one is for isotope dilution (ID) analysis, the other is for isotope composition (IC) analysis.
- Add appropriate amount of the mixed U-Pb tracer into one of the two sample beakers (spike the sample), evaporate to dryness and store for U-Pb separation.

3a. U-Pb separation technique for isotope composition (IC) analysis:

- Rinse teflon columns in deionized water and mount on racks, then load columns with 0.5 ml cleaned anion resin in 5N HCl, wait for the liquid to drain.
- Flush columns with 2 ml of 5N HCl, and label 5 ml teflon

beakers for unspiked Pb IC samples.

- Add 1 ml 1N HCl to each sample beakers, wait until all the residue is dissolved. Then load the dissolved residue onto the columns.
- Wash the columns with 1 ml 1N HCl for two times, and place 5 ml teflon beakers under columns, then elute Pb with 3 ml 5N HCl.
- Evaporate the sample to dryness and store them sealed in parafilm for the mass spectrometer runs (IC runs).

3b. U-Pb separation technique for isotope dilution (ID) analysis:

- Rinse columns in deionized water and mount on racks. Load 0.5 ml of cleand anion resin in 5N HCl to each column and let the liquid drain.
- Flush columns with 2 ml 5N HCl and label 5 ml teflon beakers for the spiked isotope dilution samples (ID's).
- Add 1 ml 3N HCl to the spiked sample beakers, wait until all the residue to dissolve. Then load the dissolved residue to the columns.
- Wash the columns with 1 ml 3N HCl for two times, and place 5 ml teflon beakers under columns.
- Elute Pb with 2 ml 5 N HCl and elute U with 2 ml deionized water.
- Evaporate the samples to dryness and store sealed in parafilm for the mass spectrometer runs (ID runs).

# APPENDIX C

## AN EXAMPLE OF THE REPROCESSED DATA USING THE DATA SMOOTHING TECHNIQUE

The results of an IC Run ($Pb^{204}/Pb^{208}$) before and after the data re-processing as well as the related data file are shown as below :

(1) Before the data re-processing :

MA-27D-IC [4/6] 3V/3.0A Run 800 18:14:35 12-14-1992
Lead IC 204/206: BLOCK NO. 1

SETTLE TIME = 5 SEC., COUNTS ON ZERO = 10 SEC.
COUNTS ON PEAK = 10 SEC., NUMBER OF SETS = 10

The FILENAME for data saving = 800C

| N | [ZERO1] | [ZERO2] | [204] | [206] |
|---|---|---|---|---|
| 1 | 0.00569 | 0.00526 | 0.00687 | 6.30762 |
| 2 | 0.00556 | 0.00646 | 0.00640 | 6.04450 |
| 3 | 0.00437 | 0.00654 | 0.00668 | 5.98698 |
| 4 | 0.00566 | 0.00580 | 0.00697 | 5.79033 |
| 5 | 0.00402 | 34.00375 | 0.00594 | 5.77477 |
| 6 | 46.00488 | 0.00584 | 0.00736 | 5.43612 |
| 7 | 30.00384 | 0.00487 | 0.00621 | 5.32017 |
| 8 | 0.00623 | 0.00570 | 0.00734 | 5.23653 |
| 9 | 0.00595 | 0.00570 | 0.00669 | 5.06851 |
| 10 | 0.00523 | 0.00624 | 0.00707 | 4.91619 |
| 11 | 0.00541 | 0.00492 | 0.00673 | 4.82289 |

| N | [ZERO] | [204]c | [ZERO]' | [206]c | [204/206] |
|---|---|---|---|---|---|
| 1 | 0.0055 | 0.00089 | 0.00541 | 6.30221 | 0.00014 |
| 2 | 0.0060 | 0.00081 | 0.00542 | 6.03909 | 0.00013 |
| 3 | 0.0055 | 0.00123 | 0.00610 | 5.98088 | 0.00021 |
| 4 | 0.0057 | -8.49835 | 0.00491 | 5.78542 | -1.46893 |
| 5 | 17.0039 | %-19.9980 | 40.00431 | %-34.2295 | 0.58423 |
| 6 | 23.0054 | %-20.9981 | 19.00484 | %-13.5687 | 1.54754 |
| 7 | 19.0044 | -9.49838 | 0.00555 | 5.31462 | -1.78722 |
| 8 | 0.0060 | 0.00112 | 0.00583 | 5.23071 | 0.00021 |
| 9 | 0.0058 | 0.00110 | 0.00547 | 5.06305 | 0.00022 |
| 10 | 0.0057 | 0.00145 | 0.00583 | 4.91036 | 0.00030 |

| | |
|---|---|
| AVG 5.90538 | -0.11232 |
| STD DEV | 0.94056 |
| STD ERROR | 0.29743 |
| PCT STD ERROR | %-264.81530 |
| NUMBER 4 DELETED | |
| NEW AVG | 0.03842 |
| STD DEV | 0.86002 |
| STD ERROR | 0.28667 |
| PCT STD ERROR | %746.20450 |
| NUMBER 5 DELETED | |
| NEW AVG | -0.02981 |
| STD DEV | 0.89298 |
| STD ERROR | 0.31572 |
| PCT STD ERROR | %-1059.122 |
| NUMBER 6 DELETED | |
| NEW AVG | -0.25514 |
| STD DEV | 0.67558 |
| STD ERROR | 0.25535 |
| PCT STD ERROR | %-100.0789 |
| NUMBER 7 DELETED | |
| NEW AVG | 0.00020 |
| STD DEV | 0.00006 |
| STD ERROR | 0.00002 |
| PCT STD ERROR | 11.96355 |

NORMALIZED Pb204/Pb206 = 0.00020 +/- 0.00002 (SE)
(Normalization factor used = 0.100 pct/mass unit)

(2) After the data re-processing :

NEW RESULT AFTER DATA PROCESSING :

(FILENAME = 800C)
The processing factor = 2

| N | [ZERO1] | [ZERO2] | [204] | [206] |
|---|---|---|---|---|
| 1 | 0.00569 | 0.00526 | 0.00667 | 6.32438 |
| 2 | 0.00556 | 0.00646 | 0.00640 | 6.03880 |
| 3 | 0.00437 | 0.00621 | 0.00670 | 5.98684 |
| 4 | 0.00540 | 0.00580 | 0.00697 | 5.79153 |
| 5 | 0.00402 | 0.00434 | 0.00594 | 5.76875 |
| 6 | 0.00505 | 0.00549 | 0.00699 | 5.43015 |
| 7 | 0.00410 | 0.00487 | 0.00621 | 5.31860 |
| 8 | 0.00623 | 0.00539 | 0.00734 | 5.23698 |
| 9 | 0.00595 | 0.00570 | 0.00669 | 5.06839 |
| 10 | 0.00523 | 0.00624 | 0.00707 | 4.91578 |
| 11 | 0.00518 | 0.00492 | 0.00673 | 4.82362 |

| N | [ZERO] | [204]c | [ZERO]' | [206]c | [204/206] |
|---|---|---|---|---|---|
| 1 | 0.0055 | 0.00079 | 0.00541 | 6.31897 | 0.00013 |
| 2 | 0.0060 | 0.00090 | 0.00542 | 6.03339 | 0.00015 |
| 3 | 0.0053 | 0.00139 | 0.00581 | 5.98104 | 0.00023 |
| 4 | 0.0056 | 0.00157 | 0.00491 | 5.78662 | 0.00027 |
| 5 | 0.0042 | 0.00174 | 0.00469 | 5.76387 | 0.00030 |
| 6 | 0.0053 | 0.00172 | 0.00479 | 5.42536 | 0.00032 |
| 7 | 0.0045 | 0.00163 | 0.00055 | 5.31305 | 0.00031 |
| 8 | 0.0058 | 0.00120 | 0.00567 | 5.23131 | 0.00023 |
| 9 | 0.0058 | 0.00110 | 0.00547 | 5.06293 | 0.00022 |
| 10 | 0.0057 | 0.00151 | 0.00571 | 4.91007 | 0.00031 |
| AVG | 0.0054 | | | | 0.00025 |
| STD DEV | | | | | 0.00007 |
| STD ERROR | | | | | 0.00002 |
| PCT STD ERROR | | | | | 8.74433 |
| NUMBER 1 DELETED | | | | | |
| NEW AVG | | | | | 0.00026 |
| STD DEV | | | | | 0.00006 |
| STD ERROR | | | | | 0.00002 |
| PCT STD ERROR | | | | | 7.25006 |
| NUMBER 2 DELETED | | | | | |
| NEW AVG | | | | | 0.00027 |
| STD DEV | | | | | 0.00004 |
| STD ERROR | | | | | 0.00001 |
| PCT STD ERROR | | | | | 5.32256 |

NORMALIZED Pb204/Pb206 = 0.00027 +/- 0.00001 (SE)
(Normalization factor used = 0.100 pct/mass unit).

(3) The related data file used in data processing :

FILENAME = 800C

N = 1

| [ZERO1] | [204] | [ZERO2] | [206] |
|---|---|---|---|
| 0.00430 | 0.00620 | 0.00430 | 6.30890 |
| 0.00530 | 0.00670 | 0.00470 | 6.31350 |
| 0.00550 | 0.00870 | 0.00500 | 6.31840 |
| 0.00570 | 0.00560 | 0.00600 | 6.31860 |
| 0.00650 | 0.00660 | 0.00610 | 6.32630 |
| 0.00660 | 0.00770 | 0.00460 | 6.34230 |
| 0.00780 | 0.00700 | 0.00450 | 6.32340 |
| 0.00370 | 0.00710 | 0.00680 | 6.33480 |
| 0.00710 | 0.00630 | 0.00630 | 6.24890 |
| 0.00440 | 0.00680 | 0.00430 | 6.24110 |

N = 2

| [ZERO1] | [204] | [ZERO2] | [206] |
|---|---|---|---|
| 0.00480 | 0.00670 | 0.00610 | 6.03900 |
| 0.00570 | 0.00690 | 0.00480 | 6.03390 |
| 0.00760 | 0.00660 | 0.00670 | 6.03120 |
| 0.00350 | 0.00620 | 0.00730 | 6.03360 |
| 0.00570 | 0.00690 | 0.00580 | 6.03910 |
| 0.00460 | 0.00660 | 0.00800 | 6.04390 |
| 0.00400 | 0.00670 | 0.00780 | 6.04810 |
| 0.00680 | 0.00530 | 0.00470 | 6.05420 |
| 0.00620 | 0.00680 | 0.00740 | 6.05880 |
| 0.00670 | 0.00530 | 0.00600 | 6.06320 |

N = 3

| [ZERO1] | [204] | [ZERO2] | [206] |
|---|---|---|---|
| 0.00520 | 0.00680 | 0.00570 | 5.99220 |
| 0.00360 | 0.00630 | 0.00690 | 5.98900 |
| 0.00420 | 0.00700 | 0.00660 | 5.99260 |
| 0.00290 | 0.00690 | 0.00950 | 5.99420 |
| 0.00370 | 0.00750 | 0.00590 | 5.99920 |
| 0.00510 | 0.00570 | 0.00720 | 6.01600 |
| 0.00490 | 0.00650 | 0.00560 | 5.98950 |
| 0.00380 | 0.00700 | 0.00620 | 5.97900 |
| 0.00460 | 0.00650 | 0.00600 | 5.97340 |
| 0.00570 | 0.00660 | 0.00580 | 5.94470 |

N = 4

| [ZERO1] | [204] | [ZERO2] | [206] |
|---|---|---|---|
| 0.00630 | 0.00660 | 0.00690 | 5.80470 |
| 0.00450 | 0.00720 | 0.00440 | 5.80170 |
| 0.00610 | 0.00730 | 0.00680 | 5.80120 |
| 0.00420 | 0.00700 | 0.00430 | 5.79650 |
| 0.00520 | 0.00820 | 0.00660 | 5.78740 |
| 0.00800 | 0.00730 | 0.00540 | 5.78610 |
| 0.00560 | 0.00610 | 0.00560 | 5.77780 |
| 0.00480 | 0.00810 | 0.00700 | 5.77900 |
| 0.00600 | 0.00610 | 0.00610 | 5.78230 |
| 0.00590 | 0.00580 | 0.00490 | 5.78660 |

N = 5

| [ZERO1] | [204] | [ZERO2] | [206] |
|---|---|---|---|
| 0.00460 | 0.00680 | 0.00430 | 5.78660 |
| 0.00440 | 0.00580 | 0.00400 | 5.79480 |
| 0.00380 | 0.00510 | 0.00430 | 5.81200 |
| 0.00410 | 0.00630 | 0.00280 | 5.81710 |
| 0.00400 | 0.00690 | 0.00360 | 5.75700 |
| 0.00350 | 0.00530 | %340.00000 | 5.74730 |
| 0.00460 | 0.00540 | 0.00480 | 5.74970 |
| 0.00310 | 0.00630 | 0.00480 | 5.76080 |
| 0.00430 | 0.00580 | 0.00410 | 5.76110 |
| 0.00380 | 0.00570 | 0.00480 | 5.76130 |

N = 6

| [ZERO1] | [204] | [ZERO2] | [206] |
|---|---|---|---|
| 0.00510 | 0.00580 | 0.00580 | 5.42190 |
| 0.00570 | 0.00650 | 0.00570 | 5.42810 |
| 0.00570 | 0.00910 | 0.00510 | 5.43470 |
| %460.0000 | 0.01070 | 0.00510 | 5.44350 |
| 0.00430 | 0.00690 | 0.00670 | 5.46970 |
| 0.00840 | 0.00580 | 0.00780 | 5.43280 |
| 0.00440 | 0.00690 | 0.00540 | 5.42590 |
| 0.00370 | 0.00860 | 0.00560 | 5.42920 |
| 0.00530 | 0.00700 | 0.00510 | 5.43180 |
| 0.00620 | 0.00630 | 0.00610 | 5.44360 |

N = 7

| [ZERO1] | [204] | [ZERO2] | [206] |
|---|---|---|---|
| 0.00550 | 0.00510 | 0.00400 | 5.31170 |
| 0.00380 | 0.00640 | 0.00580 | 5.31320 |
| 0.00430 | 0.00490 | 0.00460 | 5.31750 |
| 0.00360 | 0.00590 | 0.00530 | 5.31960 |
| %380.0000 | 0.00710 | 0.00500 | 5.32220 |
| 0.00420 | 0.00660 | 0.00610 | 5.32130 |
| 0.00450 | 0.00700 | 0.00370 | 5.32190 |
| 0.00350 | 0.00740 | 0.00500 | 5.32370 |
| 0.00470 | 0.00490 | 0.00480 | 5.32280 |
| 0.00420 | 0.00680 | 0.00440 | 5.32780 |

N = 8

| [ZERO1] | [204] | [ZERO2] | [206] |
|---|---|---|---|
| 0.00450 | 0.00720 | 0.00850 | 5.24300 |
| 0.00750 | 0.00790 | 0.00550 | 5.24560 |
| 0.00580 | 0.00680 | 0.00570 | 5.25180 |
| 0.00560 | 0.00830 | 0.00420 | 5.23970 |
| 0.00580 | 0.00740 | 0.00590 | 5.21950 |
| 0.00580 | 0.00660 | 0.00580 | 5.22300 |
| 0.00530 | 0.00860 | 0.00430 | 5.22430 |
| 0.00780 | 0.00720 | 0.00510 | 5.23190 |
| 0.00730 | 0.00690 | 0.00660 | 5.23930 |
| 0.00690 | 0.00650 | 0.00540 | 5.24720 |

N = 9

| [ZERO1] | [204] | [ZERO2] | [206] |
|---|---|---|---|
| 0.00760 | 0.00560 | 0.00720 | 5.06980 |
| 0.00450 | 0.00670 | 0.00640 | 5.06840 |
| 0.00390 | 0.00710 | 0.00530 | 5.07100 |
| 0.00680 | 0.00680 | 0.00410 | 5.07130 |
| 0.00510 | 0.00700 | 0.00460 | 5.07310 |
| 0.00470 | 0.00670 | 0.00500 | 5.06950 |
| 0.00690 | 0.00650 | 0.00630 | 5.06770 |
| 0.00690 | 0.00720 | 0.00650 | 5.06580 |
| 0.00710 | 0.00790 | 0.00560 | 5.06480 |
| 0.00600 | 0.00540 | 0.00600 | 5.06370 |

N = 10

| [ZERO1] | [204] | [ZERO2] | [206] |
|---|---|---|---|
| 0.00450 | 0.00770 | 0.00600 | 4.92060 |
| 0.00570 | 0.00690 | 0.00590 | 4.91790 |
| 0.00530 | 0.00720 | 0.00700 | 4.91590 |
| 0.00530 | 0.00710 | 0.00390 | 4.91420 |
| 0.00490 | 0.00750 | 0.00770 | 4.91370 |
| 0.00590 | 0.00600 | 0.00740 | 4.91320 |
| 0.00540 | 0.00550 | 0.00570 | 4.91410 |
| 0.00610 | 0.00820 | 0.00460 | 4.91570 |
| 0.00450 | 0.00790 | 0.00650 | 4.91670 |
| 0.00470 | 0.00670 | 0.00770 | 4.91990 |

N = 11

| [ZERO1] | [204] | [ZERO2] | [206] |
|---|---|---|---|
| 0.00550 | 0.00850 | 0.00470 | 4.83140 |
| 0.00480 | 0.00570 | 0.00440 | 4.83000 |
| 0.00540 | 0.00780 | 0.00510 | 4.82820 |
| 0.00590 | 0.00620 | 0.00630 | 4.82880 |
| 0.00540 | 0.00530 | 0.00370 | 4.82850 |
| 0.00440 | 0.00610 | 0.00470 | 4.82150 |
| 0.00560 | 0.00580 | 0.00570 | 4.81920 |
| 0.00750 | 0.00700 | 0.00440 | 4.81800 |
| 0.00430 | 0.00670 | 0.00480 | 4.81500 |
| 0.00530 | 0.00820 | 0.00540 | 4.80830 |

Note: This is original data from computer output. The erroneous numbers show up as %, there are readings correspounding to the "spikes" shown in Fig 4.1 and 4.2.

# VITA AUCTORIS

NAME: Wang, XiaoDong

BORN: April 11, 1961, Beijing, China.

HIGH SCHOOL: Beijing 101 High School, Beijing, China. 1979.

UNIVERSITY:

Ocean University of Qingdao, Qingdao, P.R. China.
1979-1983. B.Sc.

Ocean University of Qingdao, Qingdao, P.R. China.
1985-1988. M.Sc.

University of Windsor, Ontario, Canada.
1991-1993. M.Sc.

PUBLICATIONS:

Wang, X.D., 1985. A Computer program for calculating the parameter of Vo & $\beta$. A Compilation of Computer Programs Used in Petroleum Industry. Petroleum Ministry, P.R.China. (In Chinese).

Wang, X.D., and Wang, Y., 1985. A computer program for calculating the interval velocity. ( as above ).

Xu, S.Z., and Wang, X.D., 1987. Resistivity anomaly of a 2-D geological body under rugged topography. Geology and Prospecting, Vol.23, No.7. (In Chinese).

Xu, S.Z., Wang, X.D., and Ren, J.M., 1989. Geological results of 2-D terrain correction in resistivity survey. Geology and Prospecting, Vol.25, No.5. (In Chinese).

Xu, S.Z., and Wang, X.D., 1990. Boundary element method for the forward problem of a 2-D polydomain geoelectrical section in a uniform electrical field. Computer Techniques for Geophysical and Geochemical Exploration, Vol.12, No.2. (In Chinese).

Wang, X.D., and Guan, H.P., 1992 (Chinese version) and 1993 (English version). Relationship between earth resistivity precursors of an earthquake and geological environment of an observatory. Acta Seismologica Sinica (Chinese edition), Vol.14, No.3. Acta Seismologica Sinica (English edition), Vol.6, No.1.